2009

The role of the tumor suppressor gene, NF2, in the development of malignant mesothelioma

Amy Kay Erbe
The University of Montana

THE ROLE OF THE TUMOR SUPPRESSOR GENE, *NF2*, IN THE DEVELOPMENT OF MALIGNANT MESOTHELIOMA

By

Amy Kay Erbe

B.S. Chemistry with Environmental Studies Emphasis,
University of Wisconsin-La Crosse, La Crosse, WI 54601, December 2003

Dissertation

presented in partial fulfillment of the requirements
for the degree of

Doctor of Philosophy
in Toxicology

The University of Montana
Missoula, MT

January, 2009

Approved by:

Perry Brown, Associate Provost for Graduate Education
Graduate School

Mark Pershouse, Ph.D., Chairperson
Department of Biomedical and Pharmaceutical Sciences

Elizabeth Putnam, Ph.D.
Department of Biomedical and Pharmaceutical Sciences

Douglas Coffin, Ph.D.
Department of Biomedical and Pharmaceutical Sciences

J. Stephen Lodmell, Ph.D.
Division of Biological Sciences

Scott Samuels, Ph.D.
Division of Biological Sciences

Erbe, Amy, Ph.D., December 15, 2008 Toxicology

The role of the tumor suppressor gene, *NF2*, in the development of malignant mesothelioma.

Chairperson: Mark Pershouse, Ph.D.

The highly aggressive cancer, malignant mesothelioma, responds poorly to available treatment options. As most individuals diagnosed with these tumors succumb to the disease within about 2 years of diagnosis, it is imperative to develop a more thorough understanding of molecular mechanisms of the disease and thus design more suitable therapeutic options. Neurofibromatosis Type 2 (*NF2*) is one of the most commonly inactivated tumor suppressor genes in mesothelioma. The downstream signaling pathways that may be disrupted as a result of this inactivation are not entirely understood. Conversely, the tumor suppressor gene that is often referred to as the "Genome Gatekeeper," *TP53*, is rarely inactivated in mesothelioma tumors. As *TP53* is mutated in the majority of human cancers, in those cancers where *TP53* is not mutated, its function may be regulated by other mechanisms. Evidence suggests that *NF2* may be upstream in a signaling cascade of *TP53*, such that NF2 is responsible for MDM2 degradation. MDM2 is a negative regulator of p53 (the protein product of *TP53*), so that loss of *NF2* would ultimately result in decreased function of p53.

The hypothesis of this study is that inactivation of *NF2* plays a critical role in cellular growth dysregulation through altering normal regulation of MDM2 and thus p53 levels. To test this hypothesis, the role of the *NF2* gene in regulating p53 function and cellular growth in "normal" mesothelial cells and in a mesothelioma cell culture model were assessed. Normal function of *NF2* was restored by transfection of a wild-type *NF2* construct in a mesothelioma cell culture model. Additionally, NF2 expression was reduced in "normal" mesothelial cells by shRNA knockdown. In both *in vitro* models, alterations in *NF2* expression resulted in significant changes in cell cycle mechanisms, including proliferative, apoptotic, and cell cycle arrest. These events were linked to aberrant p53 function. Finally, an *in vivo* mouse model was used to determine the role *Nf2* in the development of pleural mesothelioma following asbestos exposure. A better understanding of the molecular mechanisms that are disrupted following *NF2* inactivation will help with design of more effective therapeutic strategies.

ACKNOWLEDGEMENTS

Many thanks go out to my family for their continual support throughout the pursuit of my Ph.D. I acknowledge my parents, Ann Miller and Larry Erbe, my sister, Annie, for always offering me encouragement. Also, my brother, Todd, for inspiration. I would also like to thank my fiancé, Casey, and especially our children, for their motivation and patience.

As this project could not have been achieved without the guidance of my advisor, Dr. Mark Pershouse, I would like to express my sincere gratitude to Dr. Pershouse for allowing me to join his lab and pursue my dreams of research in the field of cancer. I have learned so much, thank you Mark.

I would also like to express my appreciation to the members of my committee, Drs. Putnam, Coffin, Lodmell, and Samuels, for their guidance and input throughout this project.

In addition to my committee, I would also like to thank Dr. Melisa Bunderson Schelvan mostly for her support, encouragement, and help. Also, I thank Melisa as she contributed to some of the work done in Chapter 2.

Finally, I would like to thank the Center for Environmental Health Sciences and the Department for Biomedical and Pharmaceutical Sciences at The University of Montana for giving me this opportunity and for providing me with the financial

support needed to complete this degree. I acknowledge the following CEHS cores and their operators: Microarray Fabrication and Scanning Core (Corbin Schwanke), the Molecular Histology and Fluorscent Imaging (Lou Herritt), and the Fluorescence Cytometry (Pamela Shaw).

Additional gratitude is given to both NFS EPSCoR and EPA's Greater Research Opportunities (GRO) program Grant Number MA-91685501 for additional funding.

TABLE OF CONTENTS

LIST OF FIGURES

LIST OF TABLES

INTRODUCTION

Cell Cycle Control and Cancer

Tumor development is typified by a multitude of cellular changes including the loss of normal cell growth control, formation of new blood vessels, and acquisition of the ability to metastasize and invade foreign tissues, (Rous and Friedewald 1941; Armitage and Doll 1954; Hanahan and Weinberg 2000; Vermeulen et al. 2003a). Thought to arise from a single cell, cancer results from mutations and aberrations in the genetic code that accumulate over time, as this cell passes acquired mutations onto daughter cells (Tsuda et al. 1988; Sugimura et al. 1992). These mutations can be somatic or germline, but those that alter the function of key cell cycle regulators, such as proto-oncogenes or tumor suppressor genes (TSGs), can be critical for the eventual development of neoplasms (Shackelford et al. 1999; Evan and Vousden 2001; Croce 2008). The type and number of mutations that an individual will sustain in a lifetime is directly related to endogenous factors such as genetic predisposition and exogenous factors such as exposure to carcinogens. (Figure 1) (Sugimura et al. 1992; Minamoto et al. 1999).

FIGURE 1

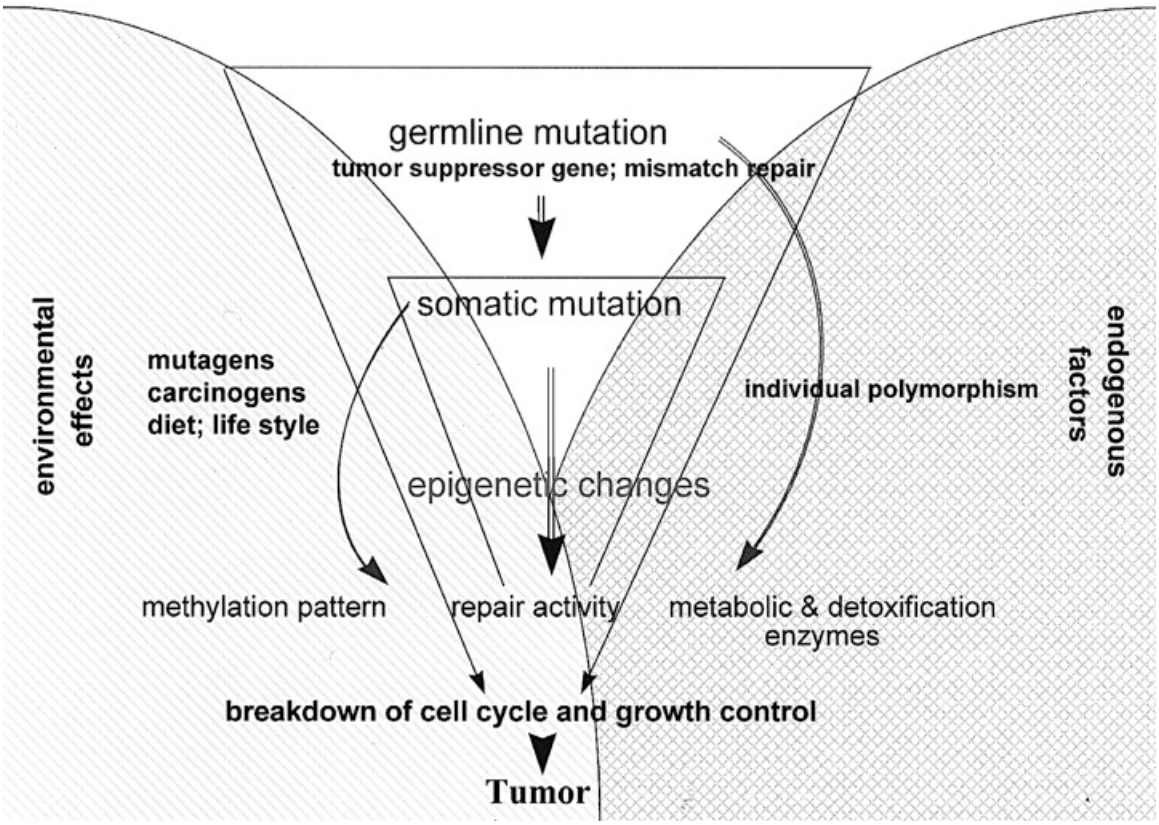

(Minamoto et al. 1999)

Figure 1. Environmental and endogenous factors can result in tumor development over time.

Cancer most often develops over long periods of time, with both endogenous and environmental factors contributing to disease formation. Germline mutations, such as those that affect TSGs or oncogenes, coupled with somatic mutations induced by environmental factors, can ultimately result in cell transformation. Another method of TSG inactivation is methylation of CpG islands in the promoter region of critical genes, which results in transcriptional silencing of the TSG. Also, in addition to germline mutations that create an increased risk to individuals for cancer susceptibility, polymorphisms in metabolic susceptibility genes create an increased cancer risk. For example, genetic variability in genes related to phase I and phase II detoxification enzymes, such that lower levels of exposure to toxicants, will cause adverse health events as the toxicant is not readily cleared from the body.

Both tumor suppressor genes and proto-oncogenes are largely involved in the regulation of cell growth. In a normal cell, proto-oncogenes act to stimulate proliferation on a controlled basis (Vermeulen et al. 2003b; Croce 2008; Johansson and Persson 2008). On the other hand, TSGs act at cell-cycle checkpoints to inhibit cell cycle progression until conditions are right for cellular division to take place. Most of these checkpoints occur at the G_1 to S phase transition of the cell cycle, but the checkpoints can also occur in S phase, at the G_2 to M phase transition, or during mitosis (Figure 2) (Shackelford et al. 1999; Tachibana et al. 2005; Johansson and Persson 2008). Mutations in proto-oncogenes, which after activation are called oncogenes, result in continued stimulation of growth. In a similar manner, inactivation of TSGs can result in the dysregulation of normal cell cycle mechanisms, allowing for progression into S phase when this transition would normally be prevented. Thus, the accumulation of changes that alter the expression level of these key genes can eventually result in tumor initiation through continual cell cycle progression (Shackelford et al. 1999; Hanahan and Weinberg 2000; Evan and Vousden 2001).

FIGURE 2

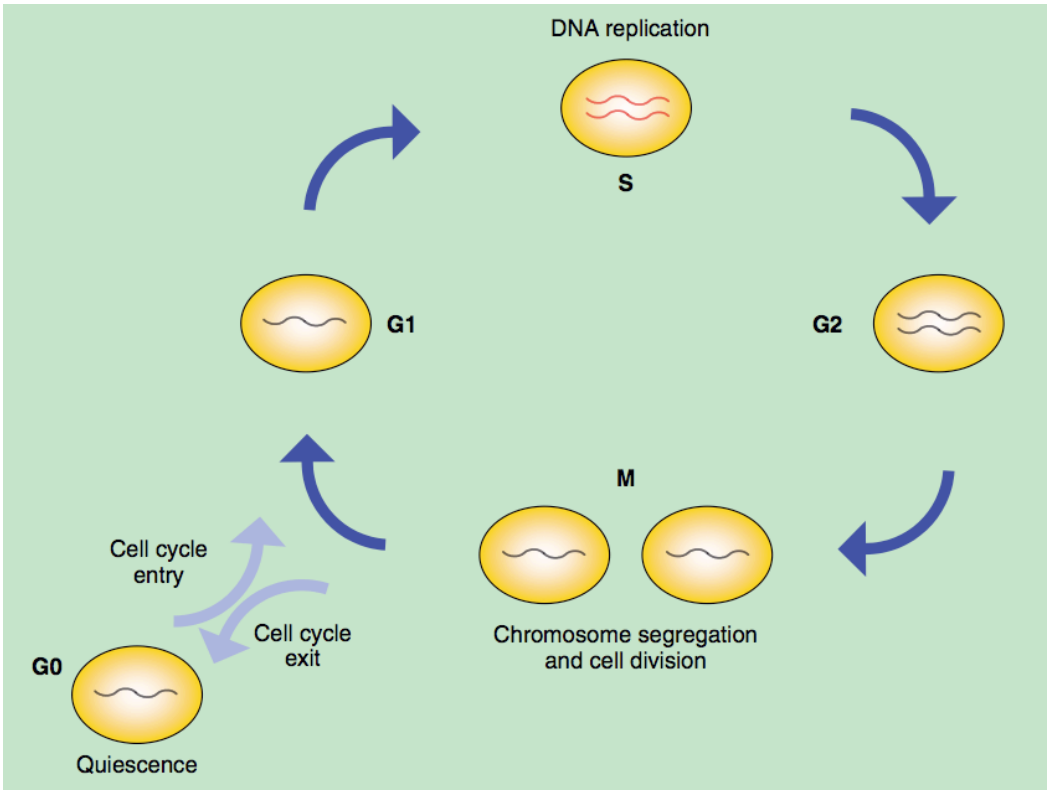

(Tachibana et al. 2005)

Figure 2. A Diagram of the Cell Cycle.

The cell cycle consists of gap 1 phase (G_1 phase), gap 0 (G_0), S phase, gap 2 (G_2), and mitosis (M phase). During G_1 , a cell prepares for DNA replication, which occurs during S phase. Following S phase, cells transition into G_2 phase while preparing for mitosis. Cells can exit the cell cycle during G_1 into G_0, a quiescent or resting state where cells are still metabolically active but are not actively cycling.

In most cases TSGs act in response to regulatory cues, often caused by cellular stress, to halt cell cycle progression. For example, depending on the type of DNA damage, the major TSG *TP53* is a transcription factor for hundreds of genes, initiating responses such as cell cycle arrest, apoptosis, and DNA repair mechanisms (Lane 1992; Rotter et al. 1994; Levine 1997; Gottlieb and Oren 1998; May and May 1999; Oren 1999). Other TSGs might not directly interact with cell cycle checkpoints, but instead function to protect and aid in the activity of other TSGs. Such is the case for p14/ARF, which is activated following DNA damaging events to inhibit MDM2 and prevent downstream p53 degradation (Chin et al. 1998; Zhang et al. 1998; Vermeulen et al. 2003b). In fact, this type of p53 deregulation is one of the possible mechanisms that may be disrupted in malignant pleural mesothelioma (MPM) contributing to loss of cellular growth control. *TP53* is rarely found mutated in this type of cancer, whereas inactivating mutations are often found in other TSGs that may protect activity of p53 (Lecomte et al. 2005).

Malignant Mesotheliomas

Malignant mesothelioma is an aggressive tumor that is strongly associated with exposure to asbestos fibers (Wagner et al. 1960). The overall incidence of these tumors is relatively rare. Individuals with these locally aggressive tumors are given a poor prognosis with a survival time of less than 2 years (Rusch 1995; Murthy and Testa 1999; Altomare et al. 2005; Jaurand and Fleury-Feith 2005; Lecomte et al. 2005; Tan and Treasure 2005). Noting the world-wide problem,

Treasure and Sedrakyan (2004) reported on the risk to workers in the UK, “One in every hundred men born in the 1940s will die of malignant pleural mesothelioma…In the developing world alone 100,000 people alive now will die from it.” In the United States, approximately 2,000 to 3,000 new cases of mesothelioma are being reported annually, and this number is expected to peak in 2015 (Murthy and Testa 1999; Hodgson et al. 2005). A latency period of 20-40 years occurs between asbestos exposure and disease diagnosis, during which time there is an accumulation of mutations (Rusch 1995; Jaurand and Fleury-Feith 2005; Kumar and Kratzke 2005). It is essential to understand the molecular mechanisms that are altered during this time to not only design more effective therapeutics, but also to improve early detection of this neoplasm.

Malignant mesotheliomas are solid tumors that arise from the mesothelium (Rusch 1995; Altomare et al. 2005; Xiao et al. 2005). The mesothelium was first described in 1827, and was reported as a single layer of flat cells that line the surfaces of certain body cavities (Whitaker et al. 1982). Body cavities where mesothelioma tumors can arise include the pleural, the peritoneal, pericardial, tunica vaginalis testis, and the ovarian epithelium, with the most common occurrence of mesothelioma cases occurring in the pleural space surrounding the lung (Tan and Treasure 2005).

The flat cells described in 1827 were later termed mesothelial cells and in the pleural space are found to overlie a basement membrane followed by a layer of connective tissue containing fibroblast-like cells, blood vessels, and lymphatics (Sahn 1998; Mutsaers et al. 2000; Mutsaers 2002). Mesothelial cells respond to

pleural injury, synthesizing and secreting inflammatory mediators to protect against physical damage and invasive organisms (Figure 3) (Jaurand and Fleury-Feith 2005). This protective barrier is formed as mesothelial cells align with tight junctions and are shielded by a “coat” predominantly composed of hyaluronan (Mutsaers 2004).

FIGURE 3

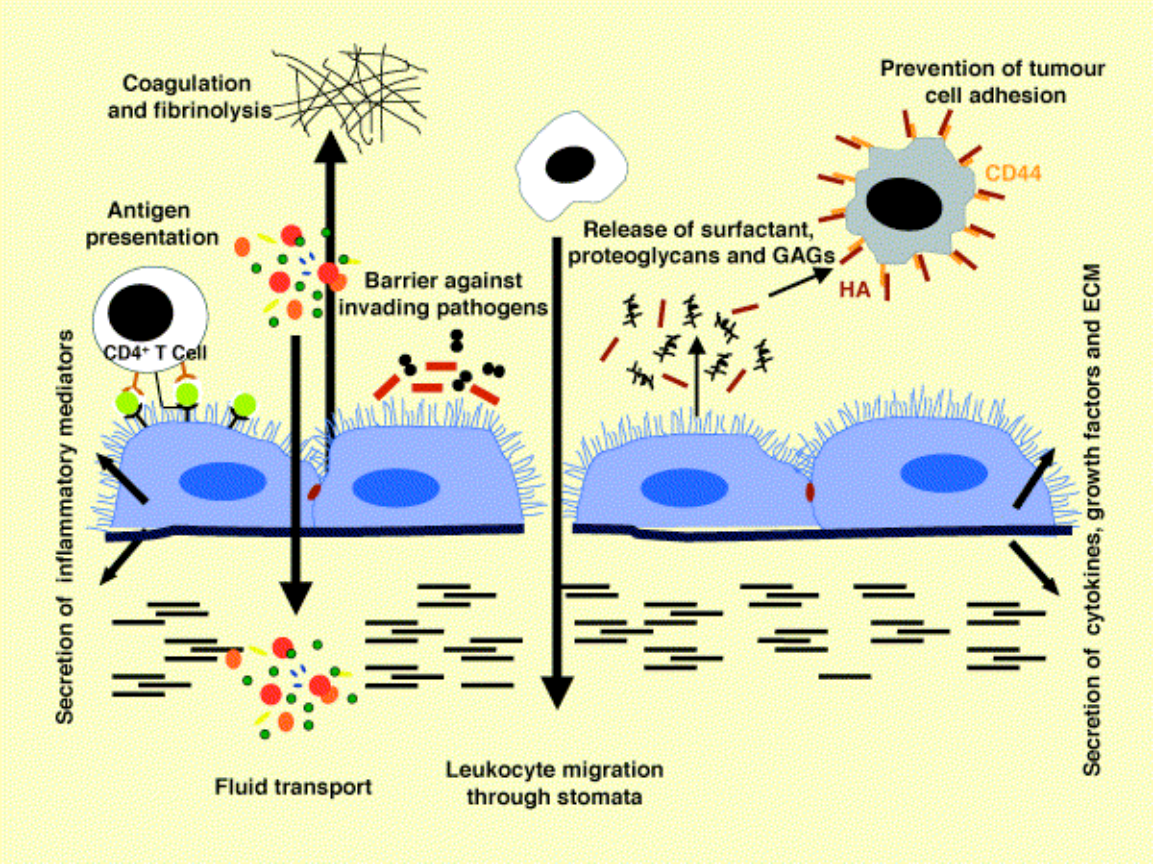

(Mutsaers 2004)

Figure 3. Mesothelial cell function.

Mesothelial cells form tight junctions and have a hyaluronic coat, which may help to provide a protective barrier against fibers and invading pathogens. In addition, these tight junctions trap fluid between the two layers of mesothelial cells, reducing friction between the two layers of the spaces that they coat allowing for more effective movement.

Mesothelial cells line the visceral and parietal surfaces of the cavities that they encompass, where they act at the border of apposing tissues to reduce friction allowing for more effective movement (Robinson et al. 2005). Thus, the visceral and parietal surfaces create the pleural space, which helps the lungs to move smoothly during breathing. Phenotypic and genetic alterations that occur in mesothelial cells result in aberrant cell cycle control, leading to uncontrolled cell growth and resistance to cell death, as well as irregular cell:cell and cell:matrix interactions, ultimately resulting in MPM (Jaurand and Fleury-Feith 2005).

MPM is most often associated with prior asbestos exposure. With a long latency period of 20 to 40 years even after exposure has stopped, development of MPM continues to progress over a long period of time. At the time of diagnosis, patients typically present with symptoms such as dyspnea (shortness of breath), difficulty sleeping, cough, chest pain, weight loss, and pleural effusion (Dunitz 2002; Robinson et al. 2005). The rare number of MPM patients that are diagnosed early (during Stage 1a) have a much better prognosis, with a median survival time of more than 5 years (Carbone et al. 2007). However, diagnosis is problematic and may take 2-3 months (Dunitz 2002; Tan and Treasure 2005).

Diagnosis of a suspected MPM usually involves an investigation into the occupational and environmental (residential) history. This is followed by a chest x-ray, which may show signs of pleural effusion, pleural thickening, pleural plaques, or asbestosis, all conditions that can be related to prior asbestos exposure. One factor complicating MPM diagnosis is that MPM is commonly

misdiagnosed as adenocarcinoma, as both of these diseases often present with multiple tan nodules in a thickened pleura. Distinction must be made between the two before treatment can begin (Robinson et al. 2005). Final diagnosis usually requires thoracocentesis and/or biopsy for cytological and histological analysis, utilizing a large panel of histological markers specific for mesothelioma or aimed at ruling out other suspected malignancies (Dunitz 2002; Robinson et al. 2005).

Adding to the complexity, there are three main histological subtypes of malignant pleural mesotheliomas (MPM). These include epithelioid (accounts for about 60%), sarcomatoid (~30%), and biphasic (~ 10%) (Dunitz 2002). The modifications that take place during mesothelial cell hyperplasia that result in these different cellular subtypes are not clear (Jaurand and Fleury-Feith 2005). However, distinguishing between these different subtypes may be a useful tool to determine the type of treatment that will best suit the patient (Dunitz 2002).

Most patients are diagnosed during a more advanced stage at which point this normally slow growing tumor becomes much more aggressive, progressing rapidly to an untreatable state (Dunitz 2002; Tan and Treasure 2005). Treatment at this stage becomes more for relief of symptoms, and most patients of this stage succumb to the disease within 4-24 months (Rusch 1995; Murthy and Testa 1999; Jaurand and Fleury-Feith 2005; Lecomte et al. 2005; Tan and Treasure 2005). Advances have been made in regards to treatment strategies in recent years, improving patient outcomes.

One therapeutic strategy is surgical resection of the tumor, involving extrapleural pneumonectomy to remove gross tumor regions followed by adjuvant therapies, typically radiotherapy, to kill any remaining cancerous tissue. However, this treatment is suitable for only certain cases of mesothelioma patients. Chemotherapeutic options for mesothelioma are currently not considered to be curative, but are used more for a palliative line of defense. (Robinson et al. 2005; Tan and Treasure 2005). Finally, a number of recent clinical trials using gene therapy have shown some promise in mesothelioma treatment. Because of their location and relative accessibility, mesothelioma tumors are considered to be a good tumor type for gene therapeutic options, as this therapy can be directly injected into the tumor to target the tumor cells. The challenge involved with this type of therapy is improving vector delivery systems to target tumor cells and also determining which genes, or types of genes, will serve to be most effective (van der Most et al. 2006).

Genomic analysis of mesotheliomas has revealed a series of related sub-chromosomal deleted regions and alterations, some of which are involved in loss of cell cycle regulation. Within these regions affected, TSGs are the type of genes most commonly affected. Included in these are *p16/INK4a* and *p14/ARF* on 9p, and *NF2* on 22q (Figure 4) (Jaurand and Fleury-Feith 2005; Musti et al. 2006; Andujar et al. 2007). Missing from the list of frequently mutated genes are *TP53* and *RB,* which is interesting as these genes are frequently found mutated in other types of human cancers (Toyooka et al. 2008).

FIGURE 4

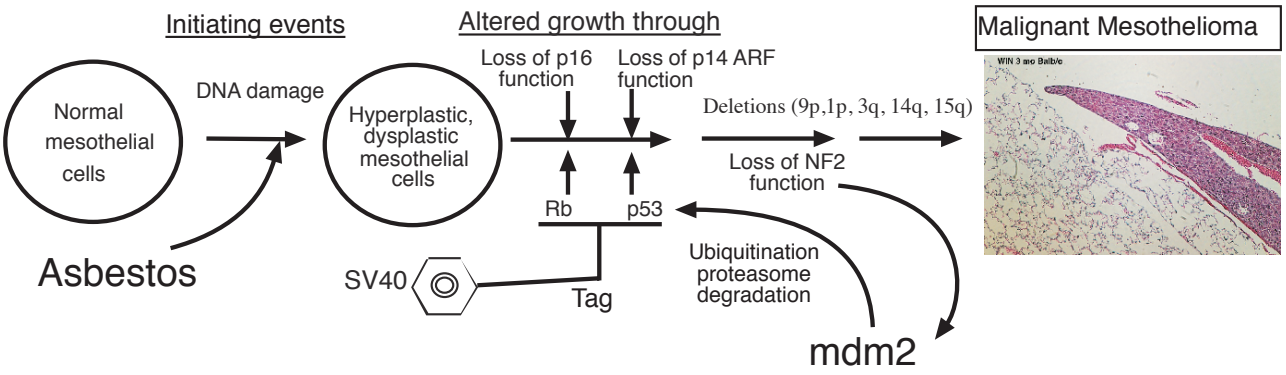

(Adapted from Murthy et al., 1999)

Figure 4. Model of mesothelioma genomic alterations.

This model is based on incidences of inactivating mutations in specific genes and genomic deletions found in human mesotheliomas. Commonly inactivated genes include p16, p14, and *NF2*. Interestingly, both *RB* and *p53* are rarely inactivated by mutation in malignant mesotheliomas. The model also includes SV40 interactions with p53, a known virus-gene interaction. While asbestos is considered the leading cause of mesothelioma tumor development, SV40 is also implicated in disease development.

A number of studies have been conducted focusing on the molecular mechanisms altered in relationship to the loss of genes that function upstream of these genes, in particular with regards to the effect that the loss of both *p16/INK4a* and *p14/ARF* might have on p53 and RB function, respectively (Lecomte et al. 2005). While there are known mechanisms whereby *p16/INK4a* and *p14/ARF* are involved with the regulation of p53 and RB, the role for *NF2* in regulation of these pathways has not been looked into as extensively. Most of the research into the role of *NF2* loss in mesothelioma tumors have focused on other pathways that the gene may be involved, but few have focused on mechanisms whereby it may interact with p53 or RB (Jung et al. 2005). The role of merlin in the regulation of these TSGs may be indirect, relaying extracellular growth signals to these downstream genes (Tsukita et al. 1994; Shaw et al. 1998b; McClatchey and Giovannini 2005).

Environmental exposures are thought to play a large role in the development of MPM tumors, with exposure to simian virus 40 (SV40), erionite, and asbestos fibers being implicated as possible causes (Carbone et al. 1999; Testa and Giordano 2001; Dogan et al. 2006; Carbone et al. 2007). Infection with SV40 has been linked to mesothelioma, brain tumors, non-Hodgkin's lymphoma, and osteosarcoma (Khalili et al. 2008). SV40 binds to and inhibits TSGs, in particular the major TSGs p53 and Rb. Many people were exposed to this oncogenic virus in the 1950s to1960s as it was a contaminant of some forms of polio vaccine (Shah 2006). The role of SV40 in mesothelioma development remains controversial, as many mesothelioma tumors are negative for SV40

infection (Aoe et al. 2006). More robust detection systems for the virus need to be developed to determine its role in carcinogenesis (Pershouse et al. 2006; Shah 2006). Erionite belongs to the zeolite group of minerals, and is considered the world's most carcinogenic mineral according to the World Health Organization (WHO), with a potency 200-1000 times greater than asbestos minerals (Carbone et al. 2002; Dogan et al. 2008). People in the Cappadocia region of Turkey were found to have a high rate of malignant mesothelioma, which was linked to erionite exposure (Dogan et al. 2006; Carbone et al. 2007). The leading cause of mesothelioma, however, is asbestos, with 80% of individuals diagnosed with the disease having had a prior documented asbestos exposure (Jaurand and Fleury-Feith 2005).

Asbestos

Asbestos is the name given to a group of fibrous silicate minerals. There are two main types of this fibrous minerals, chrysotile asbestos belongs to the serpentine family of minerals and the amphibole group, which is made up of crocidolite, tremolite, amosite, actinolite, and anthophyllite (ATSDR ; LaDou 2004). Both types of asbestos are naturally occurring in our environment, typically occurring as fiber bundles that consist of thin, separable fibers with a crystalline form. All six types of asbestos are considered hazardous to human health, with the general grouping of asbestos classified as a carcinogen (Gunter 1994; Lee et al. 2008).

The term “asbestos” is of Greek origin, meaning “unquenchable” or “inextinguishable.” These fibers were so named as they share properties of resistance to heat, chemical, and biological degradation. Virtually indestructible, asbestos has been used for centuries, dating as far back to 2000-4000 BC where it was used for the embalming of Egyptian Pharaohs (Tan and Treasure 2005). In the early 1870s, the mining of asbestos for commercial products began on a large scale, coinciding with the industrial revolution (Cugell and Kamp 2004). The flexible, fibrous shape, high tensile strength, inability to conduct electricity, thermal stability, resistance to chemical degradation, and high absorbency made asbestos a sought after element for use in commercial products (Ross et al. 2008). In fact, over 3,000 different asbestos-containing products exist, with 85% of these used in asbestos-cement construction products (LaDou 2004). However, some of these same properties that made asbestos so desirable for industrial use are also the same properties that contribute to its toxicity to human health.

Dormant and undisturbed, asbestos is relatively harmless. When the fibers separate and become airborne they can be easily inhaled. Once inhaled or swallowed, most fibers will be expelled from the body through mucous coating and cough, but those that become lodged in the lung, or elsewhere in the body, cause eventual health effects (ATSDR ; Miserocchi et al. 2008; Weiner and Neragi-Miandoab 2009). Dr J.C. Wagner first demonstrated a relationship between asbestos exposure and the development of mesotheliomas in 1960, postulating that the increase in mesothelioma in South Africa was linked to the

mining of crocidolite fibers (Wagner et al. 1960). Shortly after this discovery, reports of mesothelioma occurrences in the shipbuilding industry following WWII were linked with asbestos exposures (Sheers and Coles 1980). Since these first reports, an accumulating amount of evidence has followed linking the fibers to other asbestos-related diseases (ARDs), including pleural plaques, asbestosis, and lung cancer (ATSDR ; Sahn 1998).

The mechanism by which asbestos causes mesothelioma is not completely understood. One suggested mechanism is that asbestos generates an immune reaction, resulting in macrophage activation and asbestos phagocytosis. This results in a TNF-α mediated response in mesothelial cells, activating the NF-κB pathway, allowing mesothelial cells to be resistant to asbestos-induced apoptosis (Yang et al. 2008). A second method is through the generation of asbestos-induced reactive oxygen species, interfering with mesothelial cell homeostasis resulting in hyperplasia. A third suggestion is actual interference with mitosis, where asbestos might sever the mitotic spindle, resulting in aneuploidy and chromosomal alterations in daughter cells (Knudsen et al. 1989). Finally, constant irritation from fibers that become lodged in the pleural space can cause a continual damage/repair response from the mesothelial cells, leading to eventual uncontrolled cell growth (Figure 5) (Robinson et al. 2005; Weiner and Neragi-Miandoab 2009).

FIGURE 5

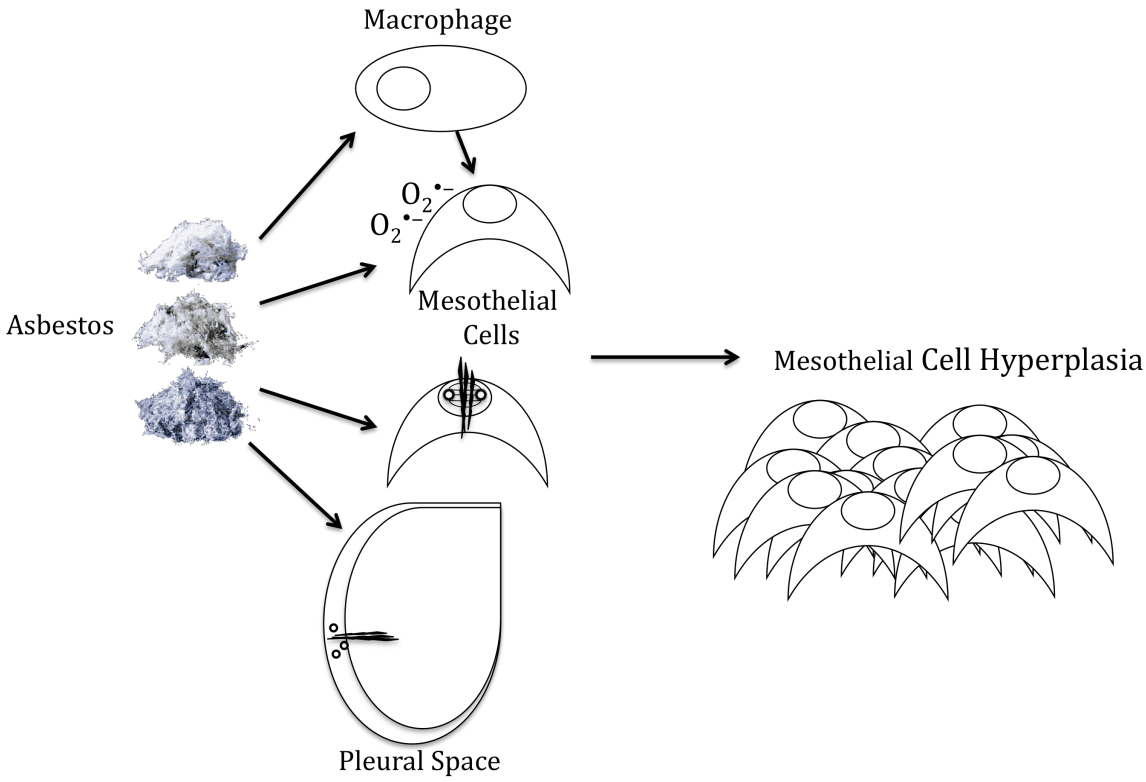
Macrophage
$O_2^{\bullet-}$
$O_2^{\bullet-}$
Asbestos
Mesothelial Cells
Mesothelial Cell Hyperplasia
Pleural Space

Figure 5. Suggested mechanisms for mesothelial cell tumorigenesis.

Mesothelial cell transformation following asbestos exposure is not completely understood. It could be that asbestos generates an immune reaction, resulting in macrophage activation and asbestos phagocytosis. This triggers in a TNF-α mediated response in mesothelial cells, activating the NF-κB pathway, allowing mesothelial cells to be resistant to asbestos-induced apoptosis. Another possibility is through the generation of asbestos-induced reactive oxygen species, interfering with mesothelial cell homeostasis resulting in hyperplasia. A third suggested mechanism is that asbestos might sever the mitotic spindle, resulting in aneuploidy and chromosomal alterations in daughter cells. Finally, fibers that become lodged in the pleural space can cause constant irritation, resulting in a continual damage/repair response from the mesothelial cells, leading to eventual uncontrolled cell growth.

Although asbestos use has been banned in many developed countries, it is not yet banned in all countries, including the United States. Considering that 95% of the asbestos mined and used today is chrysotile asbestos, this suggests that we are "safe." However, there is debate as to which asbestos fiber-types are the culprits for ARD manifestations. The majority of studies suggest that the amphiboles, namely crocidolite, are the cause of ARDs (Mossman 1993; Mossman et al. 1996; Cugell and Kamp 2004; Schneider et al. 2008). Some of these studies argue that chrysotile is relatively harmless as it can be easily cleared from the body. In contrast, numerous studies have shown that chrysotile is the more harmful fiber, with some groups indicating that it is even more toxic than the amphibole fibers (McDonald and Fry 1982; Churg et al. 1984; Huncharek 1987; Dunnigan 1988; Langer and Nolan 1989). Considering that many times these fibers are found mixed together, confounding the analysis, or that many of the studies involved a conflict of interest, it is difficult to draw conclusions as to which fibers are more prone to cause disease (Powers and Carbone 2002; Yang et al. 2008; Weiner and Neragi-Miandoab 2009).

As asbestos is the leading cause of MPM, it seems promising that its use and production have decreased over the last decade. However, in many developing countries asbestos use is not declining and will continue to create health problems in the future (Joshi and Gupta 2004). In addition, although some countries have banned the *use* of asbestos, they have not banned the *production* of the mineral for export as a commodity (Table 1) (Keith and Brophy 2004).

TABLE 1. Asbestos use in metric tons in 2003.

Region and Country		Production	Imports	Exports	Apparent Consumption
Africa					
Algeria		-	10,756	-	10,756
South Africa		6,218	1,470	4,192	3,496
Zimbabwe		147,000	1	99,262	5,000^
Other		-	7,386	377	9,158
	Total	153,218	21,944	103,831	28,642
Asia and the Middle East					
China		350,000	145,425	3,472	491,954
India		19,000	175,581	2,548	192,033
Iran		-	75,852	12	75,840
Thailand		-	133,110	127	132,983
Turkey		-	13,552	42	13,510
Other		-	159,120	-	159,013
	Total	369,000	702,640	6,307	1,065,333
Central and North America					
Canada		194,350	205	174,774	19,781
Cuba		-	9,896	-	9,896
Mexico		-	20,105	20	20,085
United States		-	4,634	3,548*	4,634#
Other		-	3,756	-	3,756
	Total	194,350	38,596	178,342	58,152
Europe					
Kazakhstan		354,500	3,340	18,349	173,891
Russia		878,000	1,050	450,031	429,020
Ukraine		-	156,393	-	156,393
Uzbekistan		-	42,362	-	42,362
Other		-	55,464	165,802	55,261
	Total	1,232,500	258,609	634,182	856,927
South America					
Brazil		194,350	28,395	144,343	78,403
Colombia		5,000	8,118	-	13,118
Other		-	4,573	-	4,739
	Total	199,516	41,086	144,343	96,260
Other		-	3,630	-	3,629
Grand Total		**2,148,584**	**1,066,566**	**1,067,006**	**2,108,943**

^ The calculated apparent consumption probably includes about 42, 739 tons going into stocks and 5,000 tons of estimated consumption.

* Includes exports and re-exports of asbestos fiber.

The apparent consumption is assumed to equal the imports.

(Adapted from the USGS 2003 Worldwide Asbestos Supply and Consumption Trend from 1900 through 2003 report)

According to Table 1, the total worldwide consumption of asbestos in 2003 was more than 2,000,000 tons. Because of this massive level of use, although these numbers have decreased from the peak of 4,360,000 tons used in the 1975 to 1977 time frame, the incidences of mesothelioma and other ARDs are going to continue to impact global health (Virta 2005). In fact, by 2020 it is predicted that the death rate from ARDs will be more than 5,000 deaths per year in the United Kingdom; the United States already exceeds that number with possibly more than 10,000 deaths per year attributed to ARDs. In Western Europe, an ARD epidemic is expected to take the lives of about 500,000 people before 2035 (Tweedale 2002). The best that we can do until the use of asbestos has stopped is continue to develop a better understanding of diseases manifestations that will result from exposure to the fibrous minerals, allowing for the design of more effective therapeutics.

Neurofibromatosis Type 2 (*NF2*)

Neurofibromatosis (NF) is a term used to describe two autosomal dominant disorders resulting in tumors of the central nervous system, NF1 and NF2 (Trofatter et al. 1993). Originally thought to be related diseases primarily because of a few clinical similarities (such as nerve sheath neoplasms) seen in patients of the two syndromes, it was later realized that these diseases are in fact distinct (Yohay 2006a). Both chromosomal location and the protein products of these two TSGs verified this fact (Trofatter et al. 1993; Gutmann 1997). The *NF1* gene is located on chromosome 17q11.2, and encodes a GTPase-activating

protein termed neurofibromin. The main function of neurofibromin as a TSG is thought to be inhibition of the proto-oncogene *Ras*. *NF2,* located on chromosome 22q12.2, encodes the 595 amino acid protein most commonly known as merlin. The exact mechanisms whereby merlin controls cell growth are not completely understood, but this protein does represent a new class of TSGs as it is thought to mediate cues from the cell membrane linking them to the cytoskeleton (Trofatter et al. 1993; Yohay 2006a).

Discovered in 1993, mutations in *NF2* are commonly associated with central nervous system tumors, including schwannomas of the eighth cranial nerve, meningiomas, and ependymomas (Rouleau et al. 1993; Trofatter et al. 1993; Baser et al. 2002; Johnson et al. 2002; Sun et al. 2002). In contrast to these normally benign tumors, *NF2* is also found inactivated by homozygous deletion mutations or loss of heterozygosity at a high frequency in malignant mesothelioma tumors (Martuza and Eldridge 1988; McClatchey 2003). Increasing evidence has shown that merlin contributes to tumor progression in many cancer types, including hepatocellular carcinoma and thyroid cancers, suggesting that the role of *NF2* in cell cycle control is more complex and broad than originally thought. As it turns out, merlin differs from the more typical TSGs in that it lacks a DNA-binding domain, instead sharing a more similar protein structure to the cytoskeleton-associated proteins and is thus considered to be a novel type of TSG (McClatchey and Giovannini 2005; Okada et al. 2007; Cole et al. 2008).

Merlin belongs to the Protein 4.1 superfamily of proteins, which have a large role in stabilization of the cellular membrane, as the members are largely involved in regulatory functions at the cell cortex. The Protein 4.1 superfamily contains over 40 members divided into five subgroups, all of which share a conserved FERM domain (*f*our.1 protein, *e*zri*n*, *r*adixin, *m*oesin) (Sun et al. 2002). Merlin is most closely related to the ERM subgroup (comprised of *e*zrin, *r*adixin, and *m*oesin), with the similarity of sharing 3 functional domains (Gutmann 1997; Yohay 2006b). These domains include a carboxy-terminal domain, an α-helical domain, and the FERM domain located in the N-terminal region of the protein. Although the C-terminal domain is more distantly related, merlin shares 63% homology to the clover-leafed FERM domain of the ERMs, and for this reason, the name "merlin" arose from the members of this group: *m*oesin-*e*zrin-*r*adixin-*l*ike prote*in* (Trofatter et al. 1993; Gautreau et al. 2002). The sequence similarities shared between merlin and the ERMs suggests that ability of merlin to regulate cell growth may be by functioning in a similar manner as the ERMs (Gutmann 1997).

The ERMs are thought to be linkers between the membrane and the cortical actin cytoskeleton (Cole et al. 2008). Merlin and the ERMs form intramolecular and intermolecular loops through interactions between the FERM and C-terminal domains. Differential function of the ERMs is dependent upon their phosphorylation status, creating secondary structures of the proteins to cycle between a closed and an open loop form. Hypo-phosphorylated ERMs result in a closed conformation, and are thought to be inactive. Phosphorylation

results in ERM activation, and has been shown to control cell morphology, adhesion, and motility, as well as the transduction of growth signals for both cell proliferation and cell survival (Gautreau et al. 2002; Sun et al. 2002). Like the ERMs, many groups have suggested that merlin is also conformationally regulated (McClatchey and Giovannini 2005; Yohay 2006b). In contrast to the ERMs, it is the hypo-phosphorylated, closed form of merlin that is considered *active*, as dephosphorylation of the protein results in membrane localization and suppression of cell growth (McClatchey 2003).

As the ERMs and merlin have been shown to share binding partners and even have been shown to interact with each other heterotypically, functional overlap is thought to occur between the proteins (McClatchey 2003). With this in mind, merlin membrane-cytoskeleton interactions have been linked to contact inhibition of growth in many different cell types (Morrison et al. 2001; Shaw et al. 2001; Lallemand et al. 2003; Curto et al. 2007; Cole et al. 2008). Although merlin and the ERMs do have some functional overlap, merlin does have many properties that are distinct from the ERMs. The only member of the ERM family that is considered a TSG, inactivation of merlin not only results in loss of cell:cell contact inhibition of growth, it is also suggested to have an effect on cell proliferation, oncogenic-induced transformation, and apoptotic response (Sainio et al. 1997; Gutmann et al. 1999; Morrison et al. 2001; Shaw et al. 2001; Sherman and Gutmann 2001; Lallemand et al. 2003; McClatchey and Giovannini 2005; Xiao et al. 2005; Curto and McClatchey 2008). Each of these phenotypic

changes are examples of loss of cell cycle control and can ultimately lead to a tumor formation.

Merlin is activated *in vitro* by dephosphorylation during conditions such as high cell density, serum deprivation, or addition of hyaluronic acid, causing localization to the cell membrane (Shaw et al. 1998b; Okada et al. 2007). At the cell membrane, merlin reportedly interacts with a number of proteins that have roles in growth factor receptor signaling, which could provide insight into the role of merlin in signal trafficking to control cell growth (McClatchey and Giovannini 2005).

At the membrane, merlin interactions include localization to adherens junctions and cell membrane receptors, such as CD44, to inhibit cell growth (Sherman et al. 1997; Shaw et al. 1998a; Shaw et al. 1998b; Cole et al. 2008; Curto and McClatchey 2008). Adherens junctions belong to the cadheren family, and form between interacting plasma membranes, prototypically of epithelial cells, creating a link between the cells through actin bundles (Alberts et al. 2002). CD44 and merlin may function together to inhibit growth as intracellular distance increases. Hyaluronic acid signaling through CD44 may induce changes in the phosphorylation status of merlin, thus affecting merlin activity (Morrison et al. 2001). Other possible roles for *NF2* in maintaining normal cellular growth may be through many possible signal transduction mechanisms, including interactions with Rac/PAK signaling, Cyclin D1, and Mouse Double Minute 2 (MDM2) (Tsukita et al. 1994; Sainio et al. 1997; Morrison et al. 2001). Because of the vast majority of cellular processes that are affected by the loss of function of this gene in

various cell types, it seems reasonable to suggest that under pathological conditions its inactivation could result in loss of cell cycle control, ultimately leading to tumor formation (Figure 6).

FIGURE 6

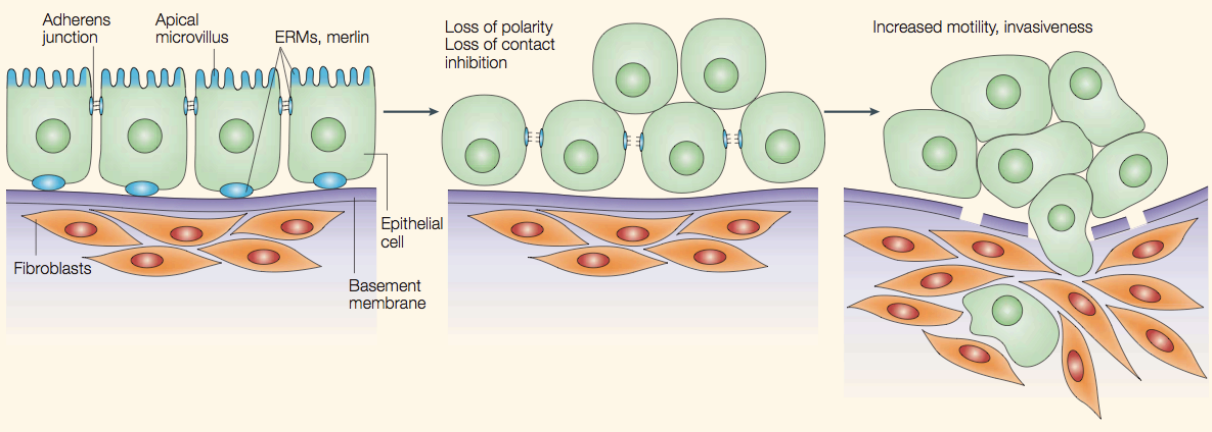

(McClatchey 2003)

Figure 6. Merlin localization and potential role in cancer.

Merlin localization to adherens junctions and cell:cell boundaries suggests that loss of the protein can contribute to cancer formation through loss of cell:cell communication. In addition, inactivation of the TSG, *NF2*, can contribute to metastatic potential through a decreased response to contact inhibition of growth and thus increased cell motility.

Localized to the cell membrane after activation, *NF2* may act upstream of p53 by helping to maintain function of the gene under normal growth conditions. Kim et al. (2004) showed that NF2 played a role in MDM2 degradation in mouse fibroblast 3T3 cells. Involved in an autoregulatory feedback loop with p53, MDM2 is responsible for degradation of the genome gatekeeper, so increases in expression of the MDM2 protein could be detrimental to p53 stability. If merlin is involved in MDM2 degradation in other cells types, loss of *NF2* could contribute to an increase in MDM2 and thus increased p53 degradation, thereby a diminished ability of p53 to function following DNA stress.

TP53

The role of the transcription factor p53 in cancer development has been widely characterized. Considered the "Guardian of the Genome," p53 plays a key role in maintaining genomic integrity by serving as a cell-cycle checkpoint (Lane 1992; Levine 1997). Under normal cellular growth conditions, p53 is kept at low-steady state levels. In response to stress, p53 is activated and acts as a transcription factor for many downstream targets, and is capable of initiating several protective pathways. UV radiation, hypoxic conditions, and overexpression of oncogenes are examples of cellular stressors that are capable of inducing p53 activity (Vogelstein et al. 2000). Depending on the type of stress, p53 is activated through mechanisms like phosphorylation or acetylation, and it is rapidly stabilized to activate downstream targets. These pathways include, but are not limited to the induction of cell-cycle arrest, DNA repair mechanisms, and

apoptosis (Gottlieb and Oren 1998; Vogelstein and Kinzler 2004; Poon et al. 2007). For example, p53 initiates cell cycle arrest following DNA damage through the upregulation of p21, a member of the CDK family of cell cycle inhibitors known as an early cell cycle response molecule (Toledo and Wahl 2006). When damage is severe, p53 is a direct transcription factor for the pro-apoptotic member of the Bcl-2 family member, Bax (Miyashita and Reed 1995; Gottlieb and Oren 1998; Kelekar and Thompson 1998). Thus, loss of p53 either through mutation or inactivation through other means can be critical for the developing cancer cell.

While *TP53* is mutated in ~50% of human cancers, in those cancers where the p53 gene is not directly mutated other mechanisms might contribute to aberrant p53 function. For example, the large T-antigen of the SV40 virus is thought to bind to both p53 and RB, inhibiting the ability of the TSGs to respond properly to DNA stress signals (Ludlow 1993; Pershouse et al. 2006; Khalili et al. 2008). Another method of wild-type p53 instability might be through the loss of other TSGs that act upstream of the gatekeeper helping to maintain its function (Chin et al. 1998; Pomerantz et al. 1998; Zhang et al. 1998; Oren 1999). Under normal conditions for cell growth, p53 levels are largely controlled through interactions with MDM2 (Brooks and Gu 2006). Following cellular stress, p53 is activated and stabilized, thereby disrupting the ability of MDM2 to bind to the protein. If protein levels are not controlled, p53 over-activity in normal cells can result in cell death. This is apparent in MDM2-deficient mice which are embryonic lethal, whereas inactivation of both MDM2 and p53 to produce double

null mice rescues this effect (Joseph and Moll 2003). Thus, to control its own activity, p53 forms an auto-regulatory feedback loop with MDM2, acting as a direct transcription factor for the ubiquitin ligase, which in turn attaches ubiquitin molecules to p53 stimulating its degradation by the proteasome (Figure 7).

FIGURE 7

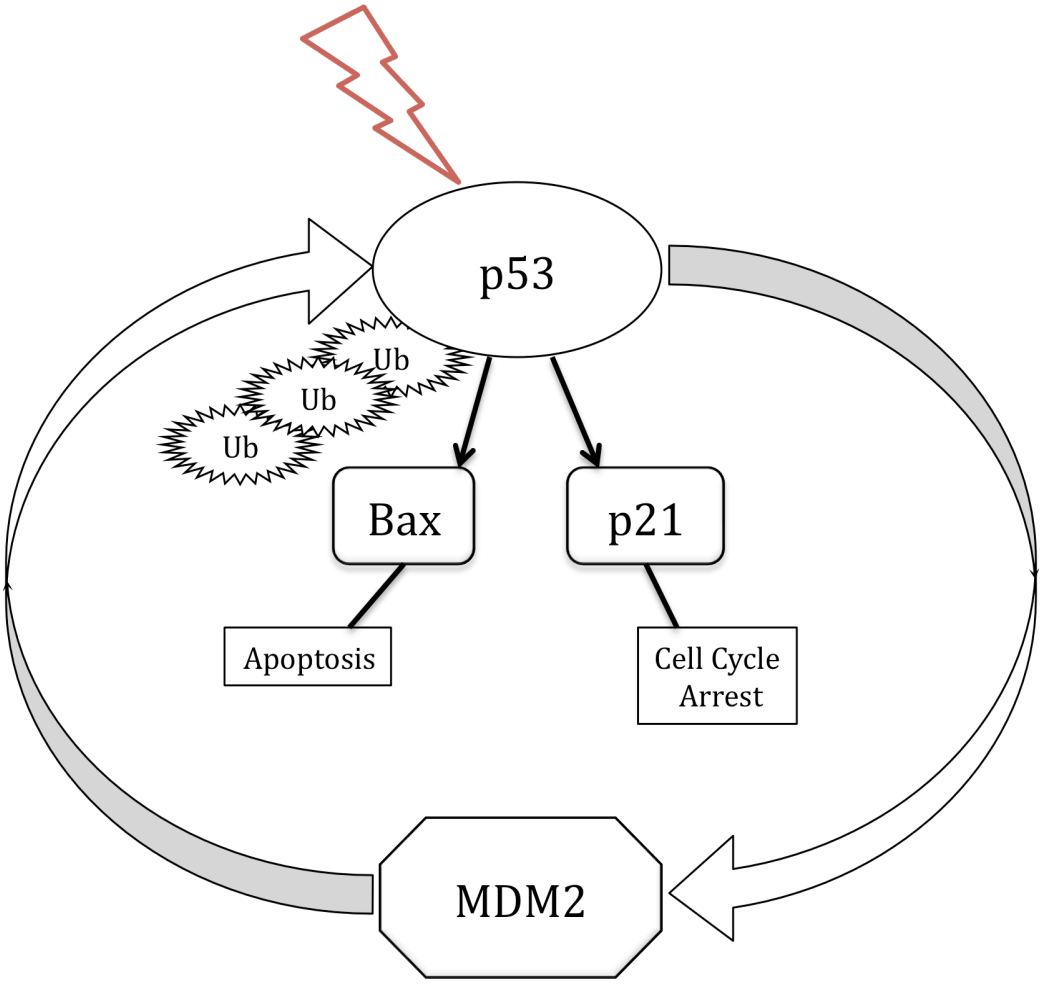

Figure 7. Example of p53 function and autoregulation following DNA damage.

After a DNA damaging event, p53 is activated to induce activities like cell-cycle arrest through the induction of p21, or if damage is more severe, p53 will activate apoptosis through the transcription of the pro-apoptotic Bcl2 family member, Bax. When p53 has carried out its protective role, it acts as a transcription factor for MDM2, which ubiquitinates the protein tagging it for proteosome degradation.

Besides inactivation by mutation, another method for decreased p53 function could be through oncogene activation that negatively regulates p53, such as can happen with MDM2. Because of the ability of the E3 ubiquitin ligase MDM2 to negatively regulate p53, MDM2 is sometimes considered to have oncogenic properties and was recently reported to be overexpressed in about 10.5% of human cancers (Michael and Oren 2002; Toledo and Wahl 2006). In fact, because of the role that MDM2 plays in p53 regulation, MDM2 has become a therapeutic target with a focus on liberation of p53 from degradation in cancers where p53 remains wild-type. Molecules that specifically target MDM2, such as small molecule inhibitors, like HLI98, are being tested *in vitro* for their therapeutic potential. The nutlins are antagonists of MDM2, and can disrupt the MDM2-p53 binding (Vassilev 2007; Shangary and Wang 2008). Studies have shown that expression of such molecules can restore the function of p53. In addition, the restoration of TSGs that act upstream of p53 through interactions with MDM2 provide gene therapeutic targets. The TSG p14/*ARF* binds to and inhibits the activity of MDM2, thereby stabilizing p53 activity (Sherr 2001). Gene therapy to re-express p14/ARF is of particular importance in the context of mesothelioma, as *p14/ARF* is often inactivated in this tumor type (Figure 4). The use of this therapy, in combination with the re-expression of other TSGs that regulate MDM2, like *NF2*, could achieve restoration of p53 function resulting in anticancer activity.

Of the common chromosomal regions commonly altered in malignant mesotheliomas (Figure 4), absent from the list is chromosome 17p, the region

that harbors *TP53* (Murthy and Testa 1999; Jaurand and Fleury-Feith 2005). Considering that the majority of mesotheliomas retain wild-type p53, the question becomes whether or not this wild-type p53 can still function properly. If enough alterations in genes that help to maintain p53 activity and function take place, it is quite possible that p53 is unable to act as a cell cycle regulator in these tumors. The critical role of p53 is made evident not only by genetic mutations present in over half of all human cancers, but also because of its critical role in host/tumor response to cancer treatments like radiation and chemotherapy (Lane and Fischer 2004). A complete understanding of the regulators of p53 function is essential for the development of more effective treatment strategies for cancer (Toledo and Wahl 2006).

Hypothesis

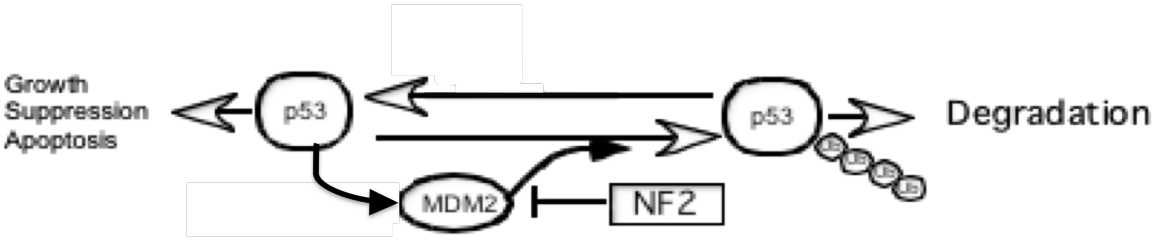

The hypothesis of this study is that inactivation of *NF2* plays a critical role in cellular growth deregulation by altering normal regulation of MDM2 and thus p53 levels. This hypothesis was tested through the following specific aims:

Specific Aim 1: Analyze the role of the *NF2* gene in regulating p53 function and cellular growth in "normal" mesothelial cells and mesothelioma cell culture models. Normal function of merlin was restored by transfection of a wild-type *NF2* construct in a mesothelioma cell culture model. Merlin function was reduced in non-cancerous mesothelial cells by shRNA knockdown.

Specific Goal 2: Analyze the role of the *NF2* gene in an *in vivo* model of pleural mesothelioma development. A heterozygous *NF2* knockout mouse model was used to follow closely the early events in tumor development. *NF2* status, time to tumor development, phenotypic and p53-related gene expression changes were monitored.

References

Alberts, B., Johnson, A., Lewis, J., Raff, M., Roberts, K., and Walter, P. 2002. Cell Junctions, Cell Adhesion, and the Extracellular Matrix. in *Molecular Biology of the Cell* (ed. S. Gibbs), pp. 1065-1075. Taylor & Francis Group, New York.

Altomare, D.A., Vaslet, C.A., Skele, K.L., De Rienzo, A., Devarajan, K., Jhanwar, S.C., McClatchey, A.I., Kane, A.B., and Testa, J.R. 2005. A mouse model recapitulating molecular features of human mesothelioma. *Cancer Res* **65**(18): 8090-8095.

Andujar, P., Lecomte, C., Renier, A., Fleury-Feith, J., Kheuang, L., Daubriac, J., Janin, A., and Jaurand, M.C. 2007. Clinico-pathological features and somatic gene alterations in refractory ceramic fibre-induced murine mesothelioma reveal mineral fibre-induced mesothelioma identities. *Carcinogenesis* **28**(7): 1599-1605.

Aoe, K., Hiraki, A., Murakami, T., Toyooka, S., Shivapurkar, N., Gazdar, A.F., Sueoka, N., Taguchi, K., Kamei, T., Takeyama, H., Sugi, K., and Kishimoto, T. 2006. Infrequent existence of simian virus 40 large T antigen DNA in malignant mesothelioma in Japan. *Cancer Sci* **97**(4): 292-295.

Armitage, P. and Doll, R. 1954. The age distribution of cancer and a multi-stage theory of carcinogenesis. *Br J Cancer* **8**(1): 1-12.

ATSDR. Agency for Toxic Substances and Disease Registry: Public Health Statement--Asbestos. In.

Baser, M.E., De Rienzo, A., Altomare, D., Balsara, B.R., Hedrick, N.M., Gutmann, D.H., Pitts, L.H., Jackler, R.K., and Testa, J.R. 2002. Neurofibromatosis 2 and malignant mesothelioma. *Neurology* **59**(2): 290-291.

Brooks, C.L. and Gu, W. 2006. p53 ubiquitination: Mdm2 and beyond. *Mol Cell* **21**(3): 307-315.

Carbone, M., Emri, S., Dogan, A.U., Steele, I., Tuncer, M., Pass, H.I., and Baris, Y.I. 2007. A mesothelioma epidemic in Cappadocia: scientific developments and unexpected social outcomes. *Nat Rev Cancer* **7**(2): 147-154.

Carbone, M., Fisher, S., Powers, A., Pass, H.I., and Rizzo, P. 1999. New molecular and epidemiological issues in mesothelioma: role of SV40. *J Cell Physiol* **180**(2): 167-172.

Carbone, M., Kratzke, R.A., and Testa, J.R. 2002. The pathogenesis of mesothelioma. *Semin Oncol* **29**(1): 2-17.

Chin, L., Pomerantz, J., and DePinho, R.A. 1998. The INK4a/ARF tumor suppressor: one gene--two products--two pathways. *Trends Biochem Sci* **23**(8): 291-296.

Churg, A., Wiggs, B., Depaoli, L., Kampe, B., and Stevens, B. 1984. Lung asbestos content in chrysotile workers with mesothelioma. *Am Rev Respir Dis* **130**(6): 1042-1045.

Cole, B.K., Curto, M., Chan, A.W., and McClatchey, A.I. 2008. Localization to the cortical cytoskeleton is necessary for Nf2/merlin-dependent epidermal growth factor receptor silencing. *Mol Cell Biol* **28**(4): 1274-1284.

Croce, C.M. 2008. Oncogene and Cancer. *The New England Journal of Medicine* **358**: 502-511.

Cugell, D.W. and Kamp, D.W. 2004. Asbestos and the pleura: a review. *Chest* **125**(3): 1103-1117.

Curto, M., Cole, B.K., Lallemand, D., Liu, C.H., and McClatchey, A.I. 2007. Contact-dependent inhibition of EGFR signaling by Nf2/Merlin. *J Cell Biol* **177**(5): 893-903.

Curto, M. and McClatchey, A.I. 2008. Nf2/Merlin: a coordinator of receptor signalling and intercellular contact. *Br J Cancer* **98**(2): 256-262.

Dogan, A.U., Baris, Y.I., Dogan, M., Emri, S., Steele, I., Elmishad, A.G., and Carbone, M. 2006. Genetic predisposition to fiber carcinogenesis causes a mesothelioma epidemic in Turkey. *Cancer Res* **66**(10): 5063-5068.

Dogan, A.U., Dogan, M., and Hoskins, J.A. 2008. Erionite series minerals: mineralogical and carcinogenic properties. *Environ Geochem Health* **30**(4): 367-381.

Dunitz, M. 2002. *Mesothelioma*. Taylor & Francis, London.

Dunnigan, J. 1988. Linking chrysotile asbestos with mesothelioma. *Am J Ind Med* **14**(2): 205-209.

Evan, G. and Vousden, K.H. 2001. Proliferation, cell cycle and apoptosis in cancer *Nature* **411**(17): 342-348.

Gautreau, A., Louvard, D., and Arpin, M. 2002. ERM proteins and NF2 tumor suppressor: the Yin and Yang of cortical actin organization and cell growth signaling. *Curr Opin Cell Biol* **14**(1): 104-109.

Gottlieb, T.M. and Oren, M. 1998. p53 and apoptosis. *Semin Cancer Biol* **8**(5): 359-368.

Gunter, M. 1994. Asbestos as a metaphor for teaching risk perception. *Journal of Geoligical Education* **42**: 17-24.

Gutmann, D.H. 1997. Molecular insights into neurofibromatosis 2. *Neurobiol Dis* **3**(4): 247-261.

Gutmann, D.H., Sherman, L., Seftor, L., Haipek, C., Hoang Lu, K., and Hendrix, M. 1999. Increased expression of the NF2 tumor suppressor gene product, merlin, impairs cell motility, adhesionand spreading. *Hum Mol Genet* **8**(2): 267-275.

Hanahan, D. and Weinberg, R.A. 2000. The Hallmarks of Cancer. *Cell* **100**: 57-70.

Hodgson, J.T., McElvenny, D.M., Darnton, A.J., Price, M.J., and Peto, J. 2005. The expected burden of mesothelioma mortality in Great Britain from 2002 to 2050. *Br J Cancer* **92**(3): 587-593.

Huncharek, M. 1987. Chrysotile asbestos exposure and mesothelioma. *Br J Ind Med* **44**(4): 287-288.

Jaurand, M.C. and Fleury-Feith, J. 2005. Pathogenesis of malignant pleural mesothelioma. *Respirology* **10**(1): 2-8.

Johansson, M. and Persson, J.L. 2008. Cancer therapy: targeting cell cycle regulators. *Anticancer Agents Med Chem* **8**(7): 723-731.
Johnson, K.C., Kissil, J.L., Fry, J.L., and Jacks, T. 2002. Cellular transformation by a FERM domain mutant of the Nf2 tumor suppressor gene. *Oncogene* **21**(39): 5990-5997.
Joseph, T.W. and Moll, U.M. 2003. Analysis of nuclear and cytoplasmic degradation of p53 in cells after stress. *Methods Mol Biol* **234**: 211-217.
Joshi, T.K. and Gupta, R.K. 2004. Asbestos in developing countries: magnitude of risk and its practical implications. *Int J Occup Med Environ Health* **17**(1): 179-185.
Jung, J.R., Kim, H., Jeun, S.S., Lee, J.Y., Koh, E.J., and Ji, C. 2005. The Phosphorylation status of merlin is important for regulating the Ras-ERK pathway. *Mol Cells* **20**(2): 196-200.
Keith, M.M. and Brophy, J.T. 2004. Participatory mapping of occupational hazards and disease among asbestos-exposed workers from a foundry and insulation complex in Canada. *Int J Occup Environ Health* **10**(2): 144-153.
Kelekar, A. and Thompson, C.B. 1998. Bcl-2-family proteins: the role of the BH3 domain in apoptosis. *Trends Cell Biol* **8**(8): 324-330.
Khalili, K., Sariyer, I.K., and Safak, M. 2008. Small tumor antigen of polyomaviruses: role in viral life cycle and cell transformation. *J Cell Physiol* **215**(2): 309-319.
Kim, H., Kwak, N.J., Lee, J.Y., Choi, B.H., Lim, Y., Ko, Y.J., Kim, Y.H., Huh, P.W., Lee, K.H., Rha, H.K., and Wang, Y.P. 2004. Merlin neutralizes the inhibitory effect of Mdm2 on p53. *J Biol Chem* **279**(9): 7812-7818.
Knudsen, N., Block, K., and Schulman, S. 1989. Malignant pleural mesothelioma. *Oncol Nurs Forum* **16**(6): 845-851.
Kumar, P. and Kratzke, R.A. 2005. Molecular prognostic markers in malignant mesothelioma. *Lung Cancer* **49 Suppl 1**: S53-60.
LaDou, J. 2004. The asbestos cancer epidemic. *Environ Health Perspect* **112**(3): 285-290.
Lallemand, D., Curto, M., Saotome, I., Giovannini, M., and McClatchey, A.I. 2003. NF2 deficiency promotes tumorigenesis and metastasis by destabilizing adherens junctions. *Genes Dev* **17**(9): 1090-1100.
Lane, D.P. 1992. Cancer. p53, guardian of the genome. *Nature* **358**(6381): 15-16.
Lane, D.P. and Fischer, P.M. 2004. Turning the key on p53. *Nature* **427**(6977): 789-790.
Langer, A.M. and Nolan, R.P. 1989. Fibre type and burden in parenchymal tissues of workers occupationally exposed to asbestos in the United States. *IARC Sci Publ*(90): 330-335.
Lecomte, C., Andujar, P., Renier, A., Kheuang, L., Abramowski, V., Mellottee, L., Fleury-Feith, J., Zucman-Rossi, J., Giovannini, M., and Jaurand, M.C. 2005. Similar tumor suppressor gene alteration profiles in asbestos-induced murine and human mesothelioma. *Cell Cycle* **4**(12): 1862-1869.

Lee, R.J., Strohmeier, B.R., Bunker, K.L., and Van Orden, D.R. 2008. Naturally occurring asbestos: a recurring public policy challenge. *J Hazard Mater* **153**(1-2): 1-21.
Levine, A.J. 1997. p53, the cellular gatekeeper for growth and division. *Cell* **88**(3): 323-331.
Ludlow, J.W. 1993. Interactions between SV40 large-tumor antigen and the growth suppressor proteins pRB and p53. *FASEB J* **7**(10): 866-871.
Martuza, R.L. and Eldridge, R. 1988. Neurofibromatosis 2 (bilateral acoustic neurofibromatosis). *N Engl J Med* **318**(11): 684-688.
May, P. and May, E. 1999. Twenty years of p53 research: structural and functional aspects of the p53 protein. *Oncogene* **18**(53): 7621-7636.
McClatchey, A.I. 2003. Merlin and ERM proteins: unappreciated roles in cancer development? *Nat Rev Cancer* **3**(11): 877-883.
McClatchey, A.I. and Giovannini, M. 2005. Membrane organization and tumorigenesis--the NF2 tumor suppressor, Merlin. *Genes Dev* **19**(19): 2265-2277.
McDonald, A.D. and Fry, J.S. 1982. Mesothelioma and the fiber type in three American asbestos factories - preliminary report. *Scand J Work Environ Health* **8 Suppl 1**: 53-58.
Michael, D. and Oren, M. 2002. The p53 and Mdm2 families in cancer. *Curr Opin Genet Dev* **12**(1): 53-59.
Minamoto, T., Mai, M., and Ronai, Z. 1999. Environmental factors as regulators and effectors of multistep carcinogenesis. *Carcinogenesis* **20**(4): 519-527.
Miserocchi, G., Sancini, G., Mantegazza, F., and Chiappino, G. 2008. Translocation pathways for inhaled asbestos fibers. *Environ Health* **7**: 4.
Miyashita, T. and Reed, J.C. 1995. Tumor suppressor p53 is a direct transcriptional activator of the human bax gene. *Cell* **80**(2): 293-299.
Morrison, H., Sherman, L.S., Legg, J., Banine, F., Isacke, C., Haipek, C.A., Gutmann, D.H., Ponta, H., and Herrlich, P. 2001. The NF2 tumor suppressor gene product, merlin, mediates contact inhibition of growth through interactions with CD44. *Genes Dev* **15**(8): 968-980.
Mossman, B.T. 1993. Mechanisms of asbestos carcinogenesis and toxicity: the amphibole hypothesis revisited. *Br J Ind Med* **50**(8): 673-676.
Mossman, B.T., Kamp, D.W., and Weitzman, S.A. 1996. Mechanisms of carcinogenesis and clinical features of asbestos-associated cancers. *Cancer Invest* **14**(5): 466-480.
Murthy, S.S. and Testa, J.R. 1999. Asbestos, chromosomal deletions, and tumor suppressor gene alterations in human malignant mesothelioma. *J Cell Physiol* **180**(2): 150-157.
Musti, M., Kettunen, E., Dragonieri, S., Lindholm, P., Cavone, D., Serio, G., and Knuutila, S. 2006. Cytogenetic and molecular genetic changes in malignant mesothelioma. *Cancer Genet Cytogenet* **170**(1): 9-15.
Mutsaers, S.E. 2002. Mesothelial cells: their structure, function and role in serosal repair. *Respirology* **7**(3): 171-191.
-. 2004. The mesothelial cell. *Int J Biochem Cell Biol* **36**(1): 9-16.

Mutsaers, S.E., Whitaker, D., and Papadimitriou, J.M. 2000. Mesothelial regeneration is not dependent on subserosal cells. *J Pathol* **190**(1): 86-92.
Okada, T., You, L., and Giancotti, F.G. 2007. Shedding light on Merlin's wizardry. *Trends Cell Biol* **17**(5): 222-229.
Oren, M. 1999. Regulation of the p53 tumor suppressor protein. *J Biol Chem* **274**(51): 36031-36034.
Pershouse, M.A., Heivly, S., and Girtsman, T. 2006. The role of SV40 in malignant mesothelioma and other human malignancies. *Inhal Toxicol* **18**(12): 995-1000.
Pomerantz, J., Schreiber-Agus, N., Liegeois, N.J., Silverman, A., Alland, L., Chin, L., Potes, J., Chen, K., Orlow, I., Lee, H.W., Cordon-Cardo, C., and DePinho, R.A. 1998. The Ink4a tumor suppressor gene product, p19Arf, interacts with MDM2 and neutralizes MDM2's inhibition of p53. *Cell* **92**(6): 713-723.
Poon, G.M., Brokx, R.D., Sung, M., and Gariepy, J. 2007. Tandem dimerization of the human p53 tetramerization domain stabilizes a primary dimer intermediate and dramatically enhances its oligomeric stability. *J Mol Biol* **365**(4): 1217-1231.
Powers, A. and Carbone, M. 2002. The role of environmental carcinogens, viruses and genetic predisposition in the pathogenesis of mesothelioma. *Cancer Biol Ther* **1**(4): 348-353.
Robinson, B.W., Musk, A.W., and Lake, R.A. 2005. Malignant mesothelioma. *Lancet* **366**(9483): 397-408.
Ross, M., Langer, A.M., Nord, G.L., Nolan, R.P., Lee, R.J., Van Orden, D., and Addison, J. 2008. The mineral nature of asbestos. *Regul Toxicol Pharmacol* **52**(1 Suppl): S26-30.
Rotter, V., Aloni-Grinstein, R., Schwartz, D., Elkind, N.B., Simons, A., Wolkowicz, R., Lavigne, M., Beserman, P., Kapon, A., and Goldfinger, N. 1994. Does wild-type p53 play a role in normal cell differentiation? *Semin Cancer Biol* **5**(3): 229-236.
Rouleau, G.A., Merel, P., Lutchman, M., Sanson, M., Zucman, J., Marineau, C., Hoang-Xuan, K., Demczuk, S., Desmaze, C., Plougastel, B., and et al. 1993. Alteration in a new gene encoding a putative membrane-organizing protein causes neuro-fibromatosis type 2. *Nature* **363**(6429): 515-521.
Rous, P. and Friedewald, W.F. 1941. The Carcinogenic Effect of Methylcholanthrene and of Tar on Rabbit Papillomas Due to a Virus. *Science* **94**(2447): 495-496.
Rusch, V.W. 1995. Clinical features and current treatment of diffuse malignant pleural mesothelioma. *Lung Cancer* **12 Suppl 2**: S127-146.
Sahn, S.A. 1998. Pleural Anatomy, Physiology, and Diagnostic Procedures. in *Textbook of Pulmonary Diseases* (ed. G.L. Baum, J.D. Crapo, B.R. Celli, and J.B. Karlinsky), pp. 255-265. Lippincott-Raven Publishers, Philadelphia.
Sainio, M., Zhao, F., Heiska, L., Turunen, O., den Bakker, M., Zwarthoff, E., Lutchman, M., Rouleau, G.A., Jaaskelainen, J., Vaheri, A., and Carpen, O. 1997. Neurofibromatosis 2 tumor suppressor protein colocalizes with ezrin

and CD44 and associates with actin-containing cytoskeleton. *J Cell Sci* **110 (Pt 18)**: 2249-2260.
Schneider, F., Sporn, T.A., and Roggli, V.L. 2008. Crocidolite and mesothelioma. *Ultrastruct Pathol* **32**(5): 171-177.
Shackelford, R.E., Kaufmann, W.K., and Paules, S.P. 1999. Cell Ceycle Control, Checkpoint Mechansisms, and Genotoxic Strees. *Environmental Health Perspectives* **107**: 5-24.
Shah, K.V. 2006. SV40 and human cancer: A review of recent data. *International Journal of Cancer* **120**: 215-223.
Shangary, S. and Wang, S. 2008. Targeting the MDM2-p53 interaction for cancer therapy. *Clin Cancer Res* **14**(17): 5318-5324.
Shaw, R.J., McClatchey, A.I., and Jacks, T. 1998a. Localization and functional domains of the neurofibromatosis type II tumor suppressor, merlin. *Cell Growth Differ* **9**(4): 287-296.
-. 1998b. Regulation of the neurofibromatosis type 2 tumor suppressor protein, merlin, by adhesion and growth arrest stimuli. *J Biol Chem* **273**(13): 7757-7764.
Shaw, R.J., Paez, J.G., Curto, M., Yaktine, A., Pruitt, W.M., Saotome, I., O'Bryan, J.P., Gupta, V., Ratner, N., Der, C.J., Jacks, T., and McClatchey, A.I. 2001. The Nf2 tumor suppressor, merlin, functions in Rac-dependent signaling. *Dev Cell* **1**(1): 63-72.
Sheers, G. and Coles, R.M. 1980. Mesothelioma risks in a naval dockyard. *Arch Environ Health* **35**(5): 276-282.
Sherman, L., Jacoby, L.B., Lampe, J., Pelton, P., Aguzzi, A., Herrlich, P., and Ponta, H. 1997. CD44 expression is aberrant in benign Schwann cell tumors possessing mutations in the neurofibromatosis type 2, but not type 1, gene. *Cancer Res* **57**(21): 4889-4897.
Sherman, L.S. and Gutmann, D.H. 2001. Merlin: hanging tumor suppression on the Rac. *Trends Cell Biol* **11**(11): 442-444.
Sherr, C.J. 2001. The INK4a/ARF network in tumour suppression. *Nat Rev Mol Cell Biol* **2**(10): 731-737.
Sugimura, T., Terada, M., Yokota, J., Hirohashi, S., and Wakabayashi, K. 1992. Multiple genetic alterations in human carcinogenesis. *Environ Health Perspect* **98**: 5-12.
Sun, C.X., Robb, V.A., and Gutmann, D.H. 2002. Protein 4.1 tumor suppressors: getting a FERM grip on growth regulation. *J Cell Sci* **115**(Pt 21): 3991-4000.
Tachibana, K.E., Gonzalez, M.A., and Coleman, N. 2005. Cell-cycle-dependent regulation of DNA replication and its relevance to cancer pathology. *J Pathol* **205**(2): 123-129.
Tan, C. and Treasure, T. 2005. Mesothelioma: time to take stock. *J R Soc Med* **98**(10): 455-458.
Testa, J.R. and Giordano, A. 2001. SV40 and cell cycle perturbations in malignant mesothelioma. *Semin Cancer Biol* **11**(1): 31-38.
Toledo, F. and Wahl, G.M. 2006. Regulating the p53 pathway: in vitro hypotheses, in vivo veritas. *Nat Rev Cancer* **6**(12): 909-923.

Toyooka, S., Kishimoto, T., and Date, H. 2008. Advances in the molecular biology of malignant mesothelioma. *Acta Med Okayama* **62**(1): 1-7.
Treasure, T. and Sedrakyan, A. 2004. Pleural mesothelioma: little evidence, still time to do trials. *Lancet* **364**(9440): 1183-1185.
Trofatter, J.A., MacCollin, M.M., Rutter, J.L., Murrell, J.R., Duyao, M.P., Parry, D.M., Eldridge, R., Kley, N., Menon, A.G., Pulaski, K., and et al. 1993. A novel moesin-, ezrin-, radixin-like gene is a candidate for the neurofibromatosis 2 tumor suppressor. *Cell* **72**(5): 791-800.
Tsuda, H., Hirohashi, S., Shimosato, Y., Terada, M., and Hasegawa, H. 1988. Clonal origin of atypical adenomatous hyperplasia of the liver and clonal identity with hepatocellular carcinoma. *Gastroenterology* **95**(6): 1664-1666.
Tsukita, S., Oishi, K., Sato, N., Sagara, J., and Kawai, A. 1994. ERM family members as molecular linkers between the cell surface glycoprotein CD44 and actin-based cytoskeletons. *J Cell Biol* **126**(2): 391-401.
Tweedale, G. 2002. Asbestos and its lethal legacy. *Nat Rev Cancer* **2**(4): 311-315.
van der Most, R.G., Robinson, B.W., and Nelson, D.J. 2006. Gene therapy for malignant mesothelioma: beyond the infant years. *Cancer Gene Ther* **13**(10): 897-904.
Vassilev, L.T. 2007. MDM2 inhibitors for cancer therapy. *Trends Mol Med* **13**(1): 23-31.
Vermeulen, K., Berneman, Z.N., and Van Bockstaele, D.R. 2003a. Cell cycle and apoptosis. *Cell Prolif* **36**(3): 165-175.
Vermeulen, K., Van Bockstaele, D.R., and Berneman, Z.N. 2003b. The cell cycle: a review of regulation, deregulation and therapeutic targets in cancer. *Cell Prolif* **36**(3): 131-149.
Virta, R.L. 2005. Mineral Commodity Profiles-Asbestos. In, pp. 1255-KK, 1256 p. U.S. Geological Survey, Reston.
Vogelstein, B. and Kinzler, K.W. 2004. Cancer genes and the pathways they control. *Nat Med* **10**(8): 789-799.
Vogelstein, B., Lane, D., and Levine, A.J. 2000. Surfing the p53 network. *Nature* **408**(6810): 307-310.
Wagner, J.C., Sleggs, C.A., and Marchand, P. 1960. Diffuse pleural mesothelioma and asbestos exposure in the North Western Cape Province. *Br J Ind Med* **17**: 260-271.
Weiner, S.J. and Neragi-Miandoab, S. 2009. Pathogenesis of malignant pleural mesothelioma and the role of environmental and genetic factors. *J Cancer Res Clin Oncol* **135**(1): 15-27.
Whitaker, D., Papadimitriou, J.M., and Walters, M.N. 1982. The mesothelium and its reactions: a review. *Crit Rev Toxicol* **10**(2): 81-144.
Xiao, G.H., Gallagher, R., Shetler, J., Skele, K., Altomare, D.A., Pestell, R.G., Jhanwar, S., and Testa, J.R. 2005. The NF2 tumor suppressor gene product, merlin, inhibits cell proliferation and cell cycle progression by repressing cyclin D1 expression. *Mol Cell Biol* **25**(6): 2384-2394.

Yang, H., Testa, J.R., and Carbone, M. 2008. Mesothelioma epidemiology, carcinogenesis, and pathogenesis. *Curr Treat Options Oncol* **9**(2-3): 147-157.

Yohay, K. 2006a. Neurofibromatosis types 1 and 2. *Neurologist* **12**(2): 86-93.

Yohay, K.H. 2006b. The genetic and molecular pathogenesis of NF1 and NF2. *Semin Pediatr Neurol* **13**(1): 21-26.

Zhang, Y., Xiong, Y., and Yarbrough, W.G. 1998. ARF promotes MDM2 degradation and stabilizes p53: ARF-INK4a locus deletion impairs both the Rb and p53 tumor suppression pathways. *Cell* **92**(6): 725-734.

CHAPTER 1

shRNA Suppression of NF2 Induces Disruption of Normal Cell Cycle Control Mechanism by Altering p53 Function

Abstract

The tumor suppressor gene neurofibromatosis type 2 (*NF2*) is inactivated in the majority of malignant mesotheliomas, an aggressive cancer strongly associated with asbestos exposure. The consequences of this inactivation are not well understood. Conversely, the major tumor suppressor gene *TP53* is rarely found mutated in mesothelioma tumors, but p53 activity may be regulated by other mechanisms during progression of this disease. Using shRNA directed against *NF2*, we assessed the possibility that loss of *NF2* negatively affects p53 function in a non-tumor mesothelial cell line. *NF2* suppression resulted in loss of cell cycle control correlating directly or indirectly with aberrant p53 function.

Introduction

Considered the “Genome Gatekeeper,” p53 (the protein product of the *TP53* gene) is a transcription factor that initiates several protective pathways following DNA damaging events (Lane 1992; Levine 1997; May and May 1999). Depending on the type of cellular stress, p53 is activated to initiate DNA repair mechanisms, cell cycle arrest, or apoptosis (Rotter et al. 1994; Gottlieb and Oren 1998; Oren 1999). Thus, loss of p53 function can be critical for the developing cancer cell. While *TP53* is mutated in most forms of human cancer, in those where *TP53* remains wild type, loss of other tumor suppressor genes upstream of *TP53* may contribute to a decrease in function of the gene (Ludlow 1993; Marine and Jochemsen 2005; Zhang et al. 2008). Such is the case for malignant pleural mesothelioma (MPM), in which the majority of MPM patients retain wild-type *TP53* genetics, but it is unknown if the p53 protein retains proper function (Murthy and Testa 1999).

MPM is a rare but aggressive cancer usually associated with exposure to asbestos (Treasure and Sedrakyan 2004; Altomare et al. 2005; Tan and Treasure 2005). Genomic analysis of mesothelioma has revealed a series of related sub-chromosomal deletion regions that could be involved in loss of cell cycle regulation. Within the regions affected, crucial regulatory genes implicated include p16 (*INK4a*) and p14 (*ARF*) on 9p, and *NF2* on 22q (Murthy and Testa 1999; Jaurand and Fleury-Feith 2005; Musti et al. 2006). It is possible that inactivation of tumor suppressor genes thought to be involved in p53 regulation,

such as *NF2* or *p14/ARF*, could hinder its ability to act as the “genome keeper” following cellular stress (Kamijo et al. 1998; Pomerantz et al. 1998; Zhang et al. 1998).

NF2 is inactivated by mutation or loss of heterozygosity in the majority of mesotheliomas, but the significance of this loss is not well understood (Baser et al. 2002; Carbone et al. 2002; Altomare et al. 2005; Tan and Treasure 2005; Yang et al. 2008; Weiner and Neragi-Miandoab 2009). Loss of function of tumor suppressor genes can be a critical step leading to abnormal growth, negatively affecting cellular processes including apoptosis, proliferation, cell-cell communication, cell motility, differentiation, as well as others (Sainio et al. 1997; Gutmann et al. 1999; Morrison et al. 2001; Shaw et al. 2001; Sherman and Gutmann 2001; Lallemand et al. 2003; McClatchey and Giovannini 2005; Xiao et al. 2005; Curto and McClatchey 2008). Merlin, the protein product of the *NF2* gene, is activated by regulatory cues to play a role in these processes, depending on cell type.

Merlin is activated *in vitro* during cellular stress events such as serum deprivation or increased cell:cell contact ratios, but the exact molecular consequences of this activation remain to be elucidated (Shaw et al. 1998b; Morrison et al. 2001; McClatchey 2003; Xiao et al. 2005). Following activation, merlin localizes to the cell membrane (Sherman et al. 1997; Shaw et al. 1998a; McClatchey and Giovannini 2005; Curto and McClatchey 2008). This translocation is considered to be rare among tumor suppressor genes, as most function intracellularly to regulate cell cycle events (McClatchey and Giovannini

2005; Curto et al. 2007). The associations that merlin forms with membrane proteins suggest that merlin may be involved in signaling cascades upstream of p53 that may be required to initiate growth arrest.

In this study, we show that suppression of *NF2* gene expression using small hairpin RNA (shRNA) in a nonmalignant mesothelial cell line results in an inability of p53 to appropriately respond to stress. Thus, p53 was unable to initiate exit of the cell cycle either by undergoing apoptosis or by activating appropriate cell cycle checkpoints. A better understanding of cell cycle regulatory changes resulting from the suppression of NF2 in mesothelial cells may provide valuable insight into the molecular mechanisms taking place in mesotheliomas as well as other tumor types with NF2 inactivation.

Results

Using an *in vitro* model for pleural mesothelial cell growth, MeT5a cells were transduced with 5 different shRNA constructs, each targeted against a different region of the *NF2* mRNA transcript (Figure 8a). The shRNA target sequences are listed in Table 2. In addition, MeT5a cells were also stably transduced with a BLAST-negative control version of the Mission shRNA construct. The BLAST-negative vector contains a shRNA insert that has at least a 4-bp mismatch with any known mouse or human gene. Following generation of stably transduced clones, three different MeT5a/*NF2*-shRNA clones (9973-6, 9974-5, and 9977-2) were chosen for further analysis (Figure 8b). Protein was harvested from cells plated at both low cellular density (LCD) and high cellular density (HCD). This was done to assess the additional role of merlin activation status, merlin being activated *in vitro* during conditions like HCD (Morrison et al. 2001; Sherman and Gutmann 2001; Lallemand et al. 2003; McClatchey and Giovannini 2005; Xiao et al. 2005). Of the selected clones, significant decreases in merlin suppression compared to the control clone (MeT5a/CNT9) were found at both LCD and HCD depending on the clone.

FIGURE 8

a) *NF2* mRNA targets of the five Mission shRNA vectors used.

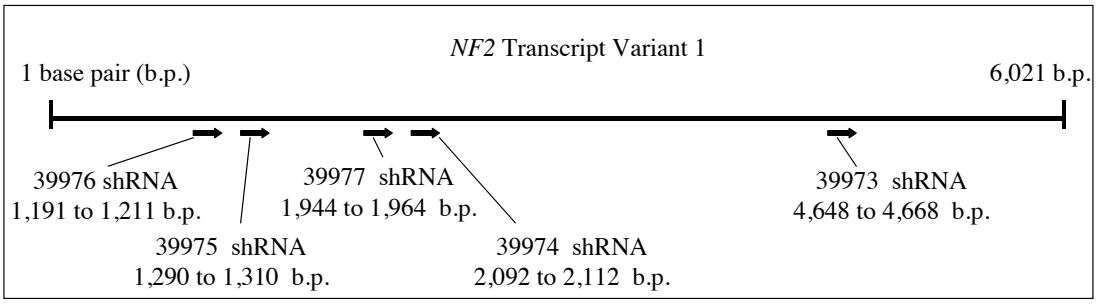

b) Merlin suppression at LCD and HCD.

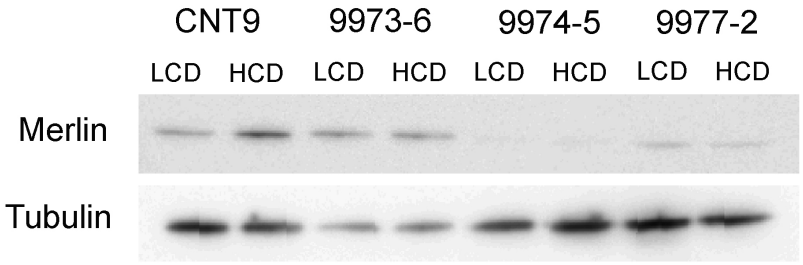

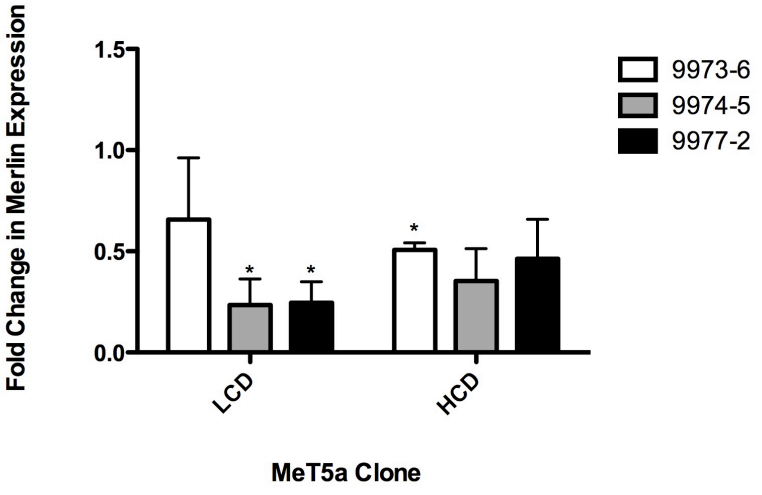

Figure 8. MeT5a cells treated with *NF2* shRNA.

Five shRNA designs were targeted against different regions of the *NF2* mRNA transcript (8a). Following selection of stably-transfected MeT5a cells, clones were selected and then analyzed for amount of merlin suppression as compared to MeT5a/CNT9 cells using Western blot analysis. The amount of merlin suppression was quantified using densitometry normalized to α-Tubulin (8b). Mean fold changes of merlin expression for each clone vs. MeT5a/CNT9 were: 9973-6 LCD=0.657±0.305, HCD=0.507±0.035*; 9974-5 LCD=0.234±0.129*, HCD=0.353±0.161; 9977-2 LCD=0.246±0.103*, HCD=0.463±0.195. Protein expression changes are representative of three individual experiments. *$p<0.05$ using unpaired t-test.

Table 2. shRNA Sequences Directed Against *NF2* mRNA.

shRNA Name	Clone ID	Target Region	shRNA Target Set Sequence
9973*	NM_000268.2-4648s1c1	3UTR	CCGGCGGGCTTTGTTTCCTTCTTTACTCGAGTAAAGAAGGAAACAAAGCCCGTTTTTG
9974*	NM_000268.2-2092s1c1	CDS	CCGGGCTCTGGATATTCTGCACAATCTCGAGATTGTGCAGAATATCCAGAGCTTTTTG
9975	NM_000268.2-1290s1c1	CDS	CCGGGCTTCGTGTTAATAAGCTGATCTCGAGATCAGCTTATTAACACGAAGCTTTTTG
9976	NM_000268.2-1191s1c1	CDS	CCGGCCCGTGGAATGAAATCCGAAACTCGAGTTTCGGATTTCATTCCACGGGTTTTTG
9977*	NM_000268.2-1944s1c1	CDS	CCGGCGACTTCAAAGATACTGACATCTCGAGATGTCAGTATCTTTGAAGTCGTTTTTG

* Clones generated from these sequence targets were used for further analysis.

Under *in vitro* conditions of HCD, normal cells will typically enter a quiescent state due to either depletion of nutrients provided in the media or limited space to proliferate. Merlin has previously been show to play a role in contact inhibition of growth, possibly through CD44 binding (Shaw et al. 1998b; Morrison et al. 2001). Suppression of merlin in MeT5a cells allowed for continued increase in cell density at confluence during growth curve analysis (Figure 9). While the growth rate of *NF2*-shRNA MeT5a clones slowed, the cell number at days 10, 14, and 18 were significantly higher than those for MeT5a/CNT9 cells. In comparison, MeT5a/CNT9 cells reached maximum growth after 10 days, and then appeared to reach a plateau phase of growth. These results indicate a role for merlin in maintaining normal growth in a mesothelial cell model.

FIGURE 9

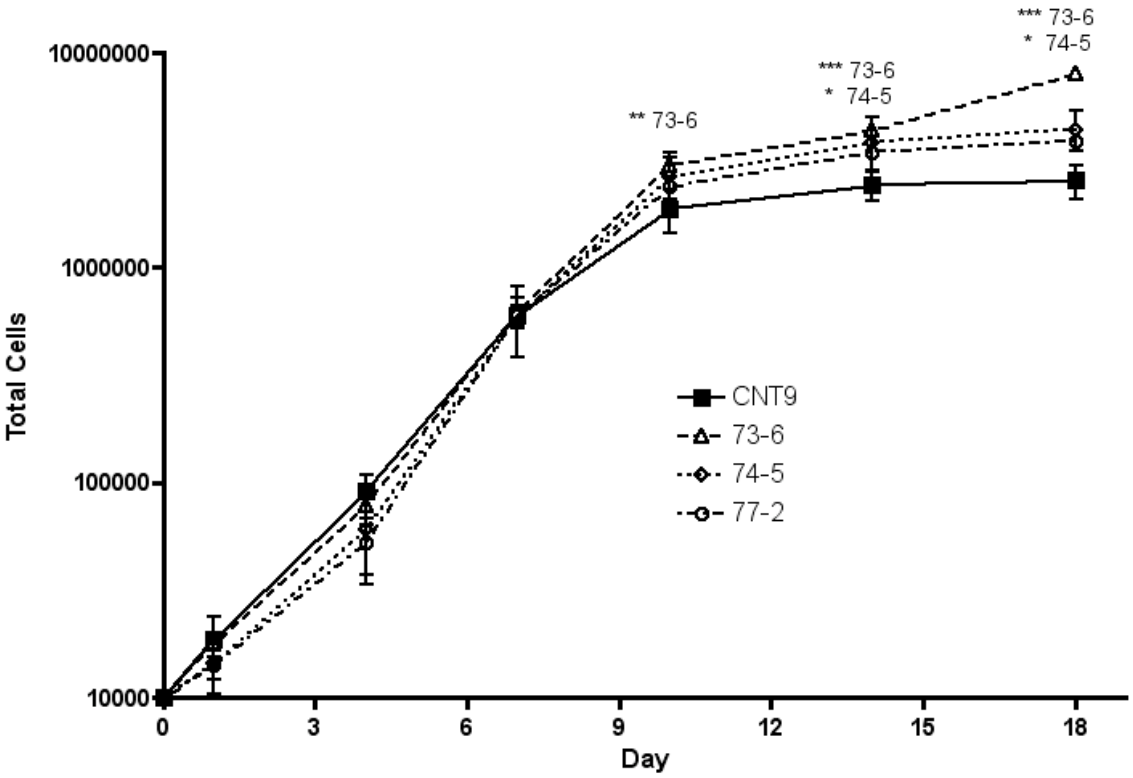
*** 73-6
* 74-5
*** 73-6
* 74-5
** 73-6
10000000
1000000
100000
10000
Total Cells
0
3
6
9
12
15
18
Day
CNT9
73-6
74-5
77-2

Figure 9. Growth curve analysis of MeT5a/CNT9 and *NF2*-shRNA transduced MeT5a cells.

As an initial analysis of cellular phenotype following shRNA suppression, growth curves were used to determine changes related to both contact inhibition of growth as well as possible proliferation rate changes. Clones generated from MeT5a transductions were plated in triplicate in 6 well plates to be counted on days 1, 4, 7, 10, 14, and 18, and average numbers from triplicate wells were used for statistical analysis. Although there was not an apparent increase in proliferation during growth phase of the growth curve, there were significant differences in saturation densities between *NF2*-shRNA transduced clones as compared to MeT5a/CNT9 cells.

n=3

*p<0.05, **p<0.01, and ***p<0.001 using a Two-way ANOVA.

The effect that merlin activation has on downstream signaling pathways in mesothelial cells is not well understood. The loss of contact inhibition of growth as seen in the growth curves suggest that normal cell cycle control mechanisms, such as proliferation and/or cell cycle exit through either apoptosis or cell cycle arrest, have been disrupted. Bromodeoxyuridine (BrDU) was used to analyze alterations in cell cycle progression, as BrDU is incorporated into proliferating cells during S phase of the cell cycle when DNA replication takes place. To determine if merlin suppression changed the ability of cells to proliferate during conditions of high cellular density (HCD), which occurs at the plateau phase of the growth curve (Figure 9), cells were incubated with BrDU for 24 hours. All merlin-suppressed clones showed an increase in BrDU incorporation, indicating that merlin suppression results in either an increased rate of proliferation or an increase in the amount of cells capable of transitioning from G_1 to S phase (Figure 10a and 10b). To exclude the possibility that cell number at the time of seeding might influence these results, two different seeding densities were used. Differences in seeding number did not change the increased ability of the NF2-suppressed clones to continue proliferating after reaching confluency.

To further assess possible proliferative advantages of merlin suppression under conditions of cellular stress, BrDU uptake was measured following exposure to 5 J/m^2 of ultraviolet radiation (UV). There was only a slight increase in BrDU uptake in *NF2*-shRNA clones as compared to MeT5a/CNT9 cells plated at 10,000 cells/well. *NF2*-shRNA clones cells plated at 20,000 cells/well were still capable of DNA replication following exposure to UV as observed through an

increase in uptake of BrDU as compared to MeT5a/CNT9 cells, although these values were not significant. The ability to proliferate even under conditions of cellular stress is evidence that merlin suppression has pushed these mesothelial cells towards a more transformed phenotype, possibly related to alterations in the p53 cell cycle checkpoint.

FIGURE 10

a) Basal BrDU uptake in MeT5a clones.

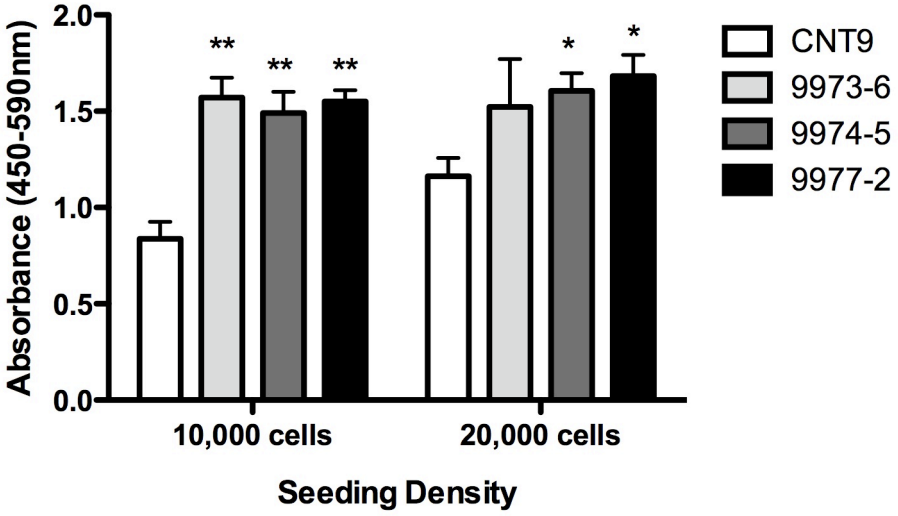

b) BrDU uptake in MeT5a clones following UV exposure.

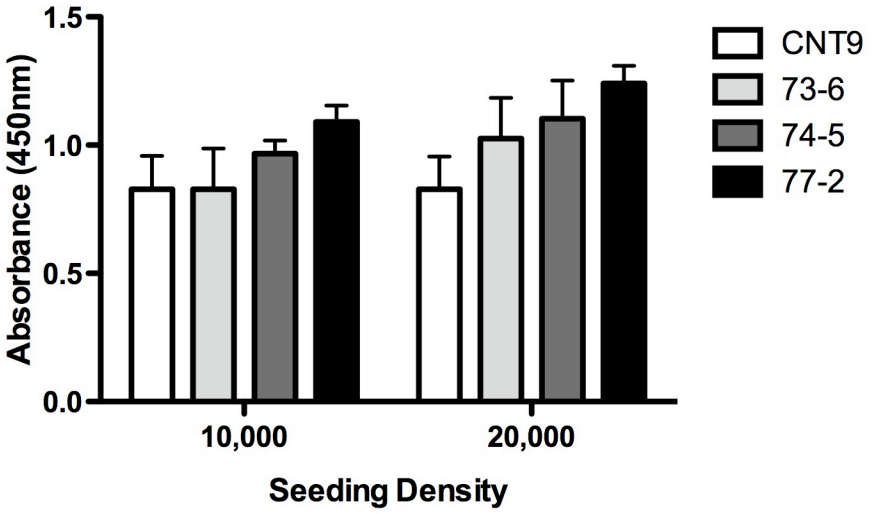

Figure 10. Alterations in BrDU incorporation in MeT5a cells.

Cells were plated at 10,000 cells/well, which is confluent in a 96 well plate. *NF2*-shRNA clones showed a significant increase in BrDU uptake as compared to MeT5a/CNT9 cells. Even at an increased cellular density, *NF2*-shRNA still were able to proliferate at an increased rate as compared to MeT5a/CNT9 cells, with significant values achieved in clones 9974-5 and 9977-2 (10a). After exposure to 5Joules/cm^2 UV, although there was little change in the amount of BrDU incorportation in cells plated at 10,000 cells/well, there was an increase in the amount of BrDU uptake in NF2-shRNA cells compared to MeT5a/CNT9 although these values were not significant (10b).

n=3. *$p<0.05$ and **$p<0.01$ using a Two-way ANOVA.

MDM2 plays a major role in p53 degradation, and there is evidence that has linked merlin to MDM2 degradation in mouse fibroblast 3T3 cells (Kim et al. 2004). We analyzed the result of merlin suppression on changes in the levels of MDM2 expression using western blot analysis, and found that in NF2-suppressed clones there was an increase in MDM2 expression as compared to MeT5a/CNT9 cells, especially at LCD (Figure 11). This increase in MDM2 may result in increased p53 degradation and thus a decrease in p53 activity, which may explain the continual BrDU uptake at both HCD and after UV exposure.

FIGURE 11

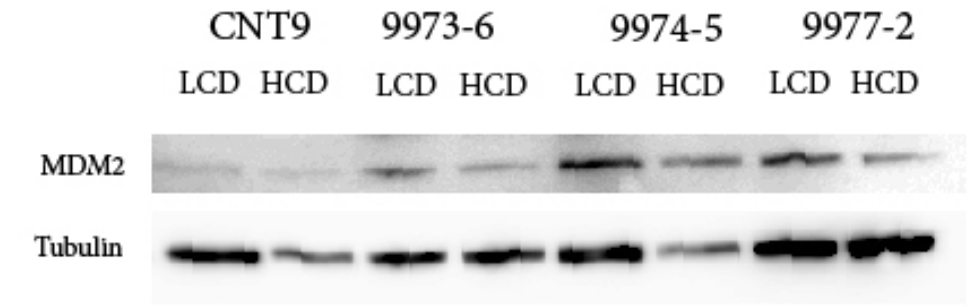
CNT9
9973-6
9974-5
9977-2
LCD HCD
LCD HCD
LCD HCD
LCD HCD
MDM2
Tubulin

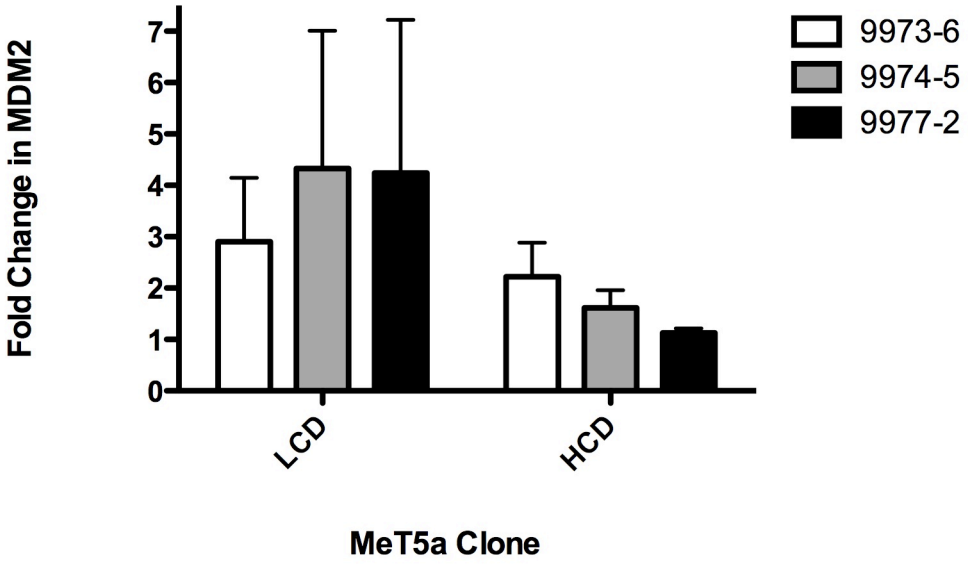
Fold Change in MDM2
0
1
2
3
4
5
6
7
LCD
HCD
9973-6
9974-5
9977-2
MeT5a Clone

Figure 11. Protein expression changes in MDM2 expression.

Alterations if the protein expression levels of MDM2 in all MeT5a clones were analyzed via Western blot analysis. *NF2*-suppressed clones had increased expression of MDM2 as compared to MeT5a/CNT9 cells, which was more pronounced during LCD conditions. Protein expression changes were quantified using densitometry normalized to α-Tubulin. Mean fold changes of MDM2 expression for each clone vs. MeT5a/CNT9 were: 9973-6 LCD=2.902±1.245, HCD=2.222±.662; 9974-5 LCD=4.646±2.682, HCD=1.613±0.347; 9977-2 LCD=4.238±2.982, HCD=1.127±0.0.090. Protein expression changes are representative of three individual experiments. While there were no significant changes found using One-way ANOVA, these data do suggest a trend towards increased MDM2 expression in merlin suppressed clones.

We further analyzed protein expression changes in key cell cycle genes that act at the G_1-S phase transition point that may be affected by merlin suppression. Merlin has been shown to inhibit Cyclin D1, which has a critical role in allowing cells to driving cells into S phase of the cell cycle (Xiao et al. 2005). Cyclin D1 is a critical integrators of mitogenic signals for cell cycle progression, thus inhibition of the protein could result in fewer cycling cells (Diehl 2002; Vermeulen et al. 2003). At both LCD and HCD, there was an increase in Cyclin D1 protein expression in all *NF2*-shRNA clones as compared to MeT5a/CNT9 cells however these increases were not significant (Figure 12a).

In addition, we assessed expression changes in the cell cycle checkpoint gene, p21(*CDNKa*). DNA stress is detected as cells are preparing to move from the phase G_1 of the cell cycle into S phase, p53 acts as a direct transcription factor for the p21 gene to initiate cell cycle arrest (el-Deiry et al. 1993; Harper et al. 1993; el-Deiry et al. 1994). As cell:cell contact increases in a HCD *in vitro* environment, this results in cellular stress that may activate p53 and subsequently p21. At both LCD and HCD, p21 was decreased in clones 9974-5 and 9977-2 as compared to MeT5a/CNT9, while there was little change in clone 9973-6 (Figure 12b). Although there was no significant differences found, these results begin to indicate that merlin may be upstream of p53.

FIGURE 12

a) Immunoblot of Cyclin D1 expression.

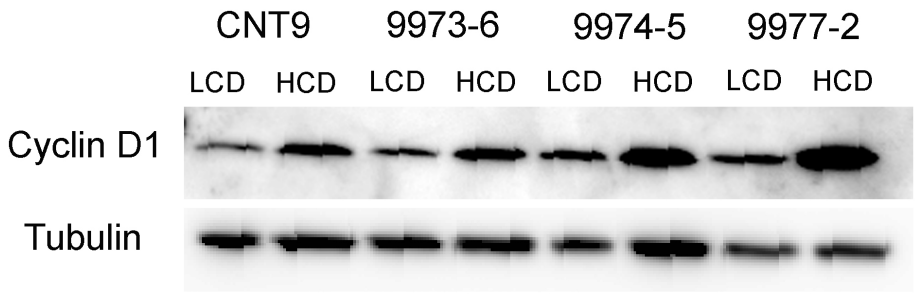

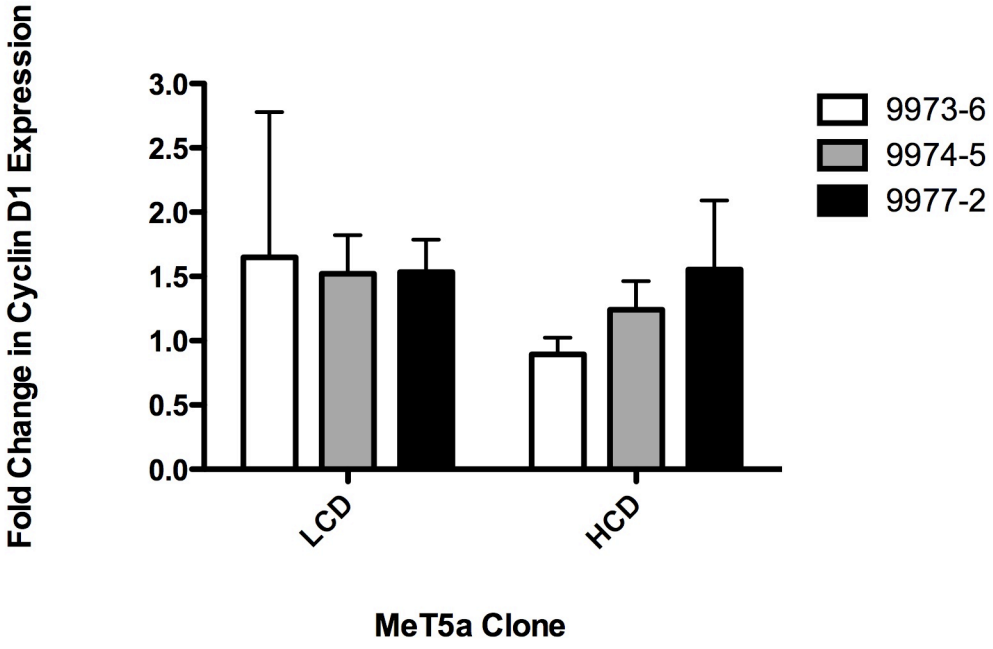

b) Immunoblot of p21 expression.

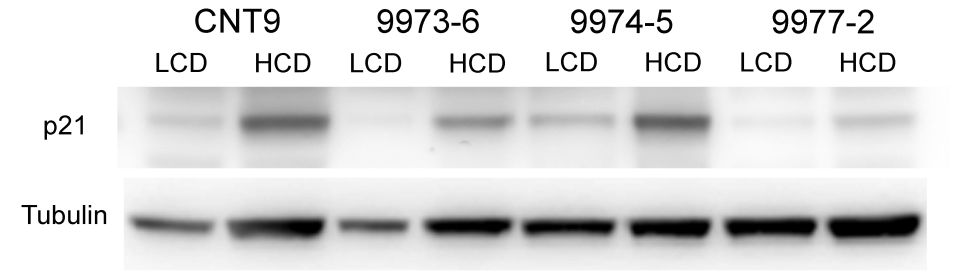

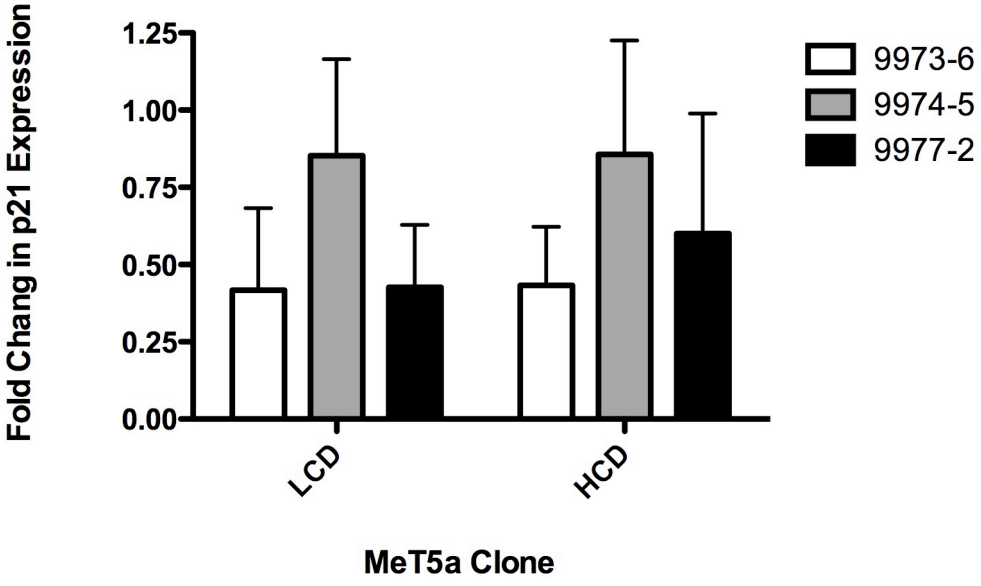

Figure 12. Protein expression in genes involved in cell cycle progression.

Western blot analysis was used to assess protein expression changes in genes involved in cell cycle progression. In all *NF2*-shRNA suppressed clones there was an increase in Cyclin D1 expression as compared to MeT5a/CNT9 cells, although these increases were not significant. At HCD, the amount of Cyclin D1 expression decreased slightly as compared to values seen at LCD (12a). Protein expression changes were quantified using densitometry normalized to α-Tubulin. Mean fold changes for Cyclin D1 expression for each clone vs. MeT5a/CNT9: 9973-6 LCD=1.648±1.131, HCD=0.895±0.130; 9974-5 LCD=1.522±0.298, HCD=1.240±0.225; 9977-2 LCD=1.533±0.255, HCD=1.553±0.0.538.

There was a decrease in p21 expression as compared to MeT5a/CNT9 cells at both LCD and HCD although not significant (12b). Protein expression changes were quantified using densitometry normalized to α-Tubulin. Mean fold changes for p21 expression for each clone vs. MeT5a/CNT9: 9973-6 LCD=0.551±0.325, HCD=0.433±0.189; 9974-5 LCD=1.012±0.375, HCD=0.8564±0.369; 9977-2 LCD=0.561±0.214, HCD=0.601±0.0.388.

Protein expression changes are representative of three individual experiments.

We also determined if cell cycle exit through apoptosis had been affected in response to decreased merlin. Exposure to UV radiation is a proven method for inducing apoptosis through p53-dependent pathways, primarily by acting as a direct transcription factor for the pro-apoptotic Bcl2 family member, Bax (Maltzman and Czyzyk 1984). As a measure of apoptosis, DNA fragmentation was quantified 24 hours post-UV exposure. *NF2*-shRNA suppressed clones had a significant decrease in the amount of apoptotic induction following UV exposure as compared to the apoptotic response seen in MeT5a-CNT9 cells (Figure 13a). Additionally, Bax protein expression changes were quantified 3 hours post-UV exposure (Figure 13b). Fold induction of Bax protein in *NF2*-shRNA suppressed clones was decreased in both basally and in UV-exposed samples compared to MeT5a/CNT9 Bax protein expression. This suggests that p53 is functioning in MeT5a/CNT9 cells as its downstream target, Bax, is activated. Even partial suppression of merlin altered this p53 responsive element indicating that merlin is an essential element for effective p53 function.

FIGURE 13

a) Apoptotic induction following UV exposure.

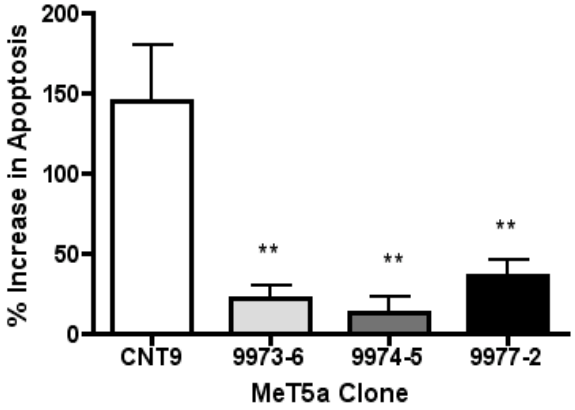

b) Bax protein expression changes.

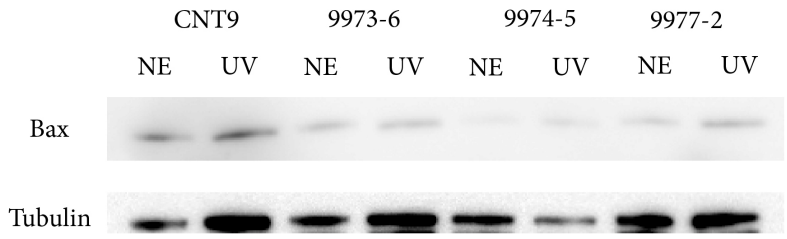

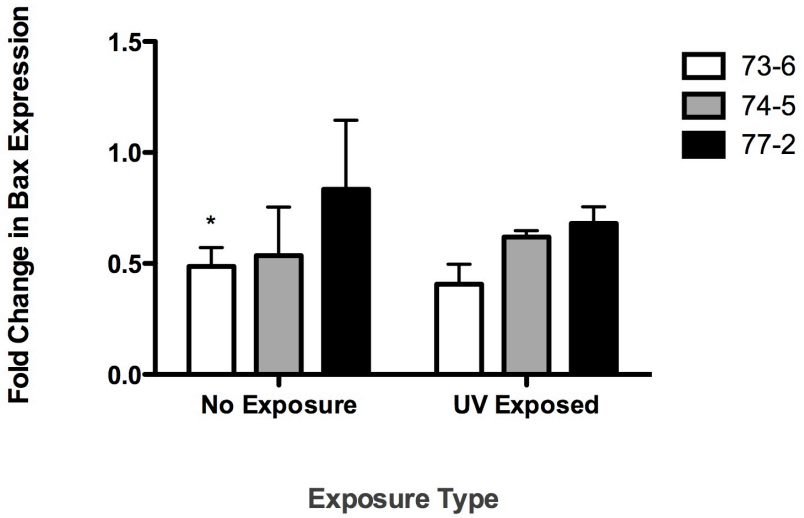

Figure 13. Changes in apoptotic response of MeT5a clones after UV exposure.

The ability to respond to apoptosis induction was analyzed by a DNA fragmentation assay (TiterTacs, Trevigen) 24 hours post-exposure to 5J/cm^2 UV. *NF2*-shRNA clones showed a significant decrease in the percent of apoptosis following exposure as compared to MeT5a/CNT9 cells (13a). A 3 hour UV exposure was also used to induce Bax protein expression, which can be correlated to p53 activity. Western blot analysis indicates that MeT5a/CNT9 cells express more Bax protein than *NF2*-shRNA clones (13b). Protein expression changes were quantified using densitometry normalized to α-Tubulin. Mean fold changes for Bax expression for each clone vs. MeT5a/CNT9: 9973-6 Basal=0.487±0.085*, UV=0.407±0.0.090*; 9974-5 Basal=0.218±0.218, UV=0.619 ±0.028**; 9977-2 Basal=0.834±0.311, UV=0.681±0.0.076.
n=3 for TiterTacs. **p<0.01 using One-way ANOVA for TiterTacs.
Protein expression changes are representative of three individual experiments.
*p<0.05 using unpaired t-test for Western blot fold change analysis.

Conclusions

Genetic mutations that result in the disruption of cell-signaling events, such as those that interfere with cell proliferation or contact inhibition of growth, can have extreme consequences (Hanahan and Weinberg 2000; Evan and Vousden 2001). When considering neoplastic development, altering these tightly regulated cellular processes results in uncontrolled cell growth as well as potential metastasic behavior (Tachibana et al. 2005; Johansson and Persson 2008). A non-cancerous pleural mesothelial cell line was used to assess cell-cycle alterations and protein expression changes that take place following merlin suppression that could contribute to mesothelioma development. Here we have shown that *NF2* contributes to dysregulation of cellular activities in mesothelial cells. Suppression of merlin resulted in loss of contact inhibition of growth as well as an increased ability to progress through the cell cycle, even in the presence of cellular stress. To this end, we found that merlin plays a crucial role in cell cycle exit, as partial suppression of merlin resulted in blockage of both apoptotic and cell cycle arrest mechanisms.

Interactions that can take place between the membrane and the cytoskeleton may be an avenue that allows merlin to react to regulatory cues signaling downstream genes for growth arrest (Tsukita et al. 1994; Sainio et al. 1997; Sherman et al. 1997; Shaw et al. 1998a; McClatchey and Giovannini 2005; Curto and McClatchey 2008). Merlin—also known as Moesin, Ezrin, and/or Radixin-like protein—is a member of the ERM family of proteins. Merlin and the

ERMs share certain structural similarities, and are a part of the superfamily band 4.1 because of the conserved four-point one, ezrin, radixin, moesin (FERM) domain (Shaw et al. 1998a; Lim et al. 2000; Morrison et al. 2001; Sun et al. 2002; McClatchey 2003). The FERM domain may be a linker between the membrane and the cytoskeleton, and ERMs are thought to be involved in the organization of cortical membrane domains that interface with the extracellular environment linking membrane-associated proteins to intracellular components (Shaw et al. 1998b; Curto and McClatchey 2008). Localization to the cytoskeletal membrane after activation suggests that, by mere proximity, merlin is not likely to directly interact with cell cycle regulators but instead may signal upstream of such regulators to inhibit cell cycle progression (McClatchey and Giovannini 2005). This upstream regulation has implications for the role of *NF2* in cell cycle control, such that merlin may be involved in both cell cycle exit and cell proliferation through p53 regulatory mechanisms. When *NF2* is mutated, merlin is incapable of localizing to cell membrane surfaces and therefore cannot respond to such environmental cues to signal p53 activity (Curto and McClatchey 2008).

Alterations in the cellular response to increased cell:cell contact following suppression of merlin suggests that the inactivation of *NF2* may directly or indirectly influence the negative regulation of p53, contributing significantly to tumor progression. *NF2*-shRNA cells had a significant advantage in their ability to progress through the cell cycle as compare to MeT5a/CNT9 cells. In the MeT5a/CNT9 cells, inadequate space for cellular division to take place, as well as lack of nutrients due to increased rate of consumption, were sufficient to

activate p53 and initiate cell cycle exit. Although no change was found in p53 protein expression between following merlin suppression (data not shown), the increase in protein expression of two p53-regulated response elements (p21 and Bax) in MeT5a/CNT9 cells is indicative of this p53 activity. Conversely, the decrease in p53 function in the MeT5a-*NF2*-shRNA clones suggests that *NF2* may be involved upstream in p53 signaling pathways. This decrease in p53 activity resulted in a decrease in the ability to exit the cell cycle through apoptosis as well as exit through cell cycle arrest, contributing to the increased proliferation seen at HCD.

The exact mechanisms by which merlin may control p53 activity has yet to be established. Kim et al. 2004 demonstrated a tight link between the merlin and MDM2, ultimately leading to the dysregulation of p53. In this report, it was shown that merlin is responsible for MDM2 degradation using 3T3 fibroblast cells (Kim et al. 2004). MDM2 is involved in an autoregulatory feedback loop with p53, whereby p53 is a transcription factor for MDM2 after which MDM2 can then ubiquitinate p53, tagging it for degradation (Levine 1997; Zhang et al. 1998; Michael and Oren 2002; Brooks and Gu 2006; Zhang et al. 2008). Here we have shown that merlin resulted in increased MDM2 expression in mesothelial cells as well, which is an unexplored avenue for tumor progression in mesothelioma tumors.

Also contributing to cell cycle progression in *NF2*-suppressed cells is increased Cyclin D1 expression. The D-type cyclins are one of the necessary components involved in entry into S phase of the cell cycle. One of the molecular

targets of Cyclin D1 is RB, responsible for phosphorylation RB allowing cells to transition into S phase (Lukas et al. 1994; Resnitzky and Reed 1995; Shackelford et al. 1999; Bali et al. 2004; Tachibana et al. 2005). *RB*, like *TP53*, is another tumor suppressor gene rarely found mutated in mesothelioma tumors (Rouleau et al. 1993; Jaurand and Fleury-Feith 2005; Kumar and Kratzke 2005). Further investigation of this pathway will provide more insight into merlin cell cycle regulation, in particular its role in the G_1 to S phase transition. If merlin is also upstream of RB, inactivation of merlin could be a critical step allowing cells to continue proliferation.

Here we have shown that merlin plays in cell cycle control includes alterations regulatory cues of both cell cycle exit mechanisms, including both apoptosis and cell cycle arrest, as well as proliferation in mesothelial cells. The vast array of cellular processes that are disrupted by decreased merlin expression strengthens our knowledge of the role *NF2* plays as a critical regulator of cell growth. In particular, our finding that the p53 response to UV damage is negatively regulated by merlin suppression provides novel insight into the molecular mechanisms involved in merlin activation. Thus, the processes involved in the activation, translocation, and regulation of merlin can ultimately affect p53 activity. Therefore future studies aimed at delineating merlin interacting molecules and their functional relationships will be critical for understanding the NF2/p53 pathway.

Methods

Cell Culture

The MeT5a cell line was grown in Medium199 with Earle's BSS, 0.75 mM L-glutamine and 1.25 g/L sodium bicarbonate supplemented with 3.3 nM epidermal growth factor (EGF), 400 nM hydrocortisone, 870 nM insulin, 20 mM HEPES, 10% fetal calf serum, penicillin streptomycin, sodium pyruvate, and non-essential amino acids. Following transduction with lentiviral vectors, the addition of puromycin (1.8 μg/ml) to the media was used for selection of stably-transduced clones.

Lentiviral shRNA Virus Production and Cell Transductions

MeT5a cells were transduced with 5 different Mission shRNA constructs (Sigma-Aldrich, St Louis, MO), each targeted against a different region of NF2 mRNA. MeT5a cells were also transduced with the PLKO.1 Mission shRNA control plasmid (Sigma-Aldrich, St Louis, MO), which consists of a scrambled insert sequence that is BLAST negative. Generated clones were screened to determine the amount of merlin suppression at 70% confluence. NF2 suppressed clones chosen to use for further analysis had a decrease in merlin expression ranging from 45-80% as compared to a control plasmid transduced MeT5a cells.

Growth Curves

Cells were plated into 6 well plates at 10,000 cells per well. Cells were covered with 3 mL of media and incubated at 37°C. Media was changed every 3 days.

At each time point, cells were counted in triplicate (3 wells of cells per count) using a hemacytometer.

ImmunoBlots

Cells were plated at 90,000 cells/well into 6 well plates for LCD and 300,000 cells/well for HCD and incubated 24 hours. At time of protein harvest, LCD samples were ~60% confluent for LCD and HCD samples were >90%. At the time of protein harvest, media was removed and cells were washed with Phosphate Buffered Saline (PBS). Protein was harvested in PBS-TDS lysis buffer (0.1% Triton X-100; 12.6 mM Sodium deoxycholate; 3.7 mM SDS; 1 mM EDTA; and 0.2 mM PMSF containing phosphatase and protease inhibitors (Sigma Alrdich, St Louis, MO)). Protein levels were measured using the BioRad Protein DC assay (Bio-Rad, Hercules, CA). Samples were loaded onto a 4-12% Bis-Tris Nupage gel (Invitrogen, Carlsbad, CA) then transferred onto a PVDF membrane (Millipore, Bedford, MA). Membranes were blocked and the primary antibody added. Following incubation with the primary antibody, membranes were washed with PBS and Tween-20 (0.1% Tween-20) (PBS-T(0.1%), and a goat anti-mouse or goat anti-rabbit secondary antibody was added. Membranes were washed with PBS-T (0.1%) prior to chemiluminescence detection using the Immobilon Detection kit (Millipore, Bedford, MA). Blots were stripped and reprobed for α-Tubulin as a loading control. Antibodies used include: NF2 (A19), MDM2 (2A10), and p21 (C-19) from Santa Cruz Biotechnology, Santa Cruz, CA; Cyclin D1 (DCS-6) and Bax (AM32) from Calbiochem, San Diego, CA; and α-Tubulin from Sigma-Aldrich, St Louis, MO.

BrdU Incorporation Assay

Cells were plated in triplicate in two 96 well plates (one for exposure, one for no exposure control) at cellular densities of 10,000 cells/well and 20,000 cells/well. 24 hours after plating, media was removed and replaced with 50 μl PBS and exposed to UV. Immediately following exposure, PBS was removed and replaced with fresh media with BrDU was added. Cells were placed in incubator for 24 hours, the amount of BrDU labeled DNA was quantified following the manufacturer's protocol (Calbiochem, San Diego, CA).

UV Exposure

For experiments utilizing UV exposure to induce DNA damage for protein expression changes, cells were plated in 6 well culture dishes at 90,000 cells/well. The next day, media was removed and wells were covered with 500 μl PBS. Cells were placed in a Stratagene Stratalinker 1800 with no plate covers and then exposed to $5J/m^2$. Following exposure, PBS was removed and replaced with media. Cells were incubated at 37°C for 3 hours, media was removed, cells were washed with PBS, and protein was harvested in protein lysis buffer as previously described.

For apoptosis and BrDU UV exposures, media was removed from incubated cells and replace with 100ul of PBS. After cells were placed in the Stratagene Stratalinker 1800, covers of plates were removed and plates were then exposed to $5J/m^2$. PBS was removed and replaced with fresh, and the cells were incubated at 37°C for 24 hours.

TiterTacs Apoptosis Assay

Cells were plated in triplicate in two 96 well plates (one plate for UV exposure, one plate served as no exposure control) at 40,000 cells/well. 48 hours after plating, cells were exposed to either UV or Camptothecin. TiterTacs (Trevigen, Helgerman, CT) was used according to manufacturers protocol to assess DNA fragmentation.

References

Altomare, D.A., Vaslet, C.A., Skele, K.L., De Rienzo, A., Devarajan, K., Jhanwar, S.C., McClatchey, A.I., Kane, A.B., and Testa, J.R. 2005. A mouse model recapitulating molecular features of human mesothelioma. *Cancer Res* **65**(18): 8090-8095.

Bali, A., O'Brien, P.M., Edwards, L.S., Sutherland, R.L., Hacker, N.F., and Henshall, S.M. 2004. Cyclin D1, p53, and p21Waf1/Cip1 expression is predictive of poor clinical outcome in serous epithelial ovarian cancer. *Clin Cancer Res* **10**(15): 5168-5177.

Baser, M.E., De Rienzo, A., Altomare, D., Balsara, B.R., Hedrick, N.M., Gutmann, D.H., Pitts, L.H., Jackler, R.K., and Testa, J.R. 2002. Neurofibromatosis 2 and malignant mesothelioma. *Neurology* **59**(2): 290-291.

Brooks, C.L. and Gu, W. 2006. p53 ubiquitination: Mdm2 and beyond. *Mol Cell* **21**(3): 307-315.

Carbone, M., Kratzke, R.A., and Testa, J.R. 2002. The pathogenesis of mesothelioma. *Semin Oncol* **29**(1): 2-17.

Curto, M., Cole, B.K., Lallemand, D., Liu, C.H., and McClatchey, A.I. 2007. Contact-dependent inhibition of EGFR signaling by Nf2/Merlin. *J Cell Biol* **177**(5): 893-903.

Curto, M. and McClatchey, A.I. 2008. Nf2/Merlin: a coordinator of receptor signalling and intercellular contact. *Br J Cancer* **98**(2): 256-262.

Diehl, J.A. 2002. Cycling to cancer with cyclin D1. *Cancer Biol Ther* **1**(3): 226-231.

el-Deiry, W.S., Harper, J.W., O'Connor, P.M., Velculescu, V.E., Canman, C.E., Jackman, J., Pietenpol, J.A., Burrell, M., Hill, D.E., Wang, Y., and et al. 1994. WAF1/CIP1 is induced in p53-mediated G1 arrest and apoptosis. *Cancer Res* **54**(5): 1169-1174.

el-Deiry, W.S., Tokino, T., Velculescu, V.E., Levy, D.B., Parsons, R., Trent, J.M., Lin, D., Mercer, W.E., Kinzler, K.W., and Vogelstein, B. 1993. WAF1, a potential mediator of p53 tumor suppression. *Cell* **75**(4): 817-825.

Evan, G. and Vousden, K.H. 2001. Proliferation, cell cycle and apoptosis in cancer *Nature* **411**(17): 342-348.

Gottlieb, T.M. and Oren, M. 1998. p53 and apoptosis. *Semin Cancer Biol* **8**(5): 359-368.

Gutmann, D.H., Sherman, L., Seftor, L., Haipek, C., Hoang Lu, K., and Hendrix, M. 1999. Increased expression of the NF2 tumor suppressor gene product, merlin, impairs cell motility, adhesionand spreading. *Hum Mol Genet* **8**(2): 267-275.

Hanahan, D. and Weinberg, R.A. 2000. The Hallmarks of Cancer. *Cell* **100**: 57-70.

Harper, J.W., Adami, G.R., Wei, N., Keyomarsi, K., and Elledge, S.J. 1993. The p21 Cdk-interacting protein Cip1 is a potent inhibitor of G1 cyclin-dependent kinases. *Cell* **75**(4): 805-816.

Jaurand, M.C. and Fleury-Feith, J. 2005. Pathogenesis of malignant pleural mesothelioma. *Respirology* **10**(1): 2-8.

Johansson, M. and Persson, J.L. 2008. Cancer therapy: targeting cell cycle regulators. *Anticancer Agents Med Chem* **8**(7): 723-731.

Kamijo, T., Weber, J.D., Zambetti, G., Zindy, F., Roussel, M.F., and Sherr, C.J. 1998. Functional and physical interactions of the ARF tumor suppressor with p53 and Mdm2. *Proc Natl Acad Sci U S A* **95**(14): 8292-8297.

Kim, H., Kwak, N.J., Lee, J.Y., Choi, B.H., Lim, Y., Ko, Y.J., Kim, Y.H., Huh, P.W., Lee, K.H., Rha, H.K., and Wang, Y.P. 2004. Merlin neutralizes the inhibitory effect of Mdm2 on p53. *J Biol Chem* **279**(9): 7812-7818.

Kumar, P. and Kratzke, R.A. 2005. Molecular prognostic markers in malignant mesothelioma. *Lung Cancer* **49 Suppl 1**: S53-60.

Lallemand, D., Curto, M., Saotome, I., Giovannini, M., and McClatchey, A.I. 2003. NF2 deficiency promotes tumorigenesis and metastasis by destabilizing adherens junctions. *Genes Dev* **17**(9): 1090-1100.

Lane, D.P. 1992. Cancer. p53, guardian of the genome. *Nature* **358**(6381): 15-16.

Levine, A.J. 1997. p53, the cellular gatekeeper for growth and division. *Cell* **88**(3): 323-331.

Lim, D.J., Rubenstein, A.E., Evans, D.G., Jacks, T., Seizinger, B.G., Baser, M.E., Beebe, D., Brackmann, D.E., Chiocca, E.A., Fehon, R.G., Giovannini, M., Glazer, R., Gusella, J.F., Gutmann, D.H., Korf, B., Lieberman, F., Martuza, R., McClatchey, A.I., Parry, D.M., Pulst, S.M., Ramesh, V., Ramsey, W.J., Ratner, N., Rutkowski, J.L., Ruttledge, M., and Weinstein, D.E. 2000. Advances in neurofibromatosis 2 (NF2): a workshop report. *J Neurogenet* **14**(2): 63-106.

Ludlow, J.W. 1993. Interactions between SV40 large-tumor antigen and the growth suppressor proteins pRB and p53. *FASEB J* **7**(10): 866-871.

Lukas, J., Pagano, M., Staskova, Z., Draetta, G., and Bartek, J. 1994. Cyclin D1 protein oscillates and is essential for cell cycle progression in human tumour cell lines. *Oncogene* **9**(3): 707-718.

Maltzman, W. and Czyzyk, L. 1984. UV irradiation stimulates levels of p53 cellular tumor antigen in nontransformed mouse cells. *Mol Cell Biol* **4**(9): 1689-1694.

Marine, J.C. and Jochemsen, A.G. 2005. Mdmx as an essential regulator of p53 activity. *Biochem Biophys Res Commun* **331**(3): 750-760.

May, P. and May, E. 1999. Twenty years of p53 research: structural and functional aspects of the p53 protein. *Oncogene* **18**(53): 7621-7636.

McClatchey, A.I. 2003. Merlin and ERM proteins: unappreciated roles in cancer development? *Nat Rev Cancer* **3**(11): 877-883.

McClatchey, A.I. and Giovannini, M. 2005. Membrane organization and tumorigenesis--the NF2 tumor suppressor, Merlin. *Genes Dev* **19**(19): 2265-2277.

Michael, D. and Oren, M. 2002. The p53 and Mdm2 families in cancer. *Curr Opin Genet Dev* **12**(1): 53-59.

Morrison, H., Sherman, L.S., Legg, J., Banine, F., Isacke, C., Haipek, C.A., Gutmann, D.H., Ponta, H., and Herrlich, P. 2001. The NF2 tumor suppressor gene product, merlin, mediates contact inhibition of growth through interactions with CD44. *Genes Dev* **15**(8): 968-980.

Murthy, S.S. and Testa, J.R. 1999. Asbestos, chromosomal deletions, and tumor suppressor gene alterations in human malignant mesothelioma. *J Cell Physiol* **180**(2): 150-157.

Musti, M., Kettunen, E., Dragonieri, S., Lindholm, P., Cavone, D., Serio, G., and Knuutila, S. 2006. Cytogenetic and molecular genetic changes in malignant mesothelioma. *Cancer Genet Cytogenet* **170**(1): 9-15.

Oren, M. 1999. Regulation of the p53 tumor suppressor protein. *J Biol Chem* **274**(51): 36031-36034.

Pomerantz, J., Schreiber-Agus, N., Liegeois, N.J., Silverman, A., Alland, L., Chin, L., Potes, J., Chen, K., Orlow, I., Lee, H.W., Cordon-Cardo, C., and DePinho, R.A. 1998. The Ink4a tumor suppressor gene product, p19Arf, interacts with MDM2 and neutralizes MDM2's inhibition of p53. *Cell* **92**(6): 713-723.

Resnitzky, D. and Reed, S.I. 1995. Different roles for cyclins D1 and E in regulation of the G1-to-S transition. *Mol Cell Biol* **15**(7): 3463-3469.

Rotter, V., Aloni-Grinstein, R., Schwartz, D., Elkind, N.B., Simons, A., Wolkowicz, R., Lavigne, M., Beserman, P., Kapon, A., and Goldfinger, N. 1994. Does wild-type p53 play a role in normal cell differentiation? *Semin Cancer Biol* **5**(3): 229-236.

Rouleau, G.A., Merel, P., Lutchman, M., Sanson, M., Zucman, J., Marineau, C., Hoang-Xuan, K., Demczuk, S., Desmaze, C., Plougastel, B., and et al. 1993. Alteration in a new gene encoding a putative membrane-organizing protein causes neuro-fibromatosis type 2. *Nature* **363**(6429): 515-521.

Sainio, M., Zhao, F., Heiska, L., Turunen, O., den Bakker, M., Zwarthoff, E., Lutchman, M., Rouleau, G.A., Jaaskelainen, J., Vaheri, A., and Carpen, O. 1997. Neurofibromatosis 2 tumor suppressor protein colocalizes with ezrin and CD44 and associates with actin-containing cytoskeleton. *J Cell Sci* **110 (Pt 18)**: 2249-2260.

Shackelford, R.E., Kaufmann, W.K., and Paules, S.P. 1999. Cell Ceycle Control, Checkpoint Mechansisms, and Genotoxic Strees. *Environmental Health Perspectives* **107**: 5-24.

Shaw, R.J., McClatchey, A.I., and Jacks, T. 1998a. Localization and functional domains of the neurofibromatosis type II tumor suppressor, merlin. *Cell Growth Differ* **9**(4): 287-296.

-. 1998b. Regulation of the neurofibromatosis type 2 tumor suppressor protein, merlin, by adhesion and growth arrest stimuli. *J Biol Chem* **273**(13): 7757-7764.

Shaw, R.J., Paez, J.G., Curto, M., Yaktine, A., Pruitt, W.M., Saotome, I., O'Bryan, J.P., Gupta, V., Ratner, N., Der, C.J., Jacks, T., and McClatchey, A.I.

2001. The Nf2 tumor suppressor, merlin, functions in Rac-dependent signaling. *Dev Cell* **1**(1): 63-72.
Sherman, L., Xu, H.M., Geist, R.T., Saporito-Irwin, S., Howells, N., Ponta, H., Herrlich, P., and Gutmann, D.H. 1997. Interdomain binding mediates tumor growth suppression by the NF2 gene product. *Oncogene* **15**(20): 2505-2509.
Sherman, L.S. and Gutmann, D.H. 2001. Merlin: hanging tumor suppression on the Rac. *Trends Cell Biol* **11**(11): 442-444.
Sun, C.X., Robb, V.A., and Gutmann, D.H. 2002. Protein 4.1 tumor suppressors: getting a FERM grip on growth regulation. *J Cell Sci* **115**(Pt 21): 3991-4000.
Tachibana, K.E., Gonzalez, M.A., and Coleman, N. 2005. Cell-cycle-dependent regulation of DNA replication and its relevance to cancer pathology. *J Pathol* **205**(2): 123-129.
Tan, C. and Treasure, T. 2005. Mesothelioma: time to take stock. *J R Soc Med* **98**(10): 455-458.
Treasure, T. and Sedrakyan, A. 2004. Pleural mesothelioma: little evidence, still time to do trials. *Lancet* **364**(9440): 1183-1185.
Tsukita, S., Oishi, K., Sato, N., Sagara, J., and Kawai, A. 1994. ERM family members as molecular linkers between the cell surface glycoprotein CD44 and actin-based cytoskeletons. *J Cell Biol* **126**(2): 391-401.
Vermeulen, K., Van Bockstaele, D.R., and Berneman, Z.N. 2003. The cell cycle: a review of regulation, deregulation and therapeutic targets in cancer. *Cell Prolif* **36**(3): 131-149.
Weiner, S.J. and Neragi-Miandoab, S. 2009. Pathogenesis of malignant pleural mesothelioma and the role of environmental and genetic factors. *J Cancer Res Clin Oncol* **135**(1): 15-27.
Xiao, G.H., Gallagher, R., Shetler, J., Skele, K., Altomare, D.A., Pestell, R.G., Jhanwar, S., and Testa, J.R. 2005. The NF2 tumor suppressor gene product, merlin, inhibits cell proliferation and cell cycle progression by repressing cyclin D1 expression. *Mol Cell Biol* **25**(6): 2384-2394.
Yang, H., Testa, J.R., and Carbone, M. 2008. Mesothelioma epidemiology, carcinogenesis, and pathogenesis. *Curr Treat Options Oncol* **9**(2-3): 147-157.
Zhang, X.C., Chen, J., Su, C.H., Yang, H.Y., and Lee, M.H. 2008. Roles for CSN5 in control of p53/MDM2 activities. *J Cell Biochem* **103**(4): 1219-1230.
Zhang, Y., Xiong, Y., and Yarbrough, W.G. 1998. ARF promotes MDM2 degradation and stabilizes p53: ARF-INK4a locus deletion impairs both the Rb and p53 tumor suppression pathways. *Cell* **92**(6): 725-734.

CHAPTER 2

Differential Protein Expression in Human Mesothelioma Cell Lines and Alterations in Cell Growth Following Reintroduction of NF2 Protein

Abstract

Malignant pleural mesothelioma (MPM) is an extremely aggressive form of cancer with a strong link to asbestos exposure. Patients diagnosed with MPM have a very poor prognosis with a median survival time of approximately 2 years. One of the most commonly inactivated tumor suppressor genes during the course of mesothelioma development is Neurofibromatosis Type 2 (NF2). Additionally, *TP53* mutations are rare in MPM, suggesting that aberrant p53 function may be due to upstream alterations in its regulation. In this study, we assessed differences in the expression of proteins with a known link to *TP53* activity in human mesothelioma cell lines and a nonmalignant mesothelial cell line. Cell cycle alterations were analyzed in response to full-length NF2 gene construct introduction using a human MPM cell line that does not express Merlin, the protein product of *NF2*.

Introduction

The *TP53* tumor suppressor gene is arguably the most important tumor suppressor gene involved in the development of human cancer (Lane 1992; Levine 1997; Oren 1999). While *TP53* is mutated in a majority of human cancers, a significant number of patients with no detectable mutations still go on to develop cancer (Danovi et al. 2004). This suggests that genetic or functional aberrations in genes that regulate p53, the protein product of *TP53*, are a factor in human cancers that retain wild-type *TP53*, including MPM.

MPM is an aggressive cancer with a complex etiology. Mesothelioma tumors form in the mesothelial layer lining certain body cavities, the most common of these occurrences is in the pleural mesothelial layers that encase the lung. Patients diagnosed with these relatively rare cancers have a poor prognosis, with patients often succumbing to the disease within 2 years post-diagnosis (Guinee and Allen 2008). It is hypothesized that in MPM, an accumulation of mutations in tumor suppressor genes, such as *p16/INK4a* (*CDKN2A*) and *p14/ARF* (*CDKN2B*) on 9p, and Neurofibromatosis type 2 (*NF2*) on 22q, occur during the latency period of 20-40 years following exposure to asbestos(Altomare et al. 2005; Kumar et al. 2005). Mutations in the *NF2* gene occur at a particularly high frequency in MPM, whereas mutations in *TP53* are rare (Sekido et al. 1995; Murthy and Testa 1999). Kim and colleagues (2004) demonstrated in 3T3 mouse fibroblast cells that inactivation of *NF2* can indirectly affect p53 function through degradation of MDM2, a negative regulator of p53.

This regulatory pathway of p53 has not yet been examined in human mesothelial cells.

In order to develop a more effective treatment strategy for patients with MPM, as well as other cancers involving wild-type *TP53*, we must gain a more thorough understanding of the molecular changes that occur during disease development. Analysis of four pleural mesothelial cell lines, nonmalignant and malignant, revealed a dramatic difference in expression of the p53 protein as well as a possible link between merlin, the protein product of *NF2*, and MDM2 protein expression. We further analyzed cell cycle changes after reintroduction of a full-length version of *NF2* in a merlin-negative mesothelioma cell line.

Results

The *TP53* tumor suppressor gene is of central importance in the regulation of cell proliferation and/or cell death following DNA damage. The activity of p53 is tightly regulated in response to cell signaling molecules, including the negative regulator MDM2*,* and its structural analog*,* MDM4 (Marine and Jochemsen 2005; Brooks and Gu 2006). Using the pleural nonmalignant mesothelial cell line, MeT5a, and the pleural mesothelioma cell lines, H-meso-1, H2052, and H28, we analyzed protein expression changes using Western blots. We did not observe a significant change in the expression of MDM4 among the cell lines in this study (Figure 14a and 14b), however there is an increased MDM2 expression in the H-meso-1 cell line when compared to MeT5a (Figure 14a and 14c). In addition, there is a significant decrease in the expression of p53 in the tumor cell lines when compared to the nonmalignant mesothelial cell line (Figure 14a and 14d). Interestingly, p53 expression in the H-meso1 cell line is nearly undetectable and significantly lower than both the H28 and H2052 lines, respectively. Of particular interest, merlin is undetectable in the H-meso1 cells (Figure 14a and 14e).

Figure 14

a) Immunoblots for merlin and MDM2 expression.

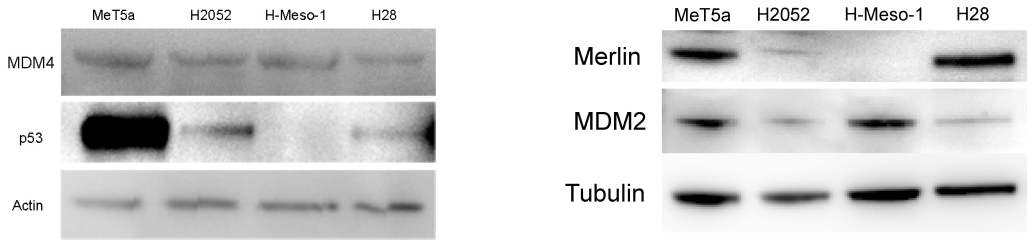

b) Densitometry analysis of immunoblots for MDM4 expression.

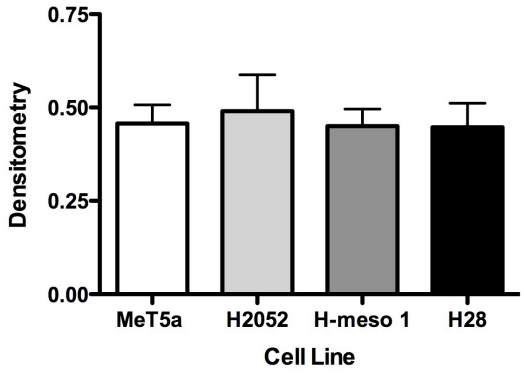

c) Densitometry analysis of immunoblots for MDM2 expression.

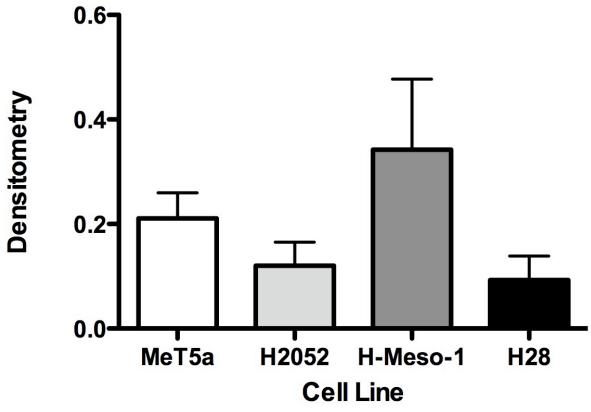

d) Densitometry analysis for p53 expression.

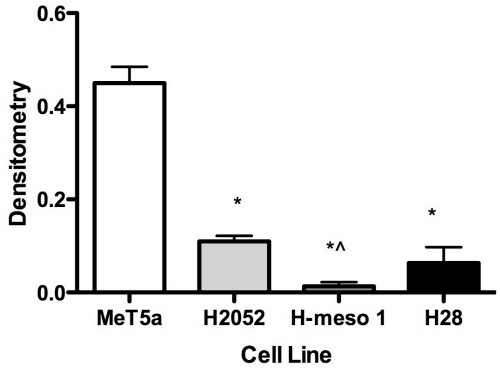

e) Densitometry analysis for merlin expression.

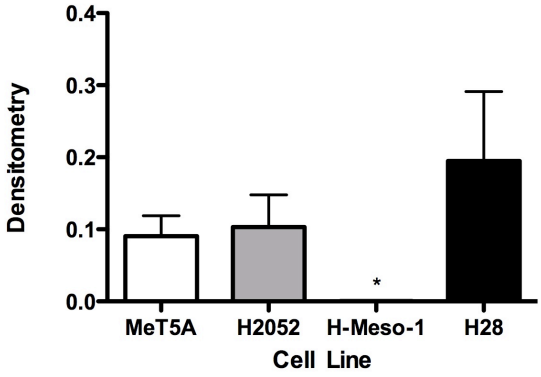

Figure 14. Immunoblots of protein expression between the MeT5a and mesothelioma cell lines.

Protein expression changes were analyzed via Western blot. The H-meso1 cell line had no detectable *NF2* expression (14a and 14b). While there was increased expression of merlin in the H2052 and H28 cell lines as compared to MeT5a, the differences were not significant (14b). A trend towards increasing expression of MDM2 was seen in the H-meso-1 cell line, although the differences were not significant (14a and 14c). The MeT5a line had significantly higher expression of p53 than all three mesothelioma cell lines (Figure 14d and 14e). Both the H2052 and the H28 lines had significantly higher expression of p53 than the H-meso-1 cells (14d and 14e).

*$p<0.05$ and indicates a significant difference when compared to MeT5a.

^$p<0.05$ and indicates a significant difference when compared to H2052 and H28. Protein expression changes were quantified using densitometry normalized to β-Actin or α-Tubulin. All statistics were conducted using densitometry from three blots from independent experiments using unpaired t-test.

To investigate cellular growth conditions and specific downstream molecular targets that may result from aberrant merlin expression, we re-introduced *NF2* in the H-meso-1 cell line. In order to achieve consistent levels of merlin expression and to achieve expression for growth curve analysis (21 days), it was important to utilize a stable transfection technique. An H-meso1 cell line already containing a Tet-repressor vector was transfected with either a pTREX control vector or a pTREX vector with a full-length open reading frame version of *NF2* (IOH23119, *NF2* Complete CDS, Invitrogen, Carlsbad, CA). Clones positive for merlin or the control vector were selected using G418. The H-meso-1 clones for the control vector (H-meso-1/CNT) or NF2 (H-meso-1/NF2), were analyzed for merlin expression using Western blot analysis (Figure 15a).

To determine the effect that merlin re-expression had on MDM2, we also analyzed changes in MDM2 protein levels in the transfected H-meso-1 clones. It has been shown that merlin is activated *in vitro* during conditions like high cellular density (HCD).(Morrison et al. 2001; Sherman and Gutmann 2001; Lallemand et al. 2003; McClatchey and Giovannini 2005; Xiao et al. 2005) Thus, protein was harvested from cells plated at both low cellular density (LCD) and high cellular density (HCD) to assess protein expression changes dependent upon merlin activity. H-meso-1/NF2 cells showed a slight decrease in MDM2 protein levels at HCD when compared to the H-meso-1/CNT cells, although these values were not significant (Figure 15b). Next, we were interested in whether or not these alterations in merlin and MDM2 protein would have an effect on p53 status and cellular phenotype.

FIGURE 15

a) Merlin expression in H-meso-1 cells.

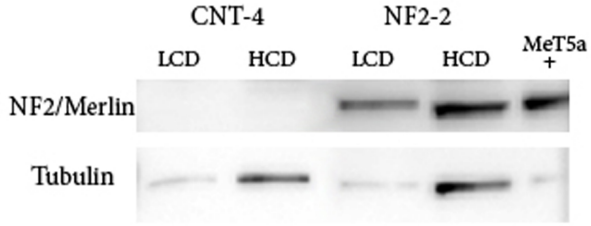

b) MDM2 expression in H-meso-1 cells.

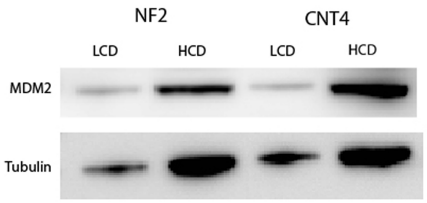

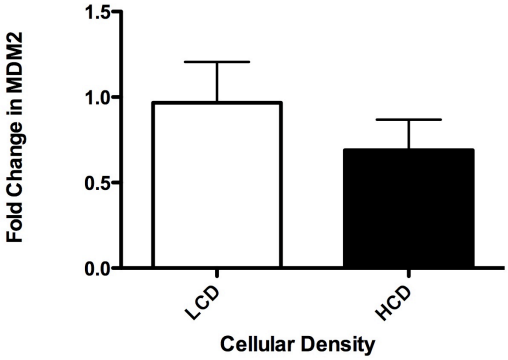

Figure 15. Western blot of NF2 and MDM2 expression changes in H-meso-1 cells.

Protein was harvested from H-meso-1/NF2 and H-meso-1/CNT cells plated at LCD and HCD to follow protein level changes related to merlin activity status. Harvested lysates were analyzed via Western blot analysis for merlin expression verification (15a) and MDM2 expression changes (15b). At HCD, when merlin is activated, there a slight decrease in MDM2 protein levels which could be related to the increase merlin expression and/or activity.

All statistics were conducted using densitometry from three blots from independent experiments using unpaired t-test.

We used growth curves to determine whether there were alterations in the cell cycle following reintroduction of *NF2* in the H-meso-1 cell line. Growth curves are a useful tool for assessing changes in both growth rate and saturation density *in vitro*, the latter being a good indicator of the degree to which a cell has been transformed. At the plateau phase of cell growth, there was a decrease in saturation density in H-Meso-1/NF2 clones as compared to H-meso-1/CNT cells (Figure 16). In addition, we found that the H-meso-1/NF2 cells show a shift in the log phase portion of the growth curve, suggesting that either H-meso-1/NF2 cells were undergoing cell cycle arrest or that growth rate itself had slowed.

FIGURE 16

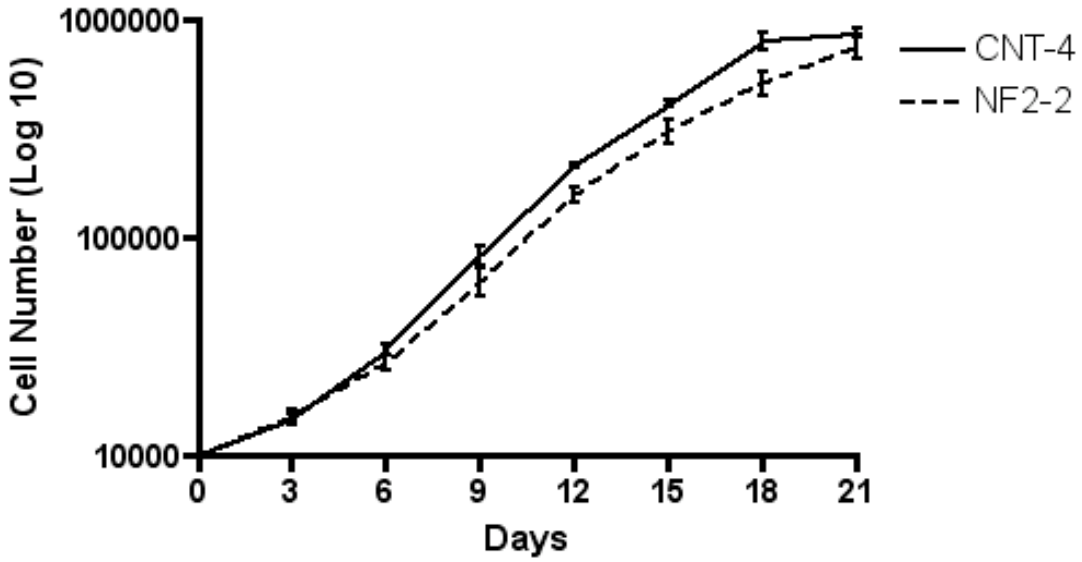
1000000
100000
10000
Cell Number (Log 10)
0
3
6
9
12
15
18
21
Days
CNT-4
NF2-2

Figure 16. Growth curves of H-meso-1/CNT and H-meso-1/NF2 cells.

Cells for each clone type were plated in triplicate into 12 well plates for each time point to be analyzed. Every three days, cells were counted and average values were used for statistical analysis. Merlin re-expression in H-meso-1 cells results in a decreased rate of growth as indicated by a shift in the log phase of the curve of H-meso-1/NF2-2 cells compared to the H-meso-1/CNT-4 log phase curve. In addition, there is a slight decrease in saturation density of H-meso-1/NF2-2 cells compared to the saturation density of the H-meso-1/CNT-4 cells.

Data were analyzed using a

n=3 for days 1-21, n=4 for days 1-18.

In order to confirm that growth rate had been altered following merlin expression, cells were labeled with BrDU. During DNA replication, BrDU is incorporated into newly synthesized DNA strands and can be correlated with the level of cellular proliferation. BrDU was added to the media and allowed to incubate for 3 hours, 12 hours, or 24 hours. The amount of BrDU incorporation was measured using an antibody directed against BrDU. At each time point, H-meso-1/CNT cells had incorporated significantly more BrDU as compared to H-meso-1/NF2 cells (Figure 17a, 17b, and 17c). This is supportive of the growth curve data that show H-meso-1/NF2 cells proliferate at a decreased rate compared to H-meso-1/CNT cells.

FIGURE 17

a) 3 Hour BrDU Label

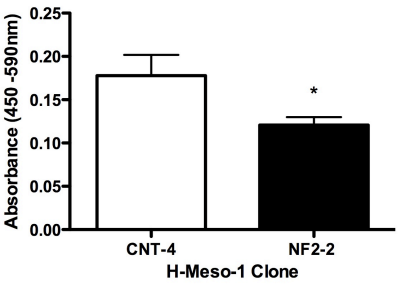

b) 12 Hour BrDU Label

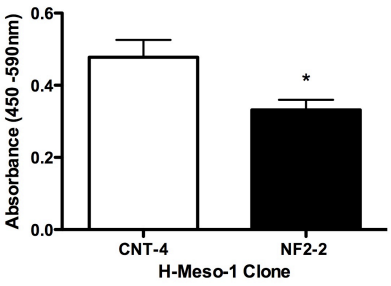

c) 24 Hour BrDU Label

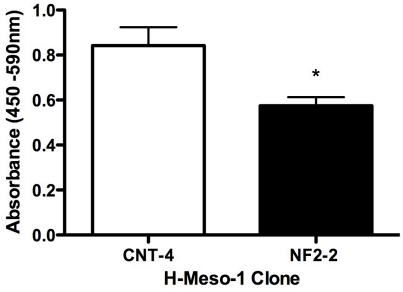

Figure 17. BrDU incorporation in H-meso-1 clones with or without merlin expression.

As a measure of DNA synthesis, incorporated BrDU was measured immunochemically. The amount of BrDU incorporation was significantly lower in H-meso-1/TR/NF2-2 clones as compared to H-meso-1/TR/CNT-4 cells at each time point analyzed. This suggests that there was a decrease in the number of cycling cells following NF2 re-expression in the mesothelioma tumor cell line.

* $p<0.05$ using t-test for each time point.

n=4 for 12 hour time point; n=5 for 3 hour and 24 hour time points.

To further dissect the nature of the cell cycle alteration following merlin reintroduction, measurement of DNA content was performed using flow cytometry. This analysis provides the percentage of cells in G_1, S, or G_2M phase at different levels of culture confluence. Cells were plated and allowed to incubate for 3 or 6 days. After 3 days, both clone types were at less than 50% confluent and determined to be LCD and the H-meso-1/NF2 cells had significantly more cells in phase G_1 compared to H-meso-1/CNT cells (Figure 18a). Although there were fewer cells cycling through S phase in H-meso-1/NF2 cells compared to H-Meso-1/CNT, this difference was not significant (Figure 18b).

After 6 days of growth, both control and NF2 clones were more than 90% confluent and considered to be HCD. At HCD, H-meso-1/NF2 clones had an increase in cells cycling through G_1 phase of the cell cycle, as well as a decrease in the number of cells cycling through S phase of the cell cycle compared to H-meso-1/CNT cells. Both of these changes in cell cycle were highly significant (Figures 18d and 18e, respectively). There was no change in the number of cells in G_2M of the cell cycle at either LCD or HCD (Figure 18c and 18f, respectively). These DNA content results suggested that H-meso-1/NF2 cells are less able to exit G_1.

FIGURE 18

a) LCD G1 Phase

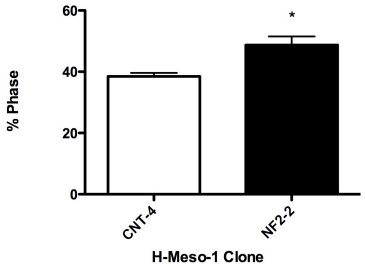

b) LCD S Phase

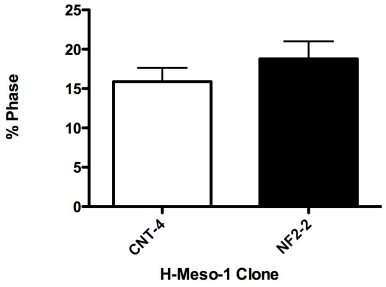

c) LCD G2 Phase

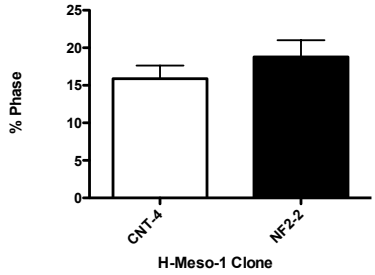

d) HCD G1 Phase

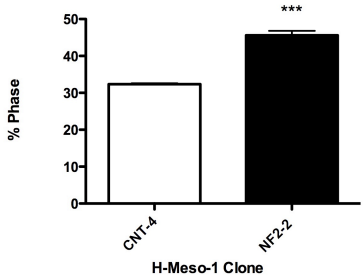

e) HCD S Phase

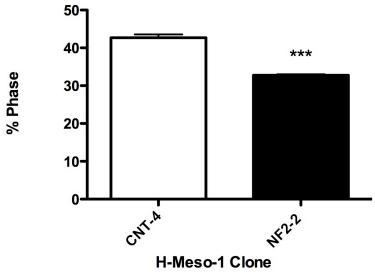

f) HCD G2 Phase

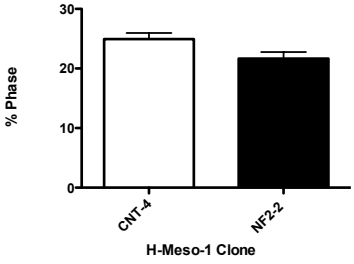

Figure 18. DNA content analysis of H-meso-1 cells to determine cell cycle phase alterations following merlin re-expression.

DNA content analysis was analyzed on a FACScalibur flow cytometer following propidium iodide staining. After 3 days of incubation, both control or merlin-expressing H-meso-1 cells were less than 50% confluent and termed LCD. There was a significant increase in G_1 cycling cells in H-meso-1/NF2-2 cells compared to H-meso-1/CNT-4 cells (18a). While there was a decrease in H-meso-1/NF2 cells cycling through S phase compared to H-meso-1/CNT-4 cells, this difference was not significant (18b). After 6 days of incubation, both clone types were more than 90% confluent and termed HCD. There were highly significant differences in phases G_1 and S of the cell cycle between the two clone types (18d and 18e). No statistical differences were found in G_2 phase between the H-meso-1 clones.

* $p<0.05$, *** $p<.001$ using unpaired t-test.

n=3

The significant increase in cells in G_1 phase of the cell cycle in H-meso-1/NF2 cells suggests cell cycle arrest mechanisms may be involved. It is generally thought that p53 initiates cell cycle arrest following DNA damage through the upregulation of p21, for which p53 is a transcription factor. The p21 protein is known to initiate cell cycle arrest (Toledo and Wahl 2006). To investigate if this pathway is involved, protein was harvested from both H-meso-1/NF2 and H-meso-1/CNT cells at LCD and HCD conditions and p21 protein expression was analyzed via Western blot. In the control cell line, there was minimal p21 protein expression and there was no change in expression as cell density increased (Figure 19a). However, in H-meso-1/NF2 cells there was an increase in p21 protein expression under both LCD and HCD conditions as compared to H-meso-1/CNT cells.

Further investigation of p53 activity involved activation of p53 by inducing apoptosis using UV exposure. In response to DNA damage, p53 is a direct transcription factor for the pro-apoptotic member of the Bcl-2 family member, Bax (Miyashita and Reed 1995; Gottlieb and Oren 1998; Kelekar and Thompson 1998). Thus, to induce apoptosis through this p53-related pathway cells were exposed to $5J/m^2$. There was no change in the amount of apoptotic induction measured by the amount of DNA fragmentation 24 hours post-exposure (Figure 19b). An additional exposure method was used to test the possibility that H-meso-1 cells were resistant to UV-induced apoptosis. Cells were exposed to the topoisomerase I inhibitor, camptothecin, and DNA fragmentation assessment showed no change in the induction of apoptosis after a 3 hour time point (Figure

19c). Lactate dehydrogenase (LDH) activity was measured following both exposure methods at varying time points to verify that the correct time point was chosen for measuring apoptosis. Apoptotic induction measured after a 24 hour exposure to UV caused the highest amount of cell death (Figure 19d).

Although there was little change in apoptotic induction between H-meso-1/NF2 and H-meso-1/CNT as assessed by DNA fragmentation assays (Figure 19b and 19c), there was an increase in Bax protein in H-meso-1/NF2 cells before and after UV exposure as compared to H-meso-1/CNT (Figure 19e). Although differences found were not significantly different, the increase in Bax protein expression suggests that p53 function is altered by the ability of the cells to express merlin.

Besides alterations in p53-responsive pathways, NF2 has been shown to inhibit Cyclin D1 (Xiao et al. 2005). Cyclin D1 is associated with the transition from a quiescent state of the cell cycle into S phase (Lukas et al. 1994; Ladha et al. 1998; Diehl 2002; Knudsen et al. 2006). We also found a significant decrease in Cyclin D1 expression following reintroduction of *NF2* into the H-meso-1 cell line (Figure 19f), suggesting that not only are cell cycle checkpoints affected by merlin but also proliferation mechanisms are responsive to merlin expression changes.

FIGURE 19.

a) p21 Protein Expression Changes

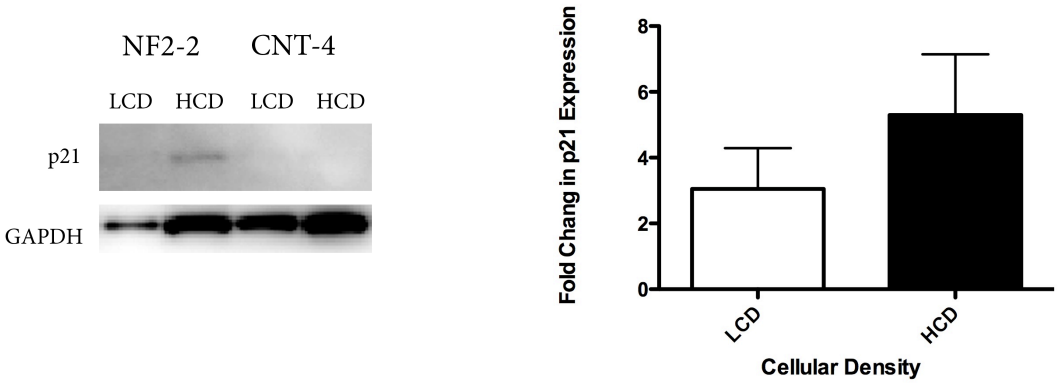

b) DNA Fragmentation in Response to Camptothecin Exposure

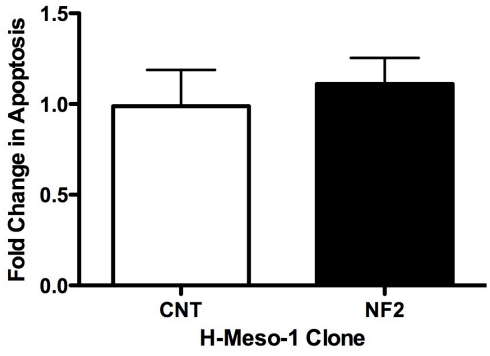

c) DNA Fragmentation in Response to UV

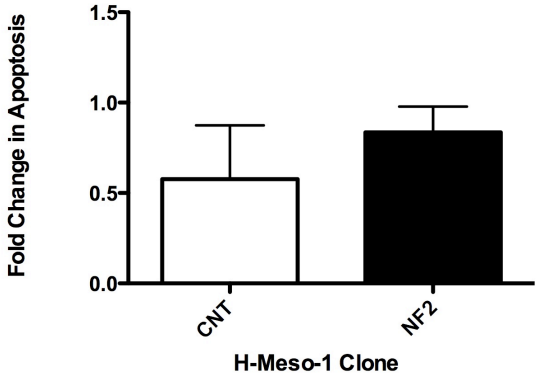

d) LDH Activity Following UV or Camptothecin Exposure

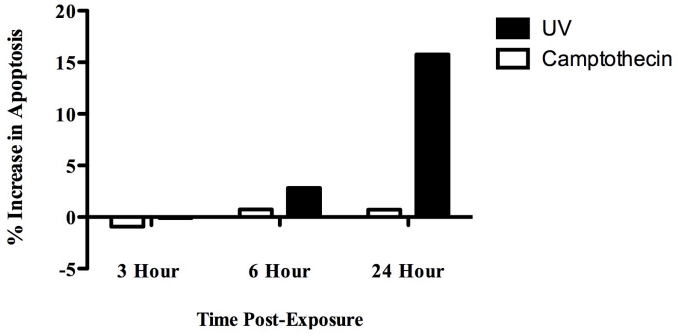

e) Bax Protein Expression Changes and Densitometry

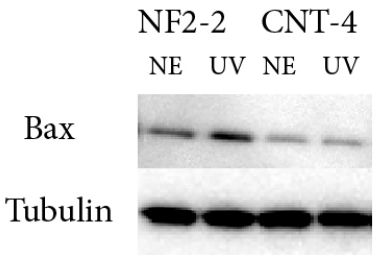

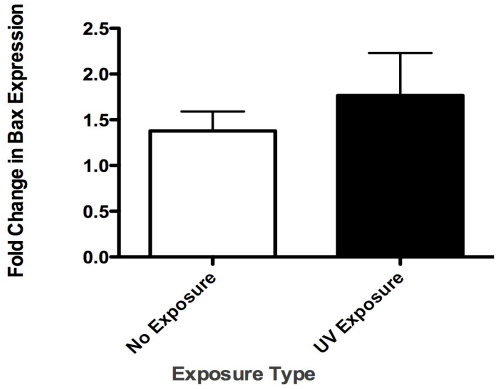

f) Cyclin D1 Protein Expression Changes and Densitometry

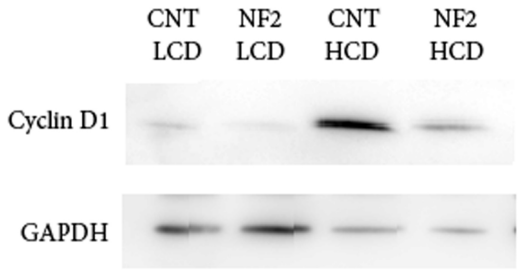

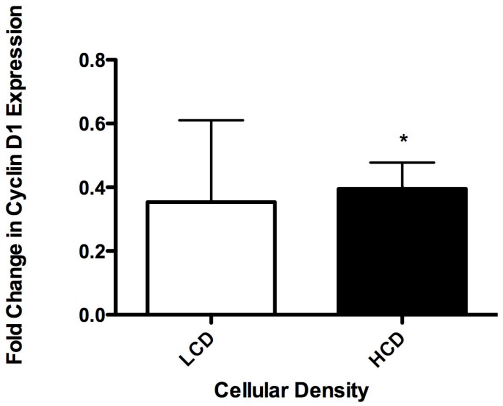

Figure 19. Protein expression in changes in genes involved in cell cycle control.

To investigate p53 activity, protein expression of p53-repsonsive genes was analyzed using Western blot analysis. At HCD, when cells should exit the cell cycle due to inadequate growth conditions, there was an increase in p21 protein expression in H-meso-1/NF2 cells as compared to H-meso-1/CNT cells (19a). Apoptotic response was measured using DNA fragmentation in response to both 3 hour camptothecin exposure and 24 hours post-UV exposure. Neither treatment-type resulted in apoptosis at the measured time points (Figure 19b and 19c, respectively). LDH activity in H-meso-1/NF2 cells determined that the highest amount of cell death could be measured at 24 hours post-UV exposure. As a measure of p53 response to DNA damage, Bax protein expression was quantified and showed an increased expression in H-meso-1/NF2 cells as compared to H-meso-1/CNT cells both basally and after UV exposure, although this difference was not significant (19e). The G_1-S phase regulator, Cyclin D1, showed a decrease in expression following reintroduction of merlin into H-meso-1 cells (19f).

* $p<0.05$ using unpaired t-test. n=4 for camptothecin-exposed apoptosis assay; n=3 for UV-exposed apoptosis assay.

Protein expression changes were quantified using densitometry normalized to α-Tubulin or GAPDH. All statistics were conducted using densitometry from three blots from independent experiments using unpaired t-test. No significant differences were found.

Conclusions

As *TP53* is inactivated by mutation in about half of human cancers analyzed to date, and many times these inactivating mutations are thought to be initiating events in tumor formation, p53 deregulation is thought to be critical for tumor development. MPM patients are generally found to have wild-type *TP53* status, despite the severity of the disease (Murthy and Testa 1999). Regulation of p53 function can include interactions with viral proteins, such as SV40 large T interactions, alterations in the levels of cellular proteins that can regulate p53 subcellular localization, for example Jab1, and inactivation of genes which may help to maintain p53 function, including *p14/ARF* and *NF2* Here we have shown that in mesothelial cells, merlin acts upstream of p53, possibly through MDM2, to help maintain function of the gene (Oliner et al. 1992; Moll et al. 1996; Chin et al. 1998; Pomerantz et al. 1998; Zhang et al. 2008).

Activation of p53 is a dynamic process involving induction of signaling molecules needed to induce cell cycle arrest, DNA repair, differentiation, or apoptosis dependent upon the type of DNA damage (May and May 1999). After p53 has carried out its protective role, p53 acts as a transcription factor for its own regulator, MDM2 (Oren 1999). MDM2 works to maintain p53 protein levels and activity through ubiquitination and subsequent degradation (Michael and Oren 2002). In the mesothelial cell lines analyzed, a trend towards increasing MDM2 expression during conditions of reduced merlin expression was apparent. This suggested that a disruption of other regulatory pathways had occurred.

Inactivation of the *NF2* tumor suppressor gene by mutation is most often associated with the cancer syndrome neurofibromatosis type 2. This familial cancer syndrome includes the development of bilateral schwannomas of the eighth cranial nerve, meningiomas, and ependymomas (Martuza and Eldridge 1988; McClatchey 2003). In contrast to these tumors, which are primarily benign cancers, mutations in *NF2* are also frequent in the asbestos-induced cancer, MPM. Interestingly, *TP53* is rarely mutated in at least two of these *NF2*-associated cancers, mesothelioma or meningiomas (Murthy and Testa 1999; Jaurand and Fleury-Feith 2005). Located on chromosome 22, *NF2* may play a role in maintaining normal cellular growth through many possible signal transduction mechanisms, including CD44 and extracellular matrix, Rac-1 proteins, and MDM2. (Tsukita et al. 1994; Sainio et al. 1997; Sherman and Gutmann 2001; Kim et al. 2004) The trend towards increasing MDM2 expression as merlin expression decreases suggests that merlin may be involved in regulation of MDM2 in mesothelial cells. To examine this possible relationship more closely, we chose to re-express merlin in the H-meso-1 cell line, which lacked merlin expression and had increased MDM2 expression.

Reintroduction of merlin into the H-meso-1 cell line resulted in both a decreased growth rate as well as a decrease in saturation density, indicating strict regulation of growth control. This is consistent with previous reports that merlin is involved in contact inhibition of growth (Morrison et al. 2001). Proliferation assays confirmed these merlin-induced changes in the cell cycle, with significant decreases in BrDU uptake at all time points examined. The

decrease in proliferation at high cellular densities, coupled with the decrease in growth rate were verified by DNA content analysis suggesting G_1-S-phase transition had been altered in H-meso-1/NF2 cells. During HCD conditions when merlin is activated, the percentage of H-meso-1/NF2 cells blocked in G_1 phase had increased significantly.

As *NF2* is a tumor suppressor gene, alterations in cell cycle were not entirely unexpected. Tumor suppressor genes may act at cell-cycle checkpoints to prevent the clonal expansion of aberrant cells through the stimulation of apoptosis, cell-cycle arrest, and DNA repair pathways. However, the increase seen in p21 expression in H-meso-1/NF2 clones as compared to H-meso-1/CNT clones suggest that merlin may be inducing this cell cycle arrest through a p53-regulated pathway. The p21 protein is a member of the CDK family of cell cycle inhibitors and an early cell cycle arrest response molecule (Toledo and Wahl 2006). Abnormalities in the expression of proteins from the CDK inhibitor family, such as p21, have also been described in MPM (Kumar and Kratzke 2005). H-meso-1/NF2 clones showed an increase in p21 expression at HCD as compared to control cells. Although no response in apoptosis was detected in these cells in response to camptothecin or UV exposures, an increase in Bax expression was found in H-meso-1/NF2 cells as compared to H-meso-1/CNT cells. This suggested that p53 function may be increased in H-meso-1 cells after merlin expression and/or activation. This alone may be insufficient to return control to the tumor cell line to allow apoptosis to take place. Multiple tumor suppressor genes are inactivated in mesothelioma, and these experiments involve the

replacement of only one. This renewal of p53 activity correlates with phenotypic changes seen in proliferation, growth curves, and DNA content analysis and is suggestive of a more “nonmalignant” or less transformed cellular phenotype.

In addition to alterations in p53-related cell cycle checkpoints altered, we also found alterations in cyclin D1 expression. Increases in cyclin D1 expression have been implicated in a number of cancers, including mantle cell lymphoma, breast cancer, uveal melanoma, and ovarian cancer (Bartkova et al. 1995; Coupland et al. 2000; Bali et al. 2004). Cyclin D1 is a critical cell cycle regulator of the G_1-S-phase transition, responsible for the phosphorylation of RB allowing cells to transition into S phase (Knudsen et al. 2006). The evidence that merlin is upstream of Cyclin D1 and plays a role in inhibition of its activity suggests that *NF2*, much like the tumor suppressor gene *p16/Ink4a*, may also be upstream of RB.

Discovered in 1993, *NF2* research has increased our knowledge that this tumor suppressor gene is a critical cell cycle regulator, responding to extracellular cues and relating signals to downstream pathways (Trofatter et al. 1993; Tsukita et al. 1994; Sherman et al. 1997; Morrison et al. 2001). As conventional cancer therapies such as radiation treatments, surgery, and chemotherapy have not significantly lengthened the survival time of patients with MPM, it is necessary to understand the molecular interactions that are altered in order to improve patient treatment paradigms (Rusch 1995; Ryan et al. 1998). Continued research of the intricacies involved in both cell cycle control and the regulation of p53 and RB pathways would aid in the search for better patient care

and earlier diagnosis in not only MPM but other cancer syndromes with similar genetic profiles.

Methods

Cell Culture and Transfections

All mesothelioma cell lines were maintained in RPMI media supplemented with 10% fetal calf serum, L-glutamine, and penicillin streptomycin. The MeT5a cell line was grown in Medium199 with Earle's BSS, 0.75 mM L-glutamine and 1.25 g/L sodium bicarbonate supplemented with 3.3 nM epidermal growth factor (EGF), 400 nM hydrocortisone, 870 nM insulin, 10% fetal calf serum, penicillin streptomycin, sodium pyruvate, and non-essential amino acids.

Following transfection with pTRex vectors (Invitrogen, Carlsbad, CA), stably transfected H-meso-1 clones had G418 (Invitrogen, Carlsbad, CA) added to the above media to maintain transformation of cells. Prior to transfection with the pTRex vectors, the H-meso-1 cell line had been transduced with the Tet-repressor pLenti6/TR vector (Invitrogen, Carlsbad, CA) and were maintained under stable selection for using blasticidin (Sigma-Aldrich, St Louis, MO). This was done to allow for controlled gene expression of merlin with the addtion of doxycycline (Sigma-Aldrich, St Louis, MO) the media as a preemptive event in case merlin reintroduction would not allow clones to grow. However, this Tet-repressor vector did not function properly and was not necessary as merlin expression was achieved without doxycyline addition to the media.

H28, MeT5a, and H2052 were purchased from ATCC, H-meso-1 was purchased from the NCI–Frederick Cancer DCTD tumor/cell line repository and was previously characterized (Reale et al. 1987).

Growth Curves

Cells were plated into 12 well plates at 10,000 cells per well. Cells were covered with 2 mL of media and incubated at 37°C. Media was changed every 3 days. At each time point, cells were counted in triplicate (3 wells of cells per count) using a hemacytometer.

DNA Content

For low cell density (LCD) and high cell density (HCD) experiments, cells were plated into 10 cm dishes at 300,000 cells/well for LCD and $1*10^6$ cells/well for HCD samples. Cells were incubated over night at 37°C.

Plates were washed with 5 ml of phosphate buffered saline (PBS), and treated with 2 ml of trypsin for 2-5 minutes at 37°C. After cells had lifted off the plate, 5 ml of PBS was added and cells were carefully harvested and then transferred to a 15 ml conical tube. Cells were centrifuged at 200*g for 6 min at room temperature (RT), followed by two washes with PBS, centrifuging between washes at 200*g for 6 min. Cells were resuspended in 500 μl of PBS, and fixed by adding 4.5 ml of ice cold 70% ethanol dropwise while gently vortexing. Samples were stored at -20°C at least 24 hours. Ethanol fixed samples were centrifuged at 200*g for 6 min at RT, followed by two washes with 5 ml PBS. Pellets were resuspended in 250 μl of propidium iodide/Triton-X 100 solution (0.1% (v/v) Triton X-100 in 5 ml PBS, DNAse-free RNAse A (0.2 mg/ml) (Sigma Aldrich, St. Louis, MO) and Propidium Iodide (0.02 mg/ml) (Sigma Aldrich, St. Louis, MO). Samples were incubated for 30 min. at RT, and then analyzed on a BD FACSCalibur. Fluorescence was read in the FL2 channel, which has a

585/402 nm filter, set and cells were excited with a 488 nm laser. Data was acquired with CellQuest version 3.3 and analyzed with ModFit version 3.1.

ImmunoBlots

Protein harvested from mesothelial cell lines was done by Dr. Melisa Bunderson Schelvan. Dr. Schelvan was also responsible for the contribution of data collected in the p53 and MDM4 Western Blot (Figure 14a). Cells were plated at 90,000 cells/well into 6 well plates for LCD and 300,000 cells/well for HCD and incubated 24 hours. At time of protein harvest, LCD samples were ~60% confluent for LCD and HCD samples were >90%. At the time of protein harvest, media was removed and cells were washed with PBS. Cells were harvested in a PBS-TDS lysis buffer (0.1% Triton X-100; 12.6 mM Sodium deoxycholate; 3.7 mM SDS; 1 mM EDTA; and 0.2 mM PMSF containing phosphatase and protease inhibitors (Sigma Alrdich, St Louis, MO). Protein levels were measured using the BioRad Protein DC assay (Bio-Rad, Hercules, CA). Samples were loaded onto a 4-12% Bis-Tris Nupage gel (Invitrogen, Carlsbad, CA) then transferred onto a PVDF membrane (Millipore, Bedford, MA). Membranes were blocked and the primary antibody added. Following incubation with the primary antibody, membranes were washed with PBS and Tween-20 (0.1% Tween-20) (PBS-t (0.1%)), and a goat anti-mouse or goat anti-rabbit secondary antibody was added. Membranes were washed with PBS-T (0.1%) prior to chemiluminescence detection using the Immobilon Detection kit (Millipore, Bedford, MA). Blots were stripped and reprobed for α-Tubulin as a loading control. Antibodies used include: MDM2 (2A10), p21 (C-19), NF2 (A19), and

p53 (DO-1) from Santa Cruz Biotechnology, Santa Cruz, CA; Bax (AM32) from Calbiochem, San Diego, CA; α-Tubulin and β-actin from Sigma-Aldrich, St Louis, MO; and GAPDH from (Cell Signaling, Danvers, MA).

Bromodeoxyuridine (BrdU) Uptake Assay

Cell were seeded at a density of 10,000 cells/well in a 96-well plate and allowed to attach overnight. BrdU labeling reagent was added and cells were allowed to incubate for 3h, 12h, or 24h. The BrdU Cell Proliferation Assay was completed following the manufacturers protocol (Calbiochem, San Diego, CA).

UV Exposure

For experiments utilizing UV exposure to induce DNA damage for protein expression changes, cells were plated in 6 well culture dishes at 90,000 cells/well. The next day, media was removed and wells were covered with 500 μl PBS. Cells were placed in a Stratagene Stratalinker 1800 with no plate covers and then exposed to 5J/m^2. Following exposure, PBS was removed and replaced with media. Cells were incubated at 37°C for 3 hours, media was removed, cells were washed with PBS, and protein was harvested in protein lysis buffer as previously described.

For apoptosis UV exposures, media was removed from incubated cells and replace with 100ul of PBS. After cells were placed in the Stratagene Stratalinker 1800, covers of plates were removed and plates were then exposed to 5J/m^2. PBS was removed and replaced with fresh, and the cells were incubated at 37°C for 24 hours.

Camptothecin Exposure

Camptothecin was prepared in DMSO at 20 mg/ml. For exposure, the prepared solution was diluted into regular media to 6 ug/ml. At time of exposure, media was removed from wells, cells were washed once with 100 μL of PBS, and 100 μL of camptothecin-media was added to the wells. Cells were incubated at 37°C for 3 hours.

TiterTacs Apoptosis Assay

Cells were plated in triplicate in two 96 well plates (one plate for UV exposure, one plate served as no exposure control) at 40,000 cells/well. 48 hours after plating, cells were exposed to either UV or Camptothecin. TiterTacs (Trevigen, Helgerman, CT) was used according to manufacturers protocol to assess DNA fragmentation.

LDH Assay

Cells were plated in triplicate in two 96 well plates (one plate for UV exposure, one plate served as no exposure control) at 40,000 cells/well. 48 hours after plating, cells were exposed to either UV or Camptothecin. The LDH-Cytotoxicity Assay Kit (BioVision, Mountain View, CA) was used according to manufacturers protocol to assess cell death or cytotoxicity.

References

Altomare, D.A., Vaslet, C.A., Skele, K.L., De Rienzo, A., Devarajan, K., Jhanwar, S.C., McClatchey, A.I., Kane, A.B., and Testa, J.R. 2005. A mouse model recapitulating molecular features of human mesothelioma. *Cancer Res* **65**(18): 8090-8095.

Bali, A., O'Brien, P.M., Edwards, L.S., Sutherland, R.L., Hacker, N.F., and Henshall, S.M. 2004. Cyclin D1, p53, and p21Waf1/Cip1 expression is predictive of poor clinical outcome in serous epithelial ovarian cancer. *Clin Cancer Res* **10**(15): 5168-5177.

Bartkova, J., Lukas, J., Strauss, M., and Bartek, J. 1995. Cyclin D1 oncoprotein aberrantly accumulates in malignancies of diverse histogenesis. *Oncogene* **10**(4): 775-778.

Brooks, C.L. and Gu, W. 2006. p53 ubiquitination: Mdm2 and beyond. *Mol Cell* **21**(3): 307-315.

Chin, L., Pomerantz, J., and DePinho, R.A. 1998. The INK4a/ARF tumor suppressor: one gene--two products--two pathways. *Trends Biochem Sci* **23**(8): 291-296.

Coupland, S.E., Anastassiou, G., Stang, A., Schilling, H., Anagnostopoulos, I., Bornfeld, N., and Stein, H. 2000. The prognostic value of cyclin D1, p53, and MDM2 protein expression in uveal melanoma. *J Pathol* **191**(2): 120-126.

Danovi, D., Meulmeester, E., Pasini, D., Migliorini, D., Capra, M., Frenk, R., de Graaf, P., Francoz, S., Gasparini, P., Gobbi, A., Helin, K., Pelicci, P.G., Jochemsen, A.G., and Marine, J.C. 2004. Amplification of Mdmx (or Mdm4) directly contributes to tumor formation by inhibiting p53 tumor suppressor activity. *Mol Cell Biol* **24**(13): 5835-5843.

Diehl, J.A. 2002. Cycling to cancer with cyclin D1. *Cancer Biol Ther* **1**(3): 226-231.

Gottlieb, T.M. and Oren, M. 1998. p53 and apoptosis. *Semin Cancer Biol* **8**(5): 359-368.

Guinee, D.G. and Allen, T.C. 2008. Primary pleural neoplasia: entities other than diffuse malignant mesothelioma. *Arch Pathol Lab Med* **132**(7): 1149-1170.

Jaurand, M.C. and Fleury-Feith, J. 2005. Pathogenesis of malignant pleural mesothelioma. *Respirology* **10**(1): 2-8.

Kelekar, A. and Thompson, C.B. 1998. Bcl-2-family proteins: the role of the BH3 domain in apoptosis. *Trends Cell Biol* **8**(8): 324-330.

Kim, H., Kwak, N.J., Lee, J.Y., Choi, B.H., Lim, Y., Ko, Y.J., Kim, Y.H., Huh, P.W., Lee, K.H., Rha, H.K., and Wang, Y.P. 2004. Merlin neutralizes the inhibitory effect of Mdm2 on p53. *J Biol Chem* **279**(9): 7812-7818.

Knudsen, K.E., Diehl, J.A., Haiman, C.A., and Knudsen, E.S. 2006. Cyclin D1: polymorphism, aberrant splicing and cancer risk. *Oncogene* **25**(11): 1620-1628.

Kumar, K., Rahman, Q., Schipper, H., Matschegewski, C., Schiffmann, D., and Papp, T. 2005. Mutational analysis of 9 different tumour-associated genes in human malignant mesothelioma cell lines. *Oncol Rep* **14**(3): 743-750.
Kumar, P. and Kratzke, R.A. 2005. Molecular prognostic markers in malignant mesothelioma. *Lung Cancer* **49 Suppl 1**: S53-60.
Ladha, M.H., Lee, K.Y., Upton, T.M., Reed, M.F., and Ewen, M.E. 1998. Regulation of exit from quiescence by p27 and cyclin D1-CDK4. *Mol Cell Biol* **18**(11): 6605-6615.
Lallemand, D., Curto, M., Saotome, I., Giovannini, M., and McClatchey, A.I. 2003. NF2 deficiency promotes tumorigenesis and metastasis by destabilizing adherens junctions. *Genes Dev* **17**(9): 1090-1100.
Lane, D.P. 1992. Cancer. p53, guardian of the genome. *Nature* **358**(6381): 15-16.
Levine, A.J. 1997. p53, the cellular gatekeeper for growth and division. *Cell* **88**(3): 323-331.
Lukas, J., Pagano, M., Staskova, Z., Draetta, G., and Bartek, J. 1994. Cyclin D1 protein oscillates and is essential for cell cycle progression in human tumour cell lines. *Oncogene* **9**(3): 707-718.
Marine, J.C. and Jochemsen, A.G. 2005. Mdmx as an essential regulator of p53 activity. *Biochem Biophys Res Commun* **331**(3): 750-760.
Martuza, R.L. and Eldridge, R. 1988. Neurofibromatosis 2 (bilateral acoustic neurofibromatosis). *N Engl J Med* **318**(11): 684-688.
May, P. and May, E. 1999. Twenty years of p53 research: structural and functional aspects of the p53 protein. *Oncogene* **18**(53): 7621-7636.
McClatchey, A.I. 2003. Merlin and ERM proteins: unappreciated roles in cancer development? *Nat Rev Cancer* **3**(11): 877-883.
McClatchey, A.I. and Giovannini, M. 2005. Membrane organization and tumorigenesis--the NF2 tumor suppressor, Merlin. *Genes Dev* **19**(19): 2265-2277.
Michael, D. and Oren, M. 2002. The p53 and Mdm2 families in cancer. *Curr Opin Genet Dev* **12**(1): 53-59.
Miyashita, T. and Reed, J.C. 1995. Tumor suppressor p53 is a direct transcriptional activator of the human bax gene. *Cell* **80**(2): 293-299.
Moll, U.M., Ostermeyer, A.G., Haladay, R., Winkfield, B., Frazier, M., and Zambetti, G. 1996. Cytoplasmic sequestration of wild-type p53 protein impairs the G1 checkpoint after DNA damage. *Mol Cell Biol* **16**(3): 1126-1137.
Morrison, H., Sherman, L.S., Legg, J., Banine, F., Isacke, C., Haipek, C.A., Gutmann, D.H., Ponta, H., and Herrlich, P. 2001. The NF2 tumor suppressor gene product, merlin, mediates contact inhibition of growth through interactions with CD44. *Genes Dev* **15**(8): 968-980.
Murthy, S.S. and Testa, J.R. 1999. Asbestos, chromosomal deletions, and tumor suppressor gene alterations in human malignant mesothelioma. *J Cell Physiol* **180**(2): 150-157.

Oliner, J.D., Kinzler, K.W., Meltzer, P.S., George, D.L., and Vogelstein, B. 1992. Amplification of a gene encoding a p53-associated protein in human sarcomas. *Nature* **358**(6381): 80-83.

Oren, M. 1999. Regulation of the p53 tumor suppressor protein. *J Biol Chem* **274**(51): 36031-36034.

Pomerantz, J., Schreiber-Agus, N., Liegeois, N.J., Silverman, A., Alland, L., Chin, L., Potes, J., Chen, K., Orlow, I., Lee, H.W., Cordon-Cardo, C., and DePinho, R.A. 1998. The Ink4a tumor suppressor gene product, p19Arf, interacts with MDM2 and neutralizes MDM2's inhibition of p53. *Cell* **92**(6): 713-723.

Reale, F.R., Griffin, T.W., Compton, J.M., Graham, S., Townes, P.L., and Bogden, A. 1987. Characterization of a human malignant mesothelioma cell line (H-MESO-1): a biphasic solid and ascitic tumor model. *Cancer Res* **47**(12): 3199-3205.

Rusch, V.W. 1995. Clinical features and current treatment of diffuse malignant pleural mesothelioma. *Lung Cancer* **12 Suppl 2**: S127-146.

Ryan, C.W., Herndon, J., and Vogelzang, N.J. 1998. A review of chemotherapy trials for malignant mesothelioma. *Chest* **113**(1 Suppl): 66S-73S.

Sainio, M., Zhao, F., Heiska, L., Turunen, O., den Bakker, M., Zwarthoff, E., Lutchman, M., Rouleau, G.A., Jaaskelainen, J., Vaheri, A., and Carpen, O. 1997. Neurofibromatosis 2 tumor suppressor protein colocalizes with ezrin and CD44 and associates with actin-containing cytoskeleton. *J Cell Sci* **110 (Pt 18)**: 2249-2260.

Sekido, Y., Pass, H.I., Bader, S., Mew, D.J., Christman, M.F., Gazdar, A.F., and Minna, J.D. 1995. Neurofibromatosis type 2 (NF2) gene is somatically mutated in mesothelioma but not in lung cancer. *Cancer Res* **55**(6): 1227-1231.

Sherman, L., Xu, H.M., Geist, R.T., Saporito-Irwin, S., Howells, N., Ponta, H., Herrlich, P., and Gutmann, D.H. 1997. Interdomain binding mediates tumor growth suppression by the NF2 gene product. *Oncogene* **15**(20): 2505-2509.

Sherman, L.S. and Gutmann, D.H. 2001. Merlin: hanging tumor suppression on the Rac. *Trends Cell Biol* **11**(11): 442-444.

Toledo, F. and Wahl, G.M. 2006. Regulating the p53 pathway: in vitro hypotheses, in vivo veritas. *Nat Rev Cancer* **6**(12): 909-923.

Trofatter, J.A., MacCollin, M.M., Rutter, J.L., Murrell, J.R., Duyao, M.P., Parry, D.M., Eldridge, R., Kley, N., Menon, A.G., Pulaski, K., and et al. 1993. A novel moesin-, ezrin-, radixin-like gene is a candidate for the neurofibromatosis 2 tumor suppressor. *Cell* **72**(5): 791-800.

Tsukita, S., Oishi, K., Sato, N., Sagara, J., and Kawai, A. 1994. ERM family members as molecular linkers between the cell surface glycoprotein CD44 and actin-based cytoskeletons. *J Cell Biol* **126**(2): 391-401.

Xiao, G.H., Gallagher, R., Shetler, J., Skele, K., Altomare, D.A., Pestell, R.G., Jhanwar, S., and Testa, J.R. 2005. The NF2 tumor suppressor gene product, merlin, inhibits cell proliferation and cell cycle progression by repressing cyclin D1 expression. *Mol Cell Biol* **25**(6): 2384-2394.

Zhang, X.C., Chen, J., Su, C.H., Yang, H.Y., and Lee, M.H. 2008. Roles for CSN5 in control of p53/MDM2 activities. *J Cell Biochem* **103**(4): 1219-1230.

CHAPTER 3

Intratracheal Injection of Asbestos in NF2$^{+/-}$ Mice Provides Insight into Cancer Susceptibility

Abstract

The neurofibromatosis type 2 gene (*Nf2*) was discovered in 1993 and shown to harbor inactivating mutations in representative tumors from neurofibromatosis 2 patients. *Nf2* is implicated in the development of other tumor types, including malignant mesotheliomas. These mesodermally derived, primarily pleural tumors display loss of chromosome 22 as one of the most common cytogenetic abnormalities. The role of *Nf2* in maintaining normal cellular growth may be through many possible signal transduction mechanisms, including CD44 and extracellular matrix, Rac-1 proteins, and MDM2. Previous studies have been shown that mice hemizygous for *Nf2* display an increased susceptibility for asbestos-induced peritoneal tumors. Thus, *Nf2* may play a central role in growth regulation in mesothelial cells.

Introduction

Malignant mesothelioma is an aggressive tumor that forms from the serous membranes lining the pleural, peritoneal, and pericardial cavities (Baser et al. 2002; Dunitz 2002; Cugell and Kamp 2004; Robinson et al. 2005; Tan and Treasure 2005; Yang et al. 2008). Mesothelioma tumor development is heavily linked to prior exposure to the fibrous mineral, asbestos, accounting for about 80% of mesothelioma cases (Wagner et al. 1960; Tweedale 2002; Cugell and Kamp 2004; Jaurand and Fleury-Feith 2005; Yang et al. 2008). The main route for exposure to asbestos is through inhalation of the fibers. Due to this common route of exposure, the pleural space surrounding the lungs is the most commonly affected mesothelial cavity, with about 70% to 95% of individuals diagnosed with the disease presenting with pleural mesothelioma (Hammar 2006; Bridda et al. 2007; Yang et al. 2008).

Investigations conducted by Fleury-Feith and colleagues (2005) showed the susceptibility of *Nf2* hemizygous mice to develop peritoneal mesotheliomas following exposure to a total of 5 mg of crocidolite asbestos via intraperitoneal injections. In their studies, mice were exposed on two different occasions, with a lag time of 2-3 months between exposures, to asbestos. This study clearly showed the role for *Nf2* in peritoneal mesothelioma development. However, as pleural mesothelioma is the predominant form of the tumor, an exposure method to induce lung injury might serve as a better model for MPM research.

In this study, a heterozygous *Nf2* knockout mouse model was used to closely follow the early events in tumor development. Mice heterozygous for the *Nf2* gene have been shown to be predisposed to the development of mesothelioma, as only one allele remains to be inactivated. *Nf2* is an autosomal dominant TSG, thus by Knudson's Two-Hit Hypothesis, inactivation of both alleles is necessary for loss of merlin function (Knudson 1971). *Nf2* homozygosity is embryonically lethal, with mice carrying this genotype dying before initiation of gastrulation (McClatchey et al. 1997). For this study, hemizygous *Nf2* knockout mice were used, and cellular and gene expression changes in the exposed lungs were monitored. The hypothesis of this *in vivo* study is that mice lacking a full complement of *Nf2* genes will develop tumors at earlier ages and in a larger percentage of animals than in control animals.

Results

Inhalation of asbestos fibers is considered the main route of human exposure to the particles, which occurs when the fibers are disturbed and become airborne (ATSDR ; Tweedale 2002). Those fibers that are not expelled can become lodged in the lung, and can continue to cause irritation over time. To best mimic this exposure route while still maintaining a controlled dose of asbestos, intratracheal injections (IT) were performed on mice using PBS as a vehicle. Both *Nf2*$^{+/+}$ mice and *Nf2*$^{+/-}$ mice were instilled with 100 μg of either crocidolite asbsestos or Libby 6 Mix amphibole asbestos. Crocidolite asbestos was used for exposures as it is generally considered the most hazardous of the amphibole fibers. Libby 6 mix amphibole is a mixture of six different samples collected from the Libby, MT mine site (Bellamy and Gunter 2008). The latency for MPM development is long (20 to 40 years). This means that even after exposure has stopped, asbestos fibers that have become lodged in the lung continue to irritate the lung, thus promoting disease over a long period of time. Thus, to mimic this latency period, after IT injections mice were monitored for a 12 month period. Following euthanasia, gross anatomy was examined and lungs were harvested for histological evaluation.

In the event that mice died before the chosen time point, or if mice needed to be sacrificed early if illness was detected, necropsy was performed and tissue was harvested for histology if possible. Of these necropsied mice, the most common event was the occurrence of osteosarcoma formation. Osteosarcoma

development was most commonly found to occur in the *Nf2*$^{+/-}$ mice and was independent of exposure type. Many groups have found that *Nf2*$^{+/-}$ mice are prone to the development of malignant tumors, in particular osteosarcoma, but these occurences are not related to loss of NF2 function (McClatchey et al. 1998; Fleury-Feith et al. 2003; McClatchey 2003; Altomare et al. 2005; Lecomte et al. 2005). Only one of the mice that died before the 12 month time point had been reached was found to have an abnormal growth on its lung, which upon gross anatomical evaluation resembled a localized, nodular mesothelioma (Figure 20). This mouse had been exposed to Libby 6 Mix amphible asbestos and was *Nf2*$^{+/-}$.

FIGURE 20

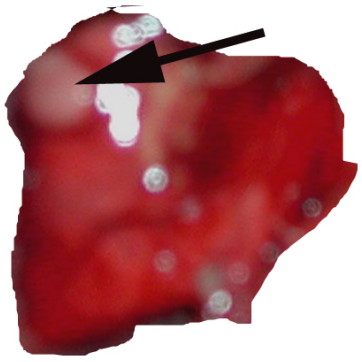

Figure 20. Gross anatomy of mouse lung from a heterozygous mouse exposed to asbestos.

The arrow points to the nodular area, that could be in this case a localized mesothelioma or pleural plaque, located on the right lung of the mouse. This was a heterzygous *Nf2* mouse exposed to Libby 6 mix amphibole asbestos. The mouse was exposed on 5/31/07 and died on 12/10/07.

Initially for mouse instillations, different groups of mice were instilled on four different occasions throughout the instillation year. Following the preliminary analysis of tissue from the first two 12 month instillation groups, we decided to include a 15 month exposure group by extending the time point for some of the mice. Changes in the structure of the lung were identified using H&E staining, which allows cell type identification as well as incidences of cellular hyperplasia. In general, the most common type of pathology identified in mouse lungs from the 12 month group were multifocal areas of epithelial cell proliferation. The areas of the lung where this pathology was most prevelent were focused around bronchioles and small airways. These lesions were regarded as hyperplastic. In addition to pre-neoplastic regions, there were fibrotic regions, as well as perivascular and peribronchiolar aggragates of lymphocytes (Figure 21). A portion of the slides from this group are still under evaluation by Dr. Donald Gardner, a pathologist at Rocky Mountain Laboratories.

FIGURE 21

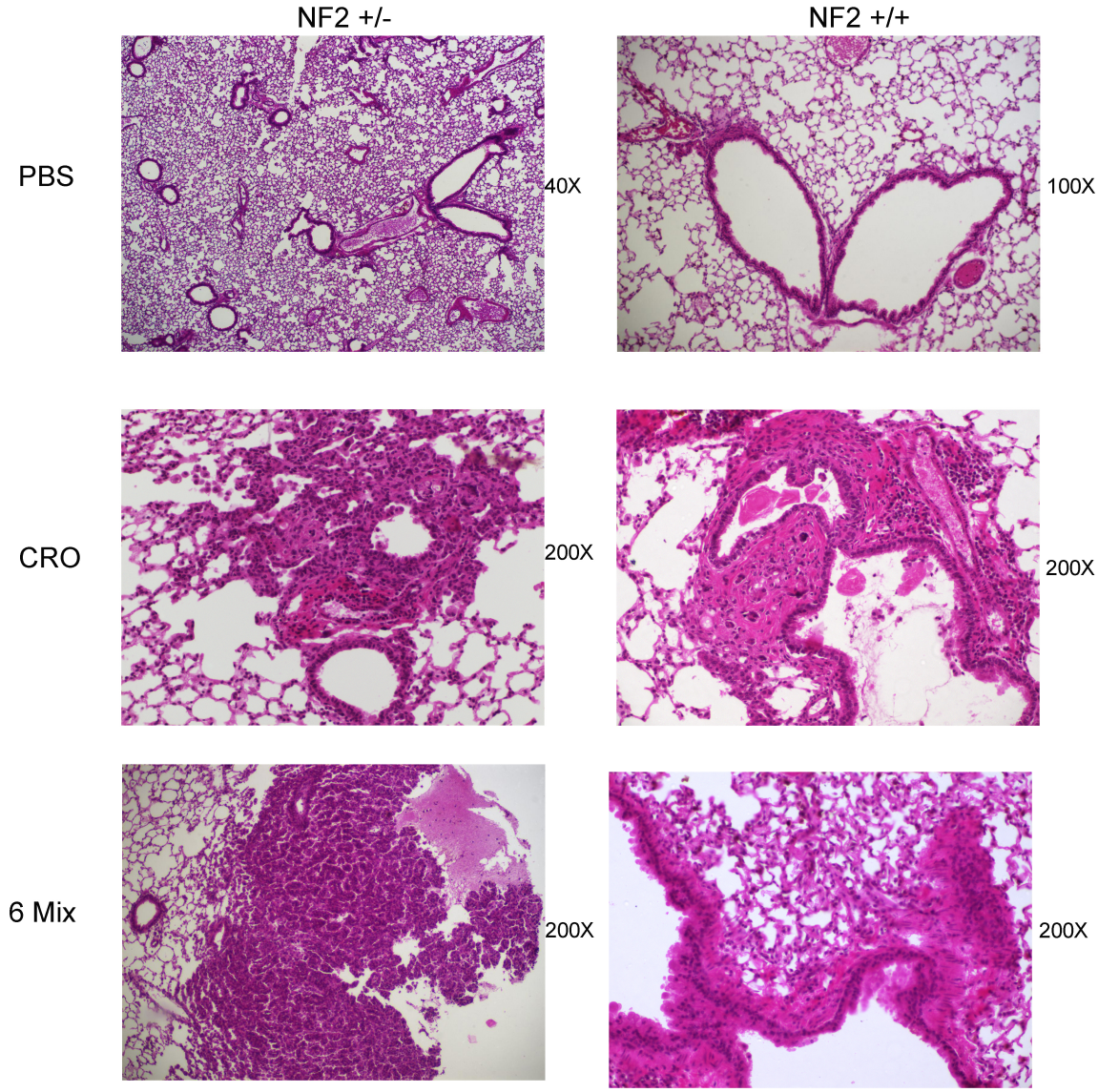

Figure 21. H&E stained sections of 12 month mouse lungs.

Images of slides stained with H&E from mice involved in 12 month exposure study. PBS exposed mice from both wild type and heterozygous groups represent lungs classified as normal. Images from 6 Mix Amphibole and crocidolite group depict hyperplasia and thus abnormal lung morphology through disease manifestation. Possible regions of fibrosis can be seen in the crocidolite and 6 mix wild type exposed mice.

Mice sacrificed following a 15 month exposure period appeared to have an increase in gross anatomical lung abnormalities. Autopsies performed at the sacrifice of the mice revealed both nodular and diffuse mesothelioma, as well as possible mice with asbestosis (Figure 22). Again, lungs were processed for histological analysis and stained with H&E to evaluate cellular alterations. As time progressed to the 15 month group, the amount and extent of cell hyperplasia seemed to increase. Various patterns of cell hyperplasia occured, with the predominant form being epithelial cell hyperplasia forming around bronchioles and airways. In addition, lesions of cell hyperplasia occured around arterioles as well. The different types of hyperplastic lesions, i.e. surrounding bronchioles or surrounding arterioles, were independent of exposure type, however again crocidolite seemed to be the most potent inducer of cell proliferation. Some of the stained sections were classified as neoplastic, with the majority of these determined to be adenocarcinomas or bronchogenic carcinomas. However, these regions were not termed mesothelioma tumors based on H&E stains. Again, fibrotic regions and lymphocyte aggregates were found in some tissue (Figure 23) (Gardner 2008). Dr. Gardner is currently evaluating H&E slides for the 15 month group.

FIGURE 22

a)

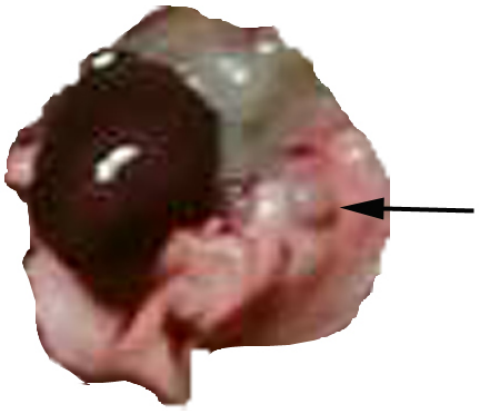

b)

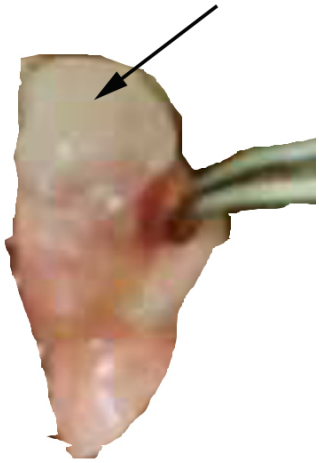

Figure 22. Gross anatomy from 15 month group.

A nodule located on the exterior surface of the left lung of the mouse, which could be a pleural plaque or a localized mesothelioma tumor (22a). Gross anatomical analysis depicting a diffuse mesothelioma on the right lung of a crocidolite exposed mouse (22b).

FIGURE 23

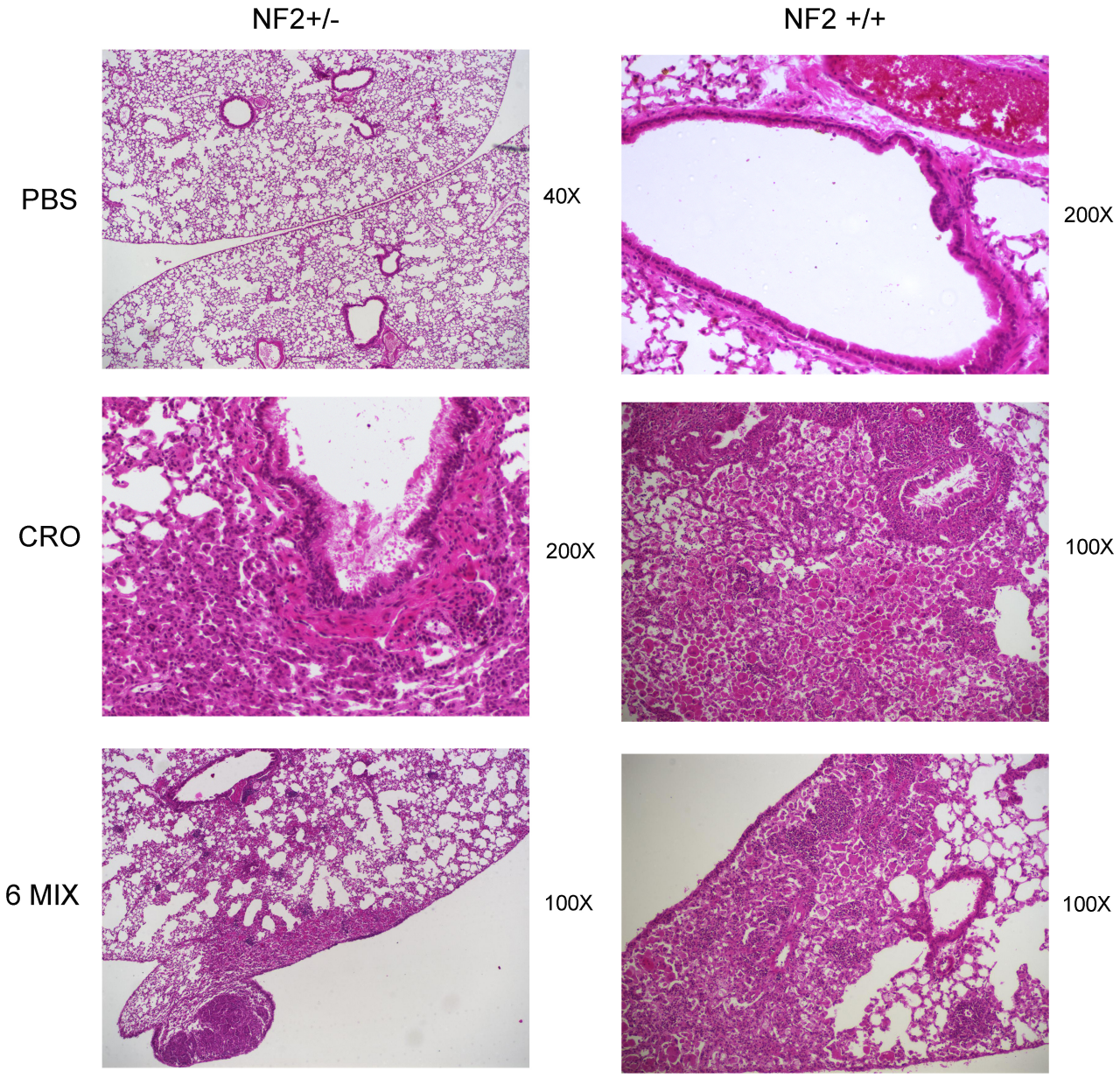

Figure 23. H&E stained sections of 15 month mouse lungs.

Images of slides stained with H&E from mice involved in 15 month exposure study. PBS exposed mice from both wild type and heterozygous groups represent lungs classified as normal. Images from 6 Mix Amphibole and crocidolite group depict hyperplasia and possible neoplastic regions in both wild type and heterozygous mice.

For statistical interpretation of these results, H&E stained sections from each group of mice were sent to Dr. Donald Gardner, a pathologist at Rocky Mountain Laboratories. Dr. Gardner is currently evaluating slides consisting of 6 mice per group for the 12 month exposure group (36 mice total) and 4 mice per group for the 15 month exposure group (24 mice total). Dr. Gardner is blinded to both mouse genotype and exposure type, and will categorize the slides based on the degree of hyperplastic alterations. Until his results arrive, I have scored these slides and graded them for cell hyperplasia. For my evalutation, I scored 3 mice per group per time point. Mice exposed to crocidolite appeared to have an increased amount of cell hyperplasia as compared to PBS and Libby 6 Mix Amphibole asbestos (Figure 24). In addition, as time progressed, the hyperplasia became more severe indicated by increases in average scores for each group. However, *Nf2* genotype appeared to not have an effect on susceptibility to cell transformation.

FIGURE 24

a) 12 Month Scores for Hyperplasia of H&E Stained Slides

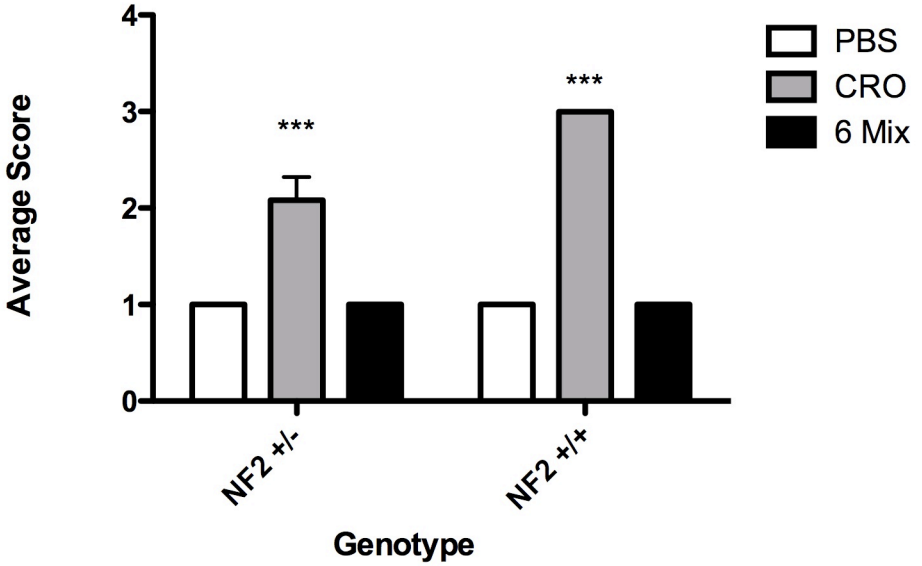

b) 15 Month Scores for Hyperplasia of H&E Stained Slides

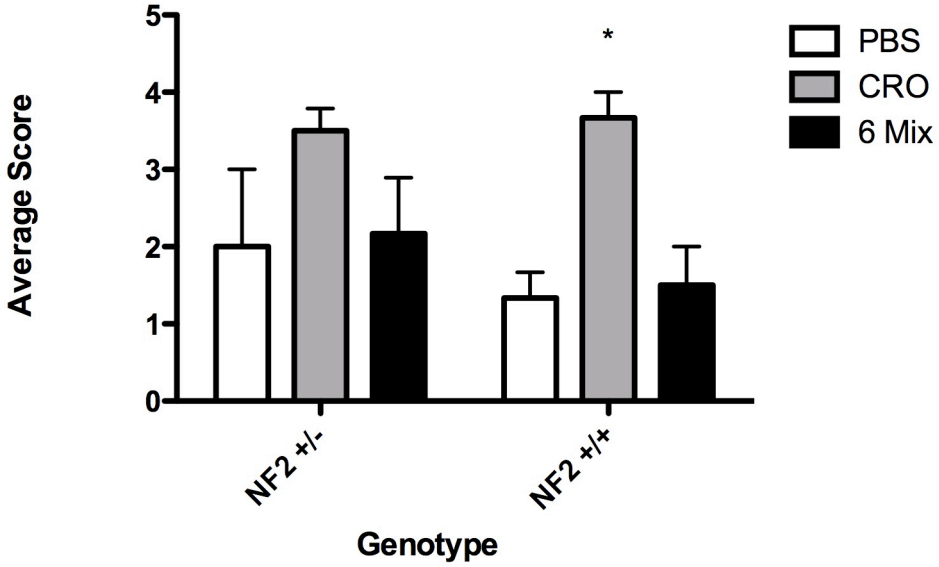

Figure 24. Graphical representation of mouse scores for hyperplasia.

Pathology scores from mice in 12 month group show a significant increase in the amount of hyperplastic lesions in crocidolite exposed mice (24a). Similarly, scores generated from mice in 15 month group showed a significant increase in the amount of hyperplasia compared to PBS control mice, with the average scores in this group higher than those seen in the 12 month group (24b).

All statistics were conducted using slides from three mice per group using Two-way ANOVA.

*$p<0.05$ and ***$p<0.001$

It was necessary to verify merlin expression status in the areas of cellular hyperplasia. Sections of lungs were dual-labeled with both merlin and p21 antibodies to determine protein expression changes, and these images are paired with the adjacent H&E stained section (sections are 7μm apart) in order to better visualize lung morphology. Merlin expression was detected in primarily Clara cells, whereas p21 expression was detected primarily in the smooth muscle cells lining airways and blood vessels (Figure 25a and 25b, respectively). Merlin also labeled cells in the alveolar space, however it is unclear what this cell type is. These cells appear more dense surrounding hyperplastic regions of the lung, and may be Type II pneumocytes (Figure 25c).

FIGURE 25

a)

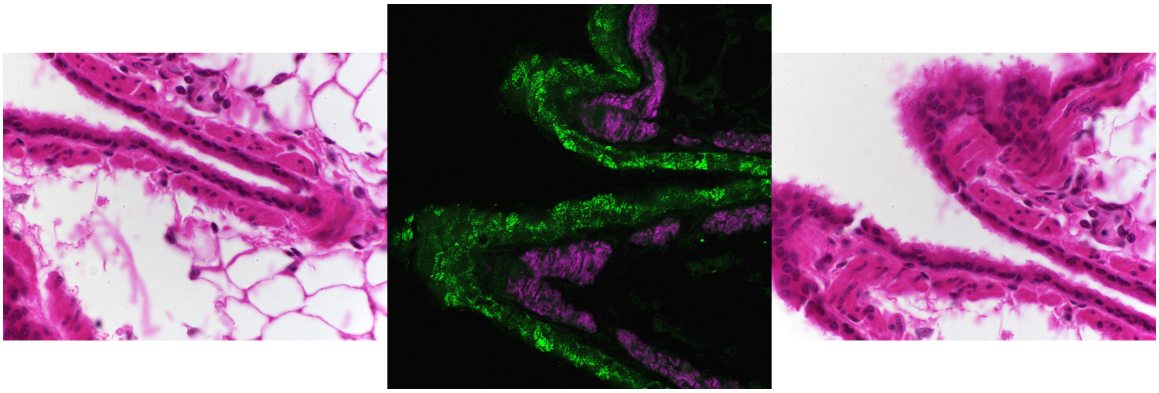

b)

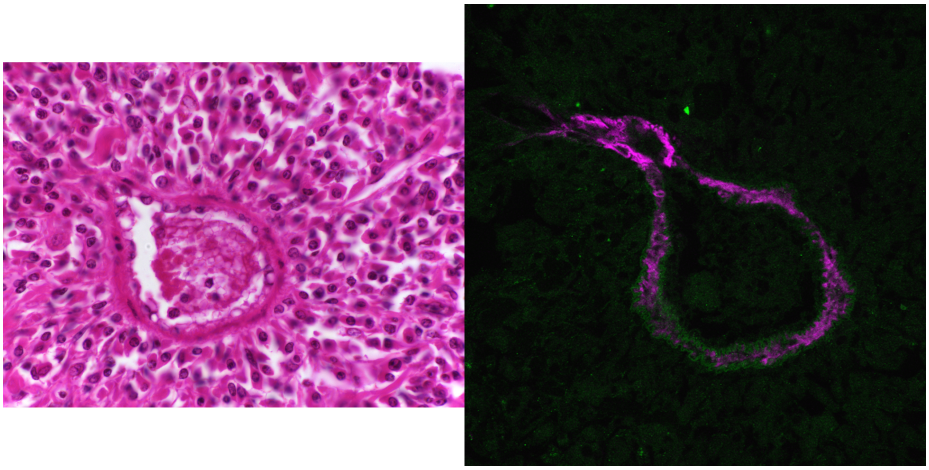

c)

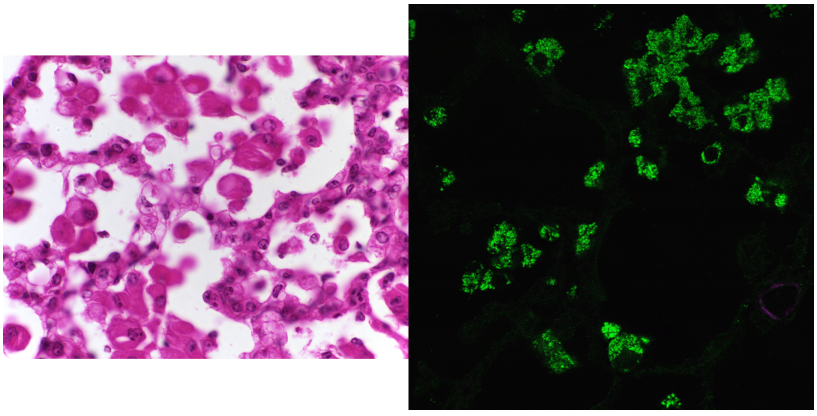

Figure 25. Cell types labeled by merlin and p21 antibodies.

Antibody labeling of merlin appears to be focused in epithelial cells lining the airways. As the predominant cell type in this region in murine lungs is Clara cells, it is likely that Clara cells are expressing merlin. p21 expression appears to be labeling airway smooth muscle cells (25a) (Gardner 2008). p21 expression also labeled smooth muscle cells lining blood vessels in the lung (25b). An additional cell type appears to express merlin in the alveolar spaces of the lung, which I believe may be Type II pneumocytes (25c).

Merlin expression was absent in almost all areas of cell hyperplasia, regardless of initial mouse genotype. However, complete examination of these same tissues revealed that in a non-hyperplastic region of the lung, merlin expression could be detected. Expression of p21 revealed a similar pattern. However, p21 expression was occasionally detected in hyperplastic areas.Loss of expression of both these cell cycle regulators in hyperplastic portions of the tissues is consistent with a model of tumorigenesis due to inactivation of TSGs. Loss seems to have contributed to uncontrolled cell growth and expression appears to be indicative of cells that are still capable of cell cycle exit (i.e. normal phenotype). Figure 26 and Figure 27 are images revealing differential protein expression in the lungs of the treated mice after 12 months and 15 months, respectively.

FIGURE 26

a) NF2 $^{+/-}$ Mice

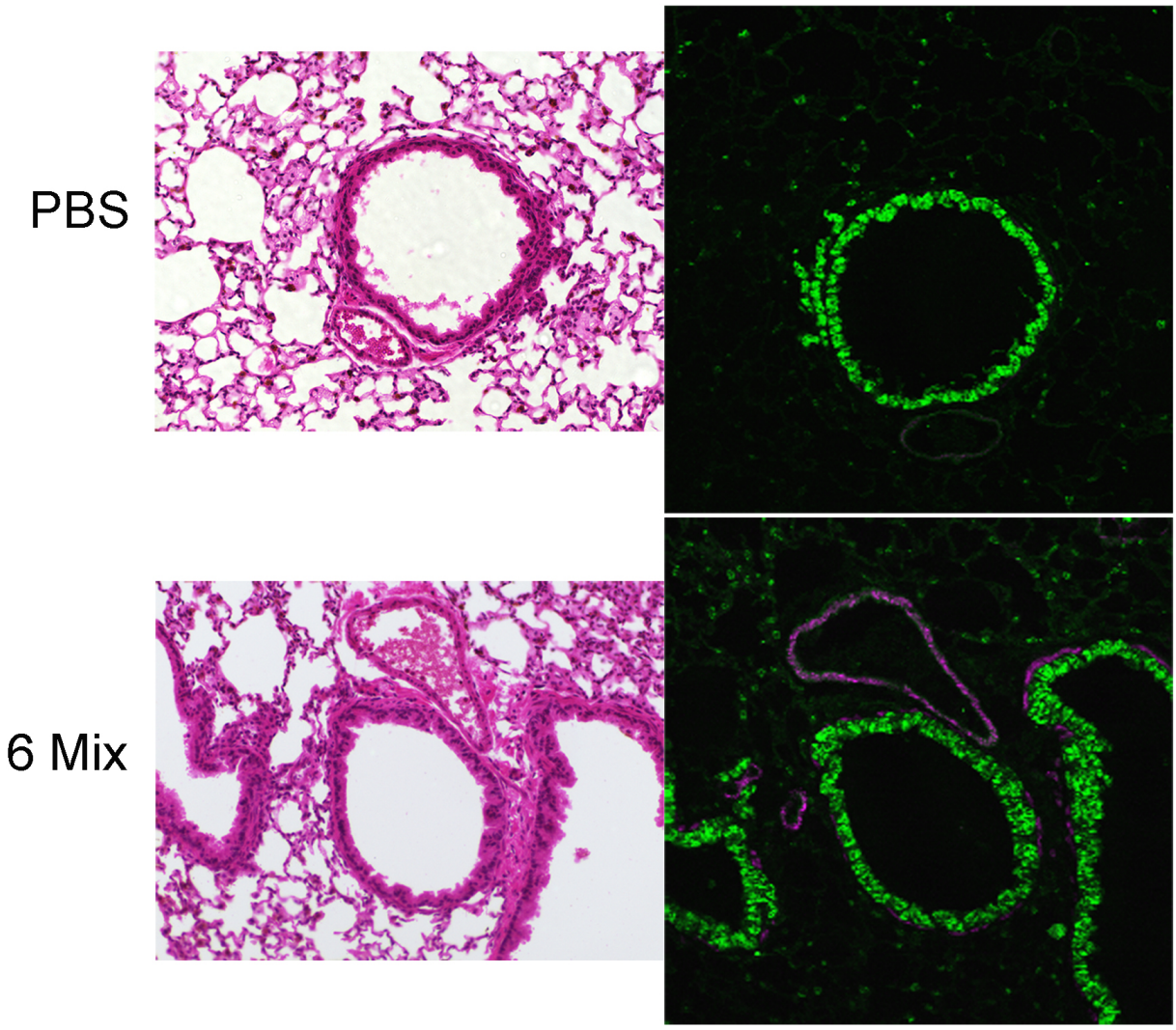

b) NF2 $^{+/-}$ Mice

CRO

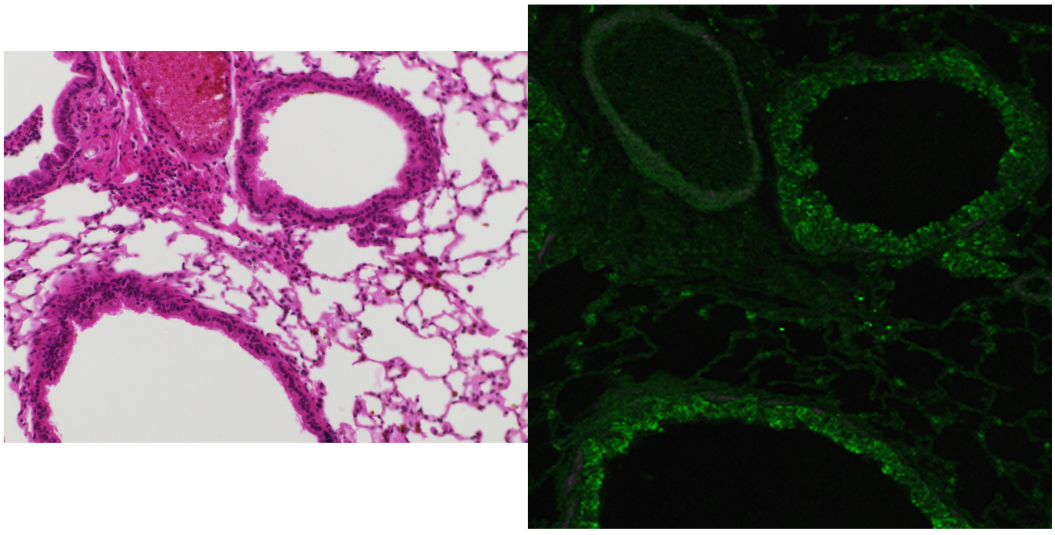

CRO

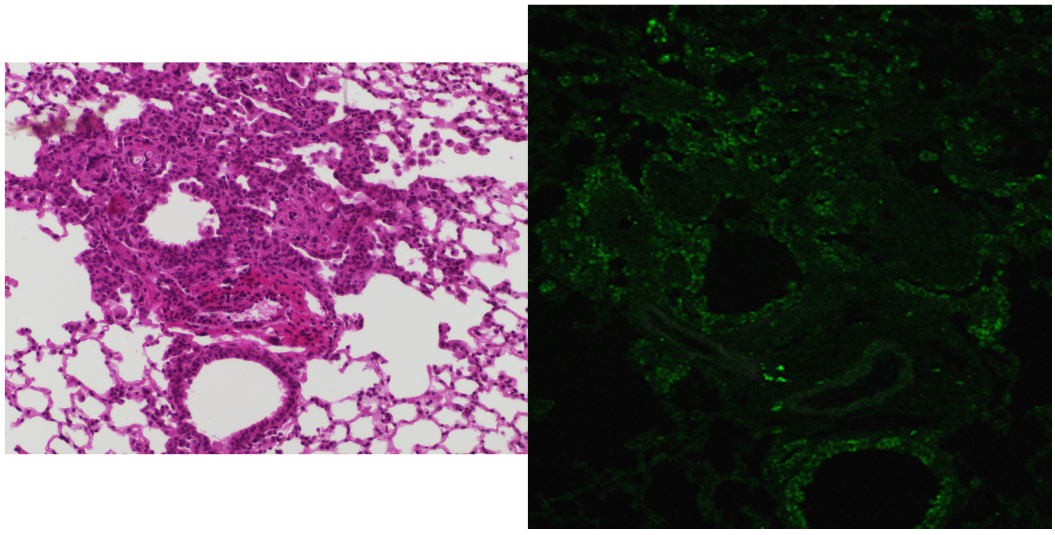

c) NF2 $^{+/+}$ Mice

PBS

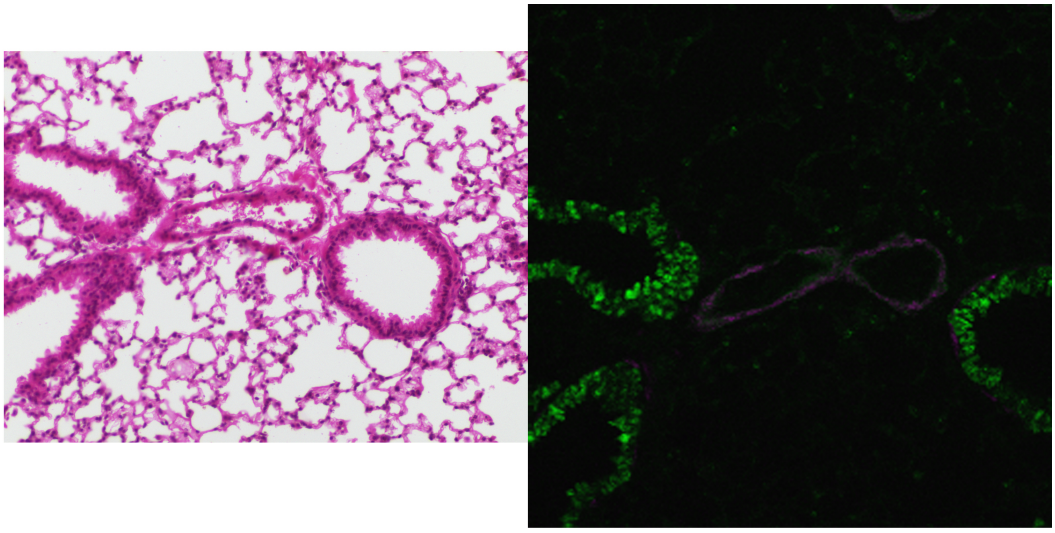

6 Mix

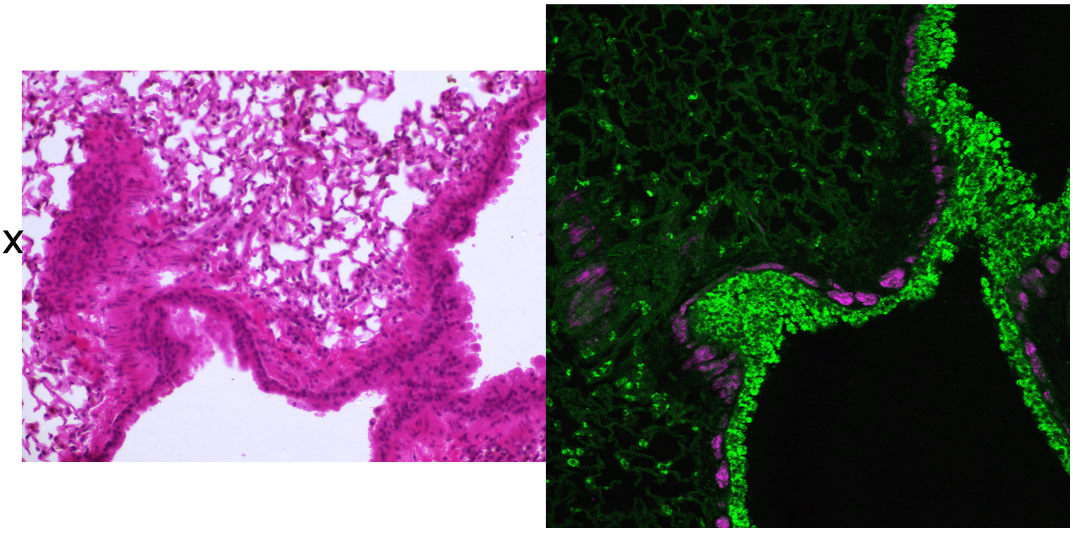

d) NF2 $^{+/+}$ Mice

CRO

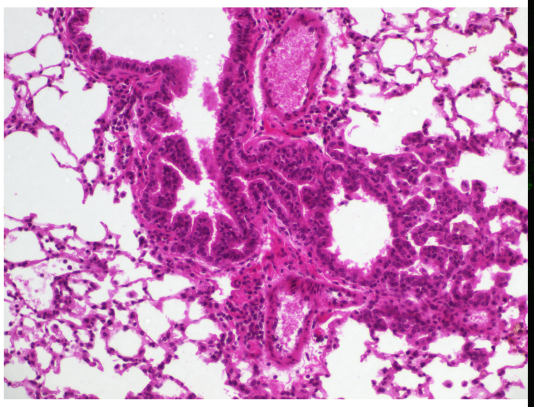

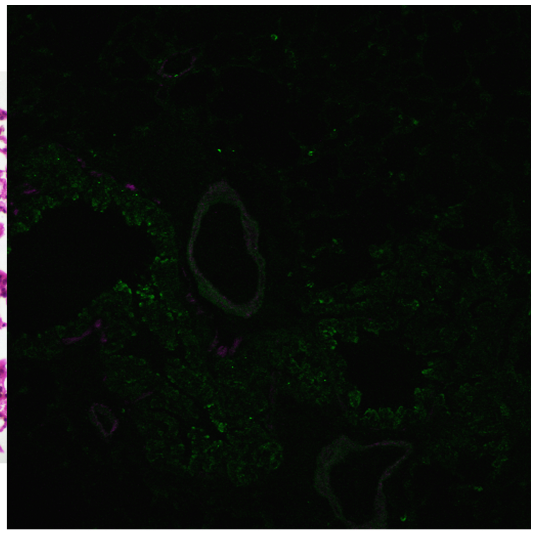

CRO

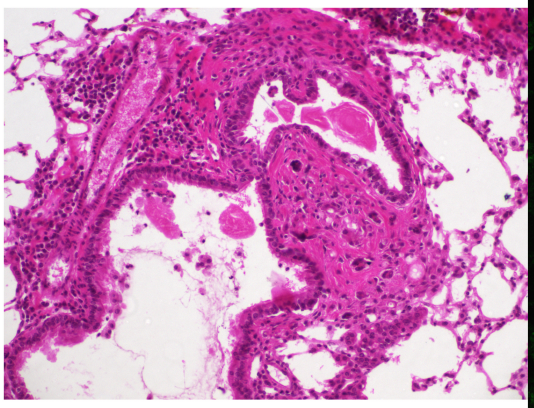

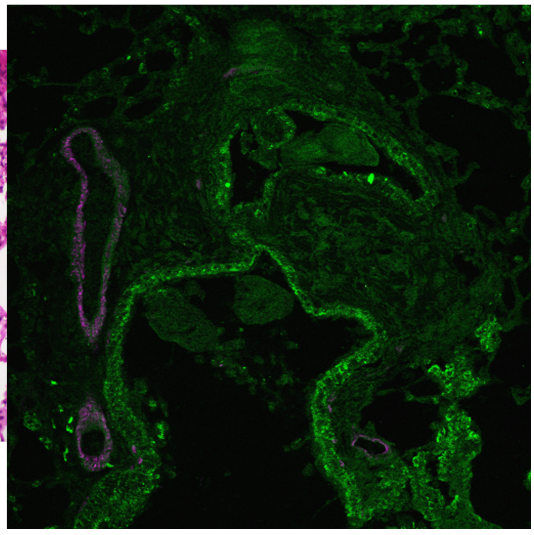

Figure 26. Immunofluorescent labeling of 12 month mouse lungs.

Immunofluorescent labeling of mice exposed to PBS and Libby 6 Mix amphibole shows merlin and p21 co-expression, with minimal p21 expression in the PBS exposed mouse, in a normal region of the lungs of a heterozygous mouse (26a). In contrast, a $NF2^{+/-}$ mouse exposed to crocidolite identifies decreased merlin expression in airway tissue and no p21 expression in hyperplastic areas. These images are from the same mouse section (26b). Analysis of wild-type lung tissue showed decreases in both merlin expression and p21 expression in lung sections of a mouse exposed to PBS. This was consistent across all three samples analyzed (26c). Merlin and p21 expression were detected in the lungs of wild type mice exposed to Libby 6 Mix amphibole (26c). In a hyperplastic region of a crocidolite exposed wild type mouse, merlin and p21 expression was absent. In the same tissue, moving toward an area where a fibrotic response seems to be occuring but not hyperplasia, expression of merlin lining the airways was detected. In this region, there was minimal p21 expression lining the airways, however it was expressed in the smooth muscle cells lining the blood vessels of this region of the lung (26d).

FIGURE 27

a) $NF2^{+/-}$ Mice

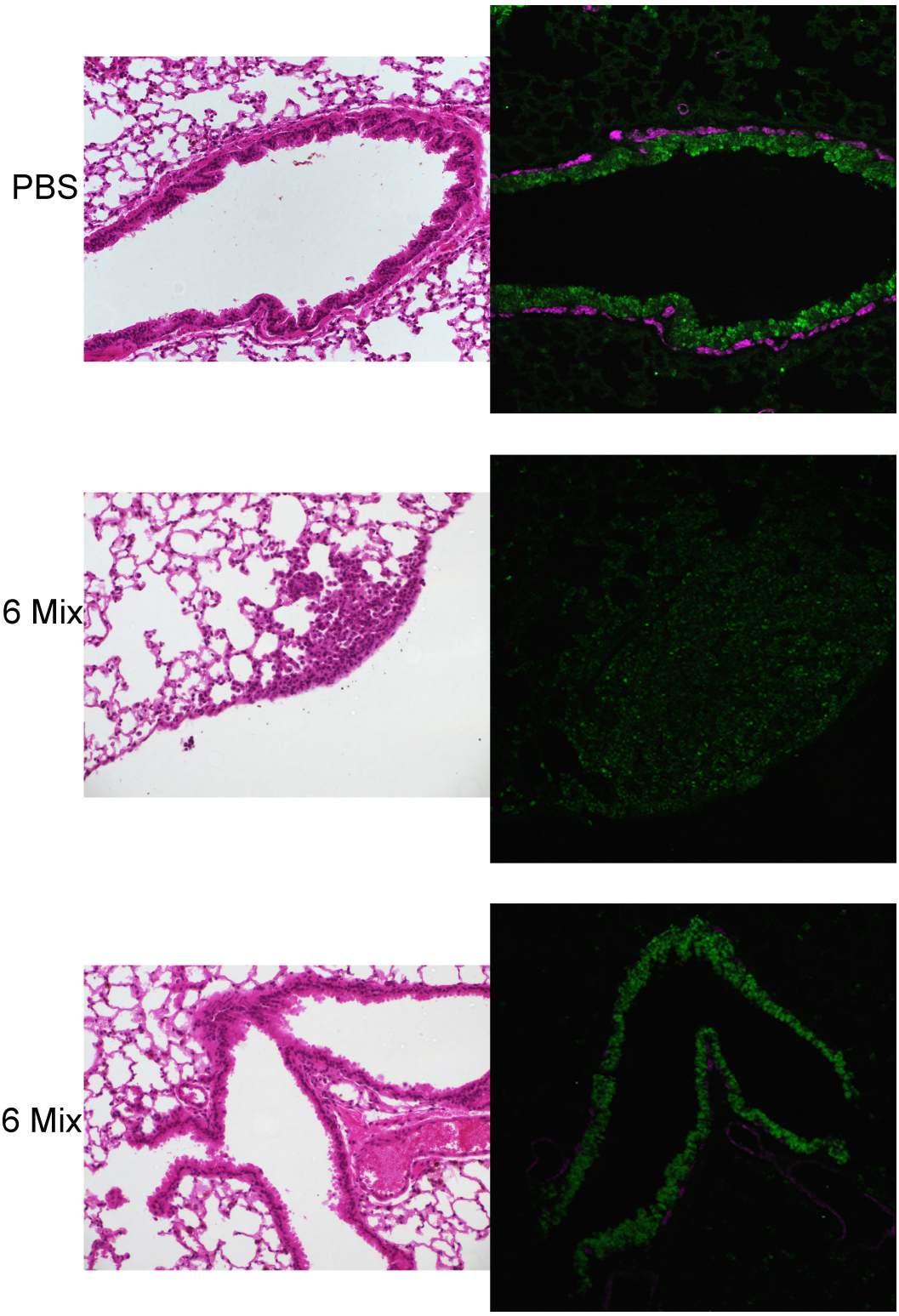

b) $NF2^{+/-}$ Mice

CRO

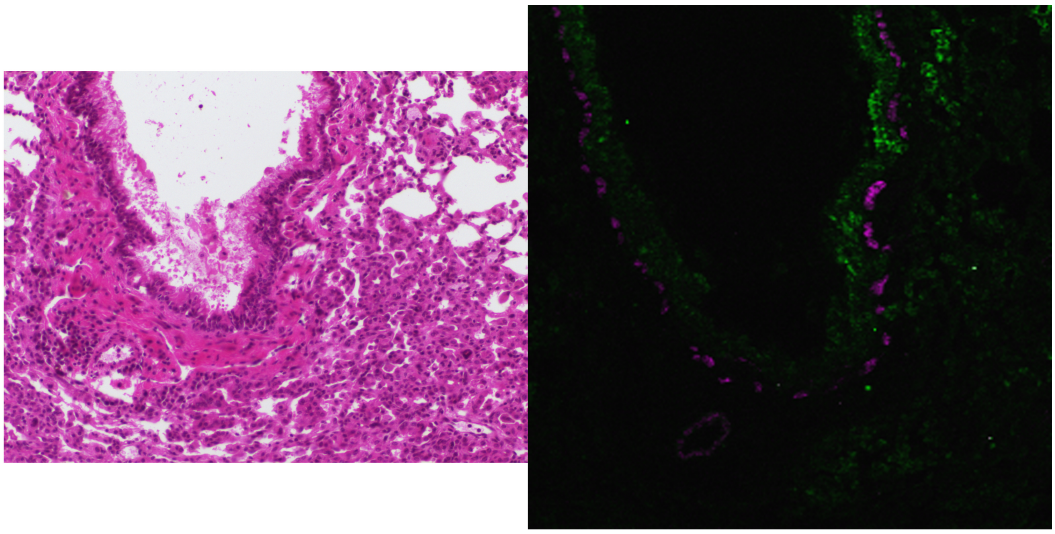

CRO

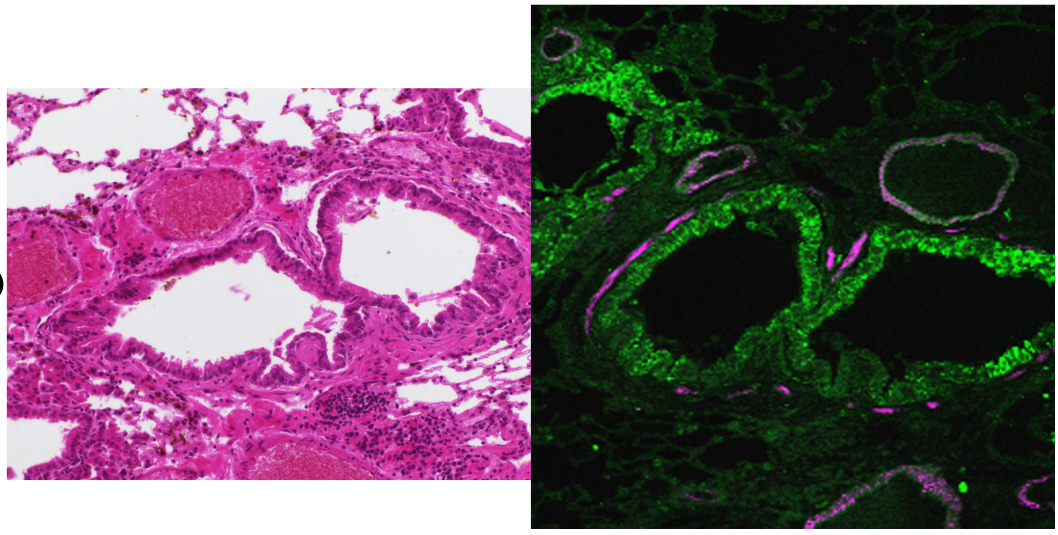

CRO 2

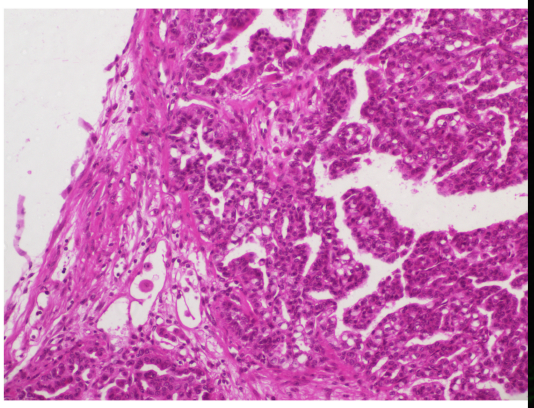

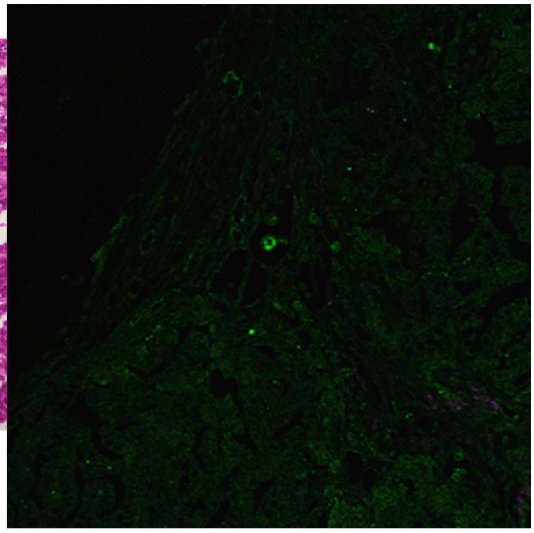

CRO 2

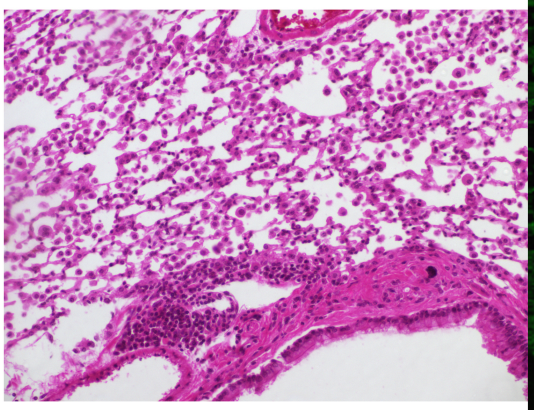

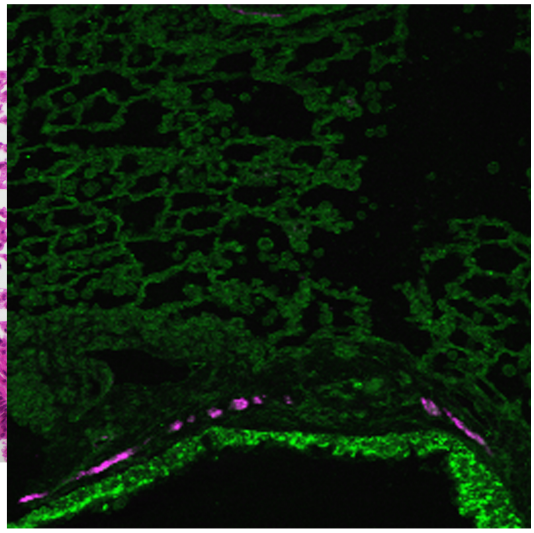

CRO 2

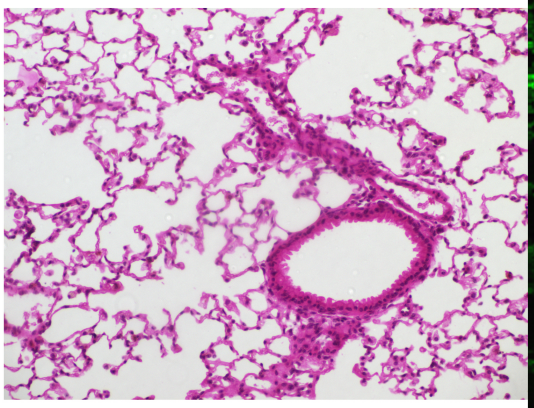

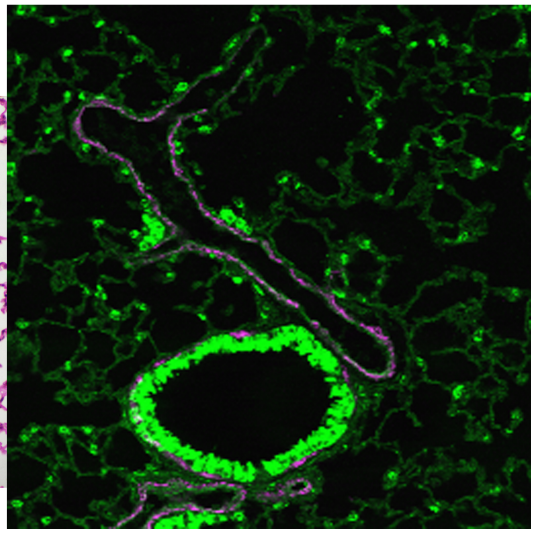

c) $NF2^{+/+}$ Mice

PBS

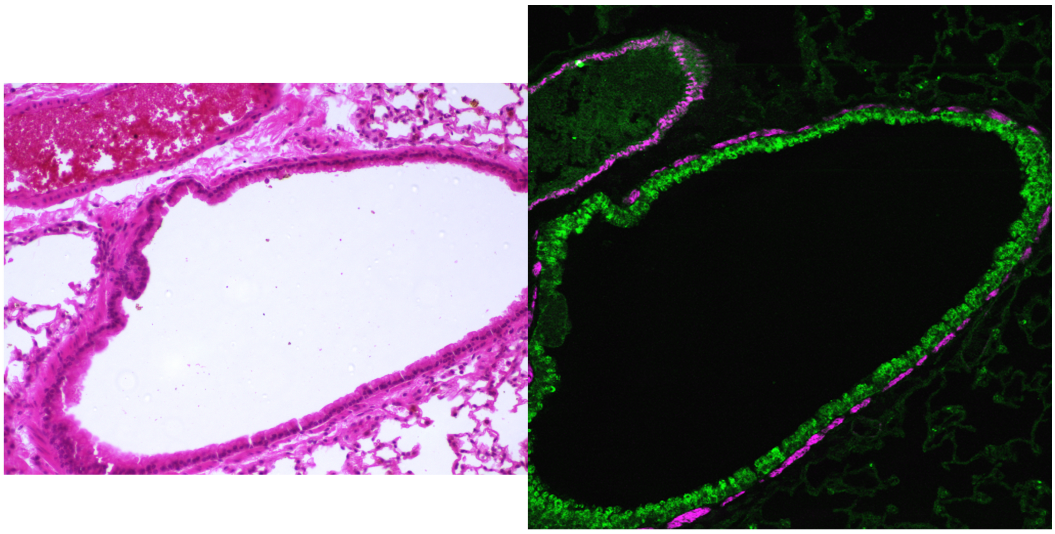

6 Mix

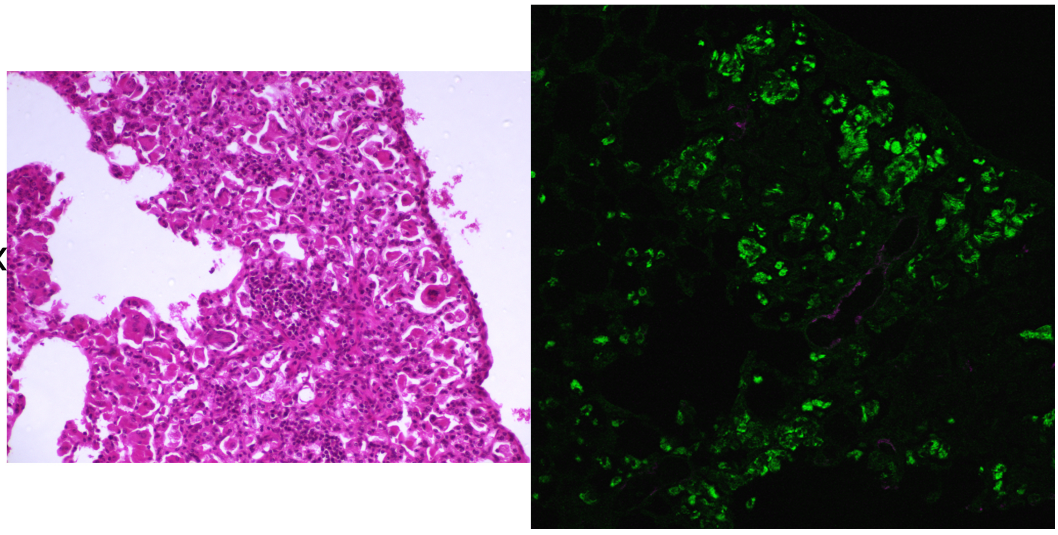

d) NF2$^{+/+}$ Mice

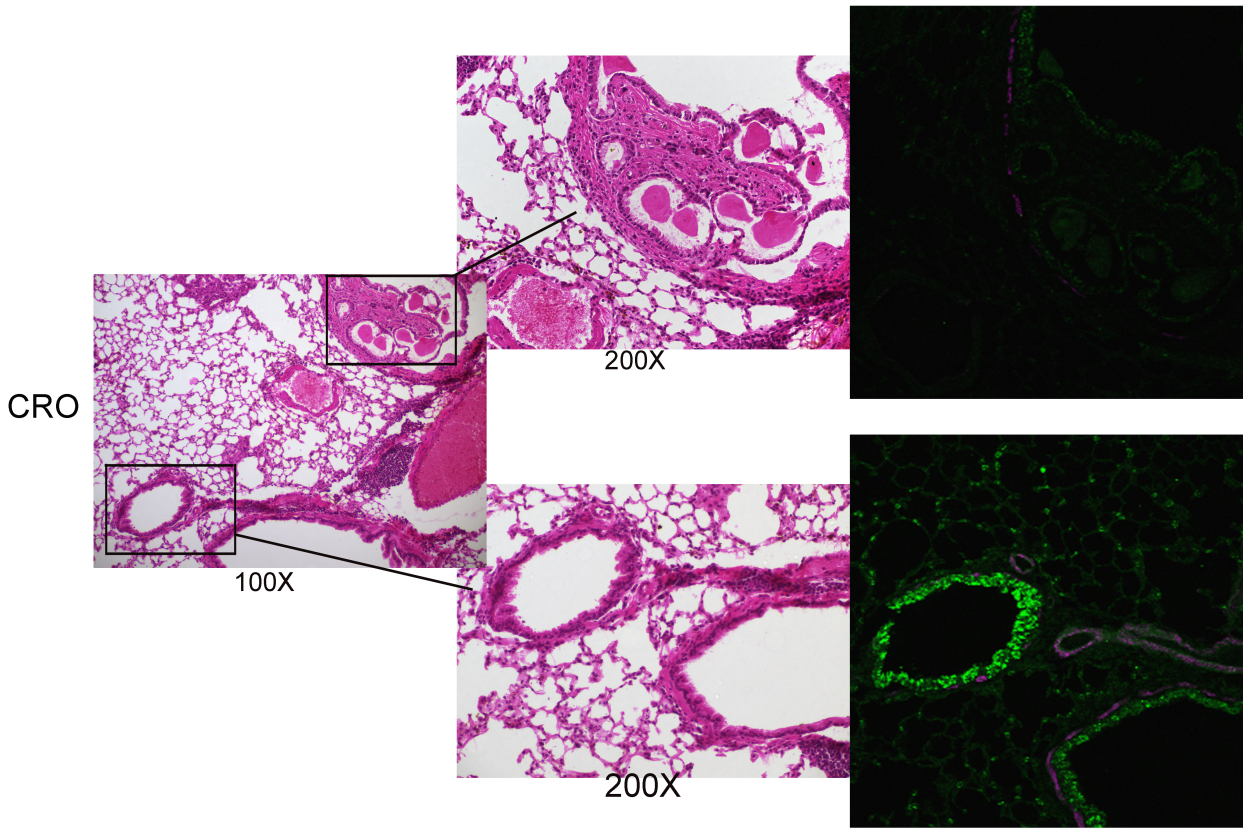

Figure 27. Immunofluorescent labeling of 15 month mouse lungs..

Immunofluorescent labeling of mice exposed to PBS shows frequent merlin and p21 co-expression in a normal region of the lungs of a heterozygous mouse (27a). In a nodular region of a section from a $NF2^{+/-}$ mouse exposed to Libby 6 Mix amphibole, merlin and p21 expression were not detected. In this same section, both merlin and p21 expression were detected around an airway with normal morphology (27a). A $NF2^{+/-}$ mouse exposed to crocidolite (labeled as CRO in figure 27b) identifies decreased merlin expression in a hyperplastic region of an airway, but expression of p21. In this same section, in a region where hyperplasia was not as abundant but a fibrotic response seems to be occuring, both merlin and p21 expression were detected (27b). Images taken from another NF2+/- mouse exposed to crocidolite (labeled as 27b CRO 2) show no labeling of merlin or p21 in a neoplastic region of a lung. Images collected further into the lung start to show p21 and merlin expression. Finally, in a different lobe of the same CRO 2 lung with normal morphology, merlin was highly expressed (27b CRO2 final image). Analysis of wild-type lung tissue showed co-expression of merlin and p21 in lung sections of a mouse exposed to PBS (27c). p21 expression was not detected in the lungs of wild type mice exposed to Libby 6 Mix amphibole in a hyperplastic area, but merlin expression in this region appeared to be labeling a cell type which has not been identified (27c). In a fibrotic region of a crocidolite exposed wild type mouse, merlin and p21 expression were absent. In the same tissue, moving toward an area of more normal lung morphology, both proteins were expressed (27d).

Conclusions

Evidence for the importance of *Nf2* as a TSG in mesothelioma is provided by the occurrence of gene inactivation in the majority of tumor incidences (Sekido et al. 1995; Baser et al. 2002; Carbone et al. 2002; Fleury-Feith et al. 2003; Lecomte et al. 2005; Robinson et al. 2005; Musti et al. 2006). *In vivo* approaches aimed at delineating this role have shown that NF2 heterozygosity contributes to early mesothelioma development. Previous studies *in vivo* have primarily focused on peritoneal mesothelioma development, which accounts for less than 10% of the already rare mesothelioma tumors (Fleury-Feith et al. 2003; Bridda et al. 2007; Yang et al. 2008). In addition, large doses of asbestos have been used to induce mesothelioma formation. Here, we were able to induce hyperplasia, as well as neoplasia in some cases, in mouse lung cells using IT injections of just 100 μg of asbestos. Although further verification is necessary, it is possible that some of the neoplastic formations were if fact pleural mesothelioma. Based on the subjective and un-blinded lungs scores that were given to H&E stained lungs on interpretation of lung hyperplasia, there appears to be no correlation with the predisposition of missing one *Nf2* allele to increased hyperplasia as compared to wild type counterparts, as both genotypes of mice developed hyperplastic regions of the lung. However, these results are subject to change upon the arrival of hyperplastic scores from Dr. Gardner.

The cell types that merlin and p21 labeled were predominantly Clara cells and smooth muscle cells, respectively. This will need to be verified by double

staining with Clara cell specific markers (CC10) or smooth muscle specific markers. In the terminal bronchioles the predominant cell type is the Clara cell, and these cells represent the precursors to ciliated cells that also line these airways. Merlin also appears to stain an additional cell type that is not identifiable, but is most likely a Type II pneumocyte. Type II pneumocytes are capable of undergoing cellular division and are progenitor cells for Type I cells. Both of these cell types, like mesothelial cells, respond to injury to repair lung tissue. In response to cell loss and injury, regenerative hyperplasia of both Type II pneumocytes and airway epithelium occurs which may lead to neoplasia (Dixon et al. 1999; Gardner 2008).

Protein expression of p21 appeared to label airway smooth muscle cells.. Airway smooth muscle cells have been regarded as contractile tissue, responding to proinflammatory mediators and bronchodilators to regulate airway size, surrounded by and reacting to the extracellular matrix (Howarth et al. 2004). Thus, in response to cues generated by the extracellular matrix, these cells respond to injury and are capable of proliferation and migration if necessary (Gounni et al. 2005). Expression of p21 was detected in both normal and hyperplastic regions of the lungs, indicating that this cell cycle checkpoint has been activated. More importantly, p21 expression was also absent in some hyperplastic regions, which could be indicative of loss of function of p53, and this absence of expression often correlated with regions where merlin was not detected. Whether these events are related has not been determined.

The majority of asbestos exposures occur through occupational means, including the mining of asbestos, the mining of asbestos-contaminated products (e.g. vermiculite or talc), or through the manufacturing of such materials. In addition, family members of those involved in such occupations can be exposed to asbestos as the particles can be brought home on one‘s clothing when the particles become aerosilized and spread throughout the environment. As many asbestos containing materials are present in our everyday environment, such as in insulation, floor tiles, roofing, etc., many people have the potential to be exposed to this hazardous material (ATSDR). Crocidolite is long regarded as the most potent of the amphibole fibers in regards to ARDs, and here we have shown that these fibers used in this study were capable of hyperplastic transformation after a 12 month exposure to the fibers, as well neoplastic transformation after 15 month exposure.

Vermiculite, a product largely used for fireproofing, soil amendments, and insulation, was mined from the Zonolite Mountain located near Libby, MT (Meeker et al. 2003). The mine was in operations from the 1920s until 1990 and was at one time the world’s largest source of vermiculite, producing 80% of the world's supply (Bandli and Gunter 2006). As early as 1959, the vermiculite was found to be contaminated with asbestos and was causing disease manifestation in workers, however the mine continued to operate until the 1990 mine closure (Meeker et al. 2003; Bandli and Gunter 2006). Since 1995, 44 cases of mesothelioma have been identified resulting from exposure to asbestos contamination in Libby, MT (Whitehouse et al. 2008).

In this study, Libby 6 Mix amphibole asbestos did not appear to have an impact on the induction cell hyperplasia as compared to PBS exposed mice. This is likely due to Libby 6 Mix amphibole fibers that were available for use at the time of mouse exposures. At the time that these exposures were performed, the fibre type that was available for use consisted of a mixture of fiber sizes. However this fraction size does not represent a respirable fraction that could cause disease. Since this time, an elutriated version of these fibers have become availble, allowing for an exposure sample more representative of the fiber type capable of causing disease. Repetition of this portion of the study using these elutriated fibers is necessary to draw conclusions on the impact that these fibers might have on mesothelioma development.

Although the degree and time to cell hyperplasia were not dependent on the predisposition of *Nf2* heterozogosity, almost all regions of where hyperplasia occured had lost merlin expression, suggesting that inactivation *Nf2* is a necessary step in the cellular transformation following asbestos exposure. Where merlin expression was not detected, loss of function appears to have contributed to cell hyperplasia. This confirmed the importance of *Nf2* in the maintenance of normal cell growth. In addition, p21 expression was absent in some areas of mild to moderate cell hyperplasia, but was absent in most neoplastic regions. Because these proteins appear not to be expressed in the same cell type, it is difficult to determine whether or not these alterations in expression were related events.

MPM is relatively untreatable, with a survival time post-diagnosis less than 2 years. As with any cancer, understanding the molecular mechanisms that are altered will help with the design of more effective treatment strategies. This becomes especially important for MPM patients, because of the poor response that this disease has to current therapies. A mouse model is a useful tool for understanding the biological changes that take place leading to tumor formation following asbestos exposure (Meuwissen and Berns 2005). Eventually, the molecular and cellular events that take place during this process can be dissected, allowing for the development of earlier diagnostic tools and treatment strategies.

Methods

Mouse Genotyping

C57BL/6/129S *Nf2*$^{+/-}$ mice were a kind gift from Dr. Joseph Kissil from the Wistar Institute in Philadelphia, PA. DNA was isolated from tail snips from the mice using DNeasy Blood and Tissue Kit (Qiagen ,Valencia, California) according to the manufacturers protocol. DNA was genotyped according to methods described by McClatchey et al. (1998). Basically, three primers (primer a: 5'-GGGGCTTCGGGAAACCTGG-3'; primer b: 5'-GTCTGGGAAGTCTGTGGAGG-3'; and primer c: 5'-CTATCAGGACATAGCGTTGG-3' were used for PCR amplification, producing two products. Primer pair a and b amplifies a 306-bp product from the wild-type allele, whereas primer pair a and c amplifies a 575-bp product from the mutant allele.

Asbestos Preparation

Mice will be exposed to two forms of asbestos particles, Libby Amphibole from U.S. Geological Survey and crocidolite from Research Triangle Institute (RTP, NC). Fibers were weighed out and suspended in PBS to a final concentration of 33.3 mg/mL. Solutions were sonicated to ensure particle suspension. As a negative control of the disease, mice (both knockout and wild type) will be exposed to sterile saline (30 uL/mouse) using the same IT procedure as described for the asbestos exposed groups.

Intratracheal Instillation

Nf2$^{+/-}$ and *Nf2*$^{+/+}$ mice were exposed to a dose of 3mg/mL (30 uL/mouse) asbestos via intratracheal (IT) instillation. The animals were anesthetized with 100μL of a ketamine (80mg/kg) and xylazine (12mg/kg) cocktail IP using a 23-25 gauge needle. The anesthesia lasts about 10-15 minutes, at which point a small incision was made into the neck (about 4-8mm). After opening the skin, the trachea was exposed and 30 μl of the above mentioned asbestos or sterile PBS was injected directly into the trachea. The skin was then closed with sterile tissue glue and the area was treated with betadine to help prevent infection. The animals were warmed on a heating pad, and usually were back to normal activity after about 1 hour.

Mice were monitored for signs of distress, which include cachexia, dypsnea, increase in chest wall mass, or cyanosis (nose and tail). If any of these signs of distress were detected, the mice were euthanized through IP injection of an overdose of 50 mg/kg pentol barbital.

Lung Fixation and Processing

Lungs were harvested from mice following euthanasia described above. Immediately following the removal of the lungs and hearts from the body cavity of the mouse, the lungs were perfused with about 200 μL of Histochoice (Amresco, Solon, Ohio), and then placed in a 15 mL conical tube with 7 mL Histochoice. Tubes were stored at 4°C at least 24 hours before processing of tissue, not to exceed 48 hours in Histochoice fixative. Lungs were processed in a Shandon

Citadel auto-processor using the following program: 30 min in 70% ethanol (EtOH), 30 min in 95% EtOH, 2 changes 1 hour each in 100% EtOH, 2 changes of 1 hour each in methyl salicylate, 45 min in paraffin, and finished in 1.5hr in a 2nd paraffin wax. Lungs were sliced in 7μm thick sections.

Hematoxylin and Eosin Stain (H&E)

For H&E staining, slides were stained in a Shandon Varistain 24-4 auto-stainer using the following program: 3*5 min in xylene, 2*3 min in 100% EtOH, 3 min in 95% EtOH, 3 min in 70% EtOH, 5 min in deionized water (dH_2O), 5 min in Harris Hematoxylin, 5 min in dH_2O, 30 sec in acid alcohol, 5 min in dH_2O, 1 min in bluing, 5 min in 70% EtOH, 2 min in eoxin, 5 min in 95% EtOH, 2*5 min in 100% EtOH, and 3*5min in xylene.

Immunohistochemistry

Sections mounted on slides were rehydrated by incubating 3*5 minutes in xylene, followed by 2*3 min incubation in 100% EtOH, a 3 min incubation in 95% EtOH, a 3 min incubation in 70% EtOH, and finished with a 5 min wash in PBS.

Slides were boiled in Citric Acid Buffer (10mM Citric Acid, pH6, with 0.1% Tween 20) for 10 minutes. After 10 minutes, the solution was removed from heat and allowed to sit in the buffer for 10 minutes. The slides were placed in a PBS wash for 5 minutes. Sections were circled with a hydrophobic pen, and blocked with 4% goat serum diluted in PAB buffer (PBS containing 2% BSA and 0.01% sodium azide). Primary NF2 antibody (A19, Santa Cruz Biotechnology, Santa Cruz, California) was diluted 1:50 in PAB and allowed to incubate overnight at

4°C. The following day, slides were washed 2*5 min in PBS. Secondary antibody (goat-anti-rabbit Alexa Fluor® 488) was added at 1:400 dilution in PAB and allowed to incubate in the dark at room temperature for 1 hour. Slides were washed 2*5 min in PBS. Primary pre-conjugated p21 Alexa Fluor® 647 antibody (C19, Santa Cruz Biotechnology, Santa Cruz, California) was added at 1:10 dilution in PAB and allowed to incubate overnight at 4°C. The following day, slides were washed 2*5 min in PBS followed by 3 quick rinses in dH_2O before coverslipping with Flurosave.

References

Altomare, D.A., Vaslet, C.A., Skele, K.L., De Rienzo, A., Devarajan, K., Jhanwar, S.C., McClatchey, A.I., Kane, A.B., and Testa, J.R. 2005. A mouse model recapitulating molecular features of human mesothelioma. *Cancer Res* **65**(18): 8090-8095.

ATSDR. Agency for Toxic Substances and Disease Registry: Public Health Statement--Asbestos. In.

Bandli, B.R. and Gunter, M.E. 2006. A review of scientific literature examining the mining history, geology, mineralogy, and amphibole asbestos health effects of the Rainy Creek igneous complex, Libby, Montana, USA. *Inhal Toxicol* **18**(12): 949-962.

Baser, M.E., De Rienzo, A., Altomare, D., Balsara, B.R., Hedrick, N.M., Gutmann, D.H., Pitts, L.H., Jackler, R.K., and Testa, J.R. 2002. Neurofibromatosis 2 and malignant mesothelioma. *Neurology* **59**(2): 290-291.

Bellamy, J.M. and Gunter, M.E. 2008. Morphological characterization of the Libby "six-mix" amphiboles used in *in vivo* studies. *Periodico di Mineralogia* **77**(2): 75-82.

Bridda, A., Padoan, I., Mencarelli, R., and Frego, M. 2007. Peritoneal mesothelioma: a review. *MedGenMed* **9**(2): 32.

Carbone, M., Kratzke, R.A., and Testa, J.R. 2002. The pathogenesis of mesothelioma. *Semin Oncol* **29**(1): 2-17.

Cugell, D.W. and Kamp, D.W. 2004. Asbestos and the pleura: a review. *Chest* **125**(3): 1103-1117.

Dixon, D., Herbert, R.A., Sills, R.C., and Boorman, G.A. 1999. *Lungs, Pleura, and Mediastinum*. Cache River Press, St. Louis.

Dunitz, M. 2002. *Mesothelioma*. Taylor & Francis, London.

Fleury-Feith, J., Lecomte, C., Renier, A., Matrat, M., Kheuang, L., Abramowski, V., Levy, F., Janin, A., Giovannini, M., and Jaurand, M.C. 2003. Hemizygosity of Nf2 is associated with increased susceptibility to asbestos-induced peritoneal tumours. *Oncogene* **22**(24): 3799-3805.

Gardner, D. 2008. Histological Evalutation of Mouse Slides. In (ed. A. Erbe), Hamilton.

Gounni, A.S., Wellemans, V., Yang, J., Bellesort, F., Kassiri, K., Gangloff, S., Guenounou, M., Halayko, A.J., Hamid, Q., and Lamkhioued, B. 2005. Human airway smooth muscle cells express the high affinity receptor for IgE (Fc epsilon RI): a critical role of Fc epsilon RI in human airway smooth muscle cell function. *J Immunol* **175**(4): 2613-2621.

Hammar, S.P. 2006. Macroscopic, histologic, histochemical, immunohistochemical, and ultrastructural features of mesothelioma. *Ultrastruct Pathol* **30**(1): 3-17.

Hesterberg, T.W., Miiller, W.C., McConnell, E.E., Chevalier, J., Hadley, J.G., Bernstein, D.M., Thevenaz, P., and Anderson, R. 1993. Chronic inhalation toxicity of size-separated glass fibers in Fischer 344 rats. *Fundam Appl Toxicol* **20**(4): 464-476.

Howarth, P.H., Knox, A.J., Amrani, Y., Tliba, O., Panettieri, R.A., Jr., and Johnson, M. 2004. Synthetic responses in airway smooth muscle. *J Allergy Clin Immunol* **114**(2 Suppl): S32-50.

Jaurand, M.C. and Fleury-Feith, J. 2005. Pathogenesis of malignant pleural mesothelioma. *Respirology* **10**(1): 2-8.

Knudson, A.G., Jr. 1971. Mutation and cancer: statistical study of retinoblastoma. *Proc Natl Acad Sci U S A* **68**(4): 820-823.

Lecomte, C., Andujar, P., Renier, A., Kheuang, L., Abramowski, V., Mellottee, L., Fleury-Feith, J., Zucman-Rossi, J., Giovannini, M., and Jaurand, M.C. 2005. Similar tumor suppressor gene alteration profiles in asbestos-induced murine and human mesothelioma. *Cell Cycle* **4**(12): 1862-1869.

McClatchey, A.I. 2003. Merlin and ERM proteins: unappreciated roles in cancer development? *Nat Rev Cancer* **3**(11): 877-883.

McClatchey, A.I., Saotome, I., Mercer, K., Crowley, D., Gusella, J.F., Bronson, R.T., and Jacks, T. 1998. Mice heterozygous for a mutation at the Nf2 tumor suppressor locus develop a range of highly metastatic tumors. *Genes Dev* **12**(8): 1121-1133.

McClatchey, A.I., Saotome, I., Ramesh, V., Gusella, J.F., and Jacks, T. 1997. The Nf2 tumor suppressor gene product is essential for extraembryonic development immediately prior to gastrulation. *Genes Dev* **11**(10): 1253-1265.

Meeker, G.P., Bern, A.M., Brownfield, I.K., Lowers, H.A., Sutley, S.J., Hoefen, T.M., and Vance, J.S. 2003. The Composition and Morphology of Amphiboles from the Rainy Creek Complex, Near Libby, Montana. *American Mineralogist* **88**: 1955-1969.

Meuwissen, R. and Berns, A. 2005. Mouse models for human lung cancer. *Genes Dev* **19**(6): 643-664.

Musti, M., Kettunen, E., Dragonieri, S., Lindholm, P., Cavone, D., Serio, G., and Knuutila, S. 2006. Cytogenetic and molecular genetic changes in malignant mesothelioma. *Cancer Genet Cytogenet* **170**(1): 9-15.

Robinson, B.W., Musk, A.W., and Lake, R.A. 2005. Malignant mesothelioma. *Lancet* **366**(9483): 397-408.

Sekido, Y., Pass, H.I., Bader, S., Mew, D.J., Christman, M.F., Gazdar, A.F., and Minna, J.D. 1995. Neurofibromatosis type 2 (NF2) gene is somatically mutated in mesothelioma but not in lung cancer. *Cancer Res* **55**(6): 1227-1231.

Tan, C. and Treasure, T. 2005. Mesothelioma: time to take stock. *J R Soc Med* **98**(10): 455-458.

Tweedale, G. 2002. Asbestos and its lethal legacy. *Nat Rev Cancer* **2**(4): 311-315.

Wagner, J.C., Sleggs, C.A., and Marchand, P. 1960. Diffuse pleural mesothelioma and asbestos exposure in the North Western Cape Province. *Br J Ind Med* **17**: 260-271.

Whitehouse, A.C., Black, C.B., Heppe, M.S., Ruckdeschel, J., and Levin, S.M. 2008. Environmental exposure to Libby Asbestos and mesotheliomas. *Am J Ind Med* **51**(11): 877-880.

Yang, H., Testa, J.R., and Carbone, M. 2008. Mesothelioma epidemiology, carcinogenesis, and pathogenesis. *Curr Treat Options Oncol* **9**(2-3): 147-157.

DISCUSSION

Since its discovery, *NF2* has been suggested to be a unique tumor suppressor gene, mainly because of its subcellular localization and connection with the cell membrane (Trofatter et al. 1993; Brault et al. 2001; McClatchey and Giovannini 2005). Researchers have shown that this gene is involved in cellular growth regulation through its involvement in contact inhibition of growth, cell proliferation alterations, and apoptotic response. Here, we have shown that *NF2* is not only involved in the relaying of signals involved in these pathways, but activity of the gene may ultimately affect the function and/or activity of *two* key TSGs, *TP53* and *RB*.

This study has primarily focused on how *NF2* inactivation might be involved upstream in the regulation of p53, attributed to its possible involvement in the degradation of MDM2. MDM2 helps to maintain low steady-state p53 levels through ubiquitination and subsequent proteasome degradation. We were able to show that alterations in the protein level of merlin (the *NF2* gene product) resulted in inverse alterations in MDM2 protein levels. MDM2 protein level changes also correlated with alterations in p53 activity. For example, in Chapter 1 we showed that suppression of merlin resulted in increased MDM2 protein and subsequently decreased p21 and Bax expression, indicating p53 activity had been negatively affected by merlin loss. It remains unclear whether merlin is degrading MDM2 in this pathway or inhibiting its activity through other

mechanisms. Future studies could assess the ubiquitination status of p53 and could provide more information regarding MDM2 activity levels.

As the major TSGs *RB* and *TP53* are commonly found mutated in other cancers, how malignant mesothelioma tumors arise while still retaining these two major TSG in their wild-type form is unclear. Alterations in the cell that might contribute to loss of function of these genes need to be elucidated. In mesothelioma, it seems plausible that both p53 and RB are not capable of functioning properly, thus the hyperplastic cells do not require inactivation of the p53 or RB to progress to neoplasms. The mechanisms for this malfunction of both RB and p53 has largely been attributed to p16 and p14, respectively. Here we have shown that merlin not only contributes to loss of p53 activity, but via mechanisms such as Cyclin D1, it may also contribute to Rb loss of function as well (Figure 28). We were able to confirm a role for merlin in the regulation of Cyclin D1, which is involved in the progression from G_1 to S phase of the cell cycle. One of the means by which Cyclin D1 initiates this transition is via phosphorylation of Rb. Investigations aimed at the phosphorylation status of Rb following merlin expression level alterations might provide insight into this pathway.

FIGURE 28

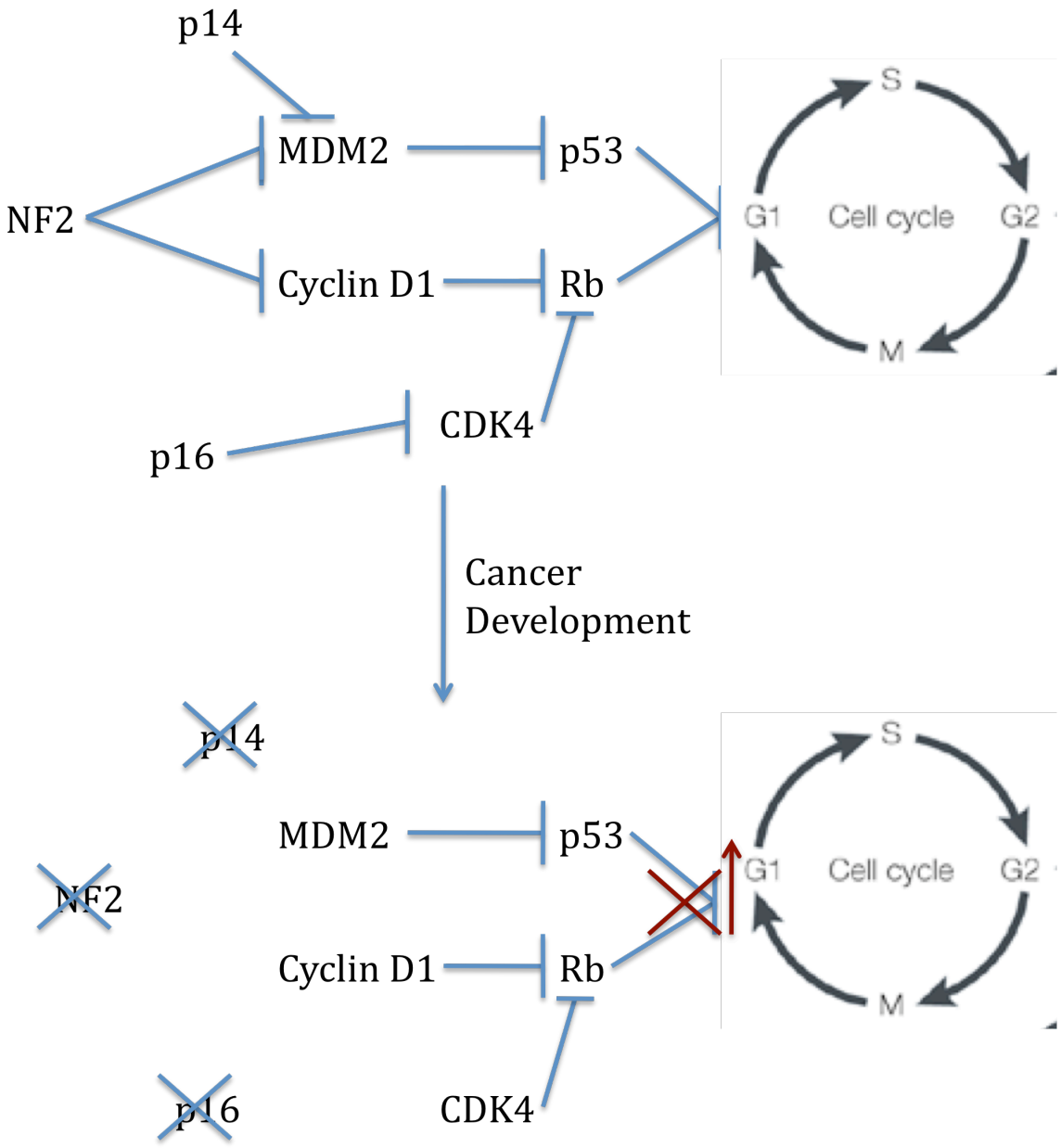
p14
MDM2
p53
NF2
Cyclin D1
Rb
S
G1
Cell cycle
G2
M
CDK4
p16
Cancer
Development
p14
MDM2
p53
NF2
Cyclin D1
Rb
S
G1
Cell cycle
G2
M
p16
CDK4

Figure 28. A possible mechanism for *NF2* in the control of the activity of p53 and RB.

Merlin, the protein product of *NF2*, may act upstream of p53 to regulate activity of the TSG by negatively regulating MDM2. Similarly, merlin may act upstream of Rb by inhibiting Cyclin D1. When *NF2* is inactivated, in combination with the inactivation other genes like *p16* and *p14*, an increase in inhibition of p53 and Rb can occur resulting in continual transition into S phase and thus loss of cell cycle control.

Using a mouse model to recapitulate genetic alterations that occur in humans following asbestos exposure, we were able to demonstrate the toxicity of asbestos in terms the carcinogenic potential of the fibers. While cell hyperplasia occurred in many of the asbestos-exposed mice, the majority of these cases were not termed mesothelioma by the pathologist. Further analysis of these samples using histological markers to verify the type of tumor formation may provide more information into the tumor types seen. Instead, as this study could be considered a pilot study of mesothelioma development using an IT exposure route, it might be useful to repeat this study including an additional exposure time point. Such an approach would be more similar to human exposure to asbestos, as most asbestos exposures are not likely one-time occurrences, but occur over a period of time. Another advantage to repeating this portion would be the inclusion of additional time points, both shorter and longer, in an attempt to determine the time of *NF2* inactivation and possible information on earlier diagnosis. Once a consistent *in vivo* approach for the development of mesothelioma is achieved, this model could be used in the testing of therapeutics, possible testing gene therapy targeting mesothelial cells expressing *NF2*.

Genetic variance among patients involved in Phase I clinical trials, which typically include about 30 people, usually results in at least one death due toxicity of the drug being tested (Ames 2008). This is primarily due to genetic variability in genes responsible metabolism of the drugs being administered, but it can also be applied to gene alterations that occur in the cancer tissue. Genotyping of

individuals prior to treatment will be a critical step for improving clinical outcomes. In the case of mesothelioma, genotyping can be further focused to commonly inactivated genes for targeted gene therapy approaches. There is genetic testing available for *NF2*, including both mutation analysis and linkage analysis, for NF2 patients (Yohay 2006). As this tool is available, gene therapy could be used to specifically target those tumors where *NF2* is inactivated to re-express the gene with the hopes of slowing tumor growth. In addition, in mesothelioma patients that retain wild-type *NF2,* it may be that overexpression of *NF2* will be useful. Of the possible uses for *NF2*-targeted gene therapy, one that involves a combination of this approach with other therapeutic options will likely be the most effective treatment to benefit patients. Jongsma et al. (2008) found that co-deletion of NF2 along with the INK4a locus in mice without asbestos exposure was sufficient to induce mesothelioma, highlighting the importance of these genes in tumor development. In particular, combination gene therapeutic options that include both the INK4a locus, which houses the TSGs p14 and p16, and *NF2* may have promising results, where these genes could stabilize p53 and Rb resulting in the restoration of cell-cycle checkpoints and tumor suppression.

This study has provided useful information regarding the tumor suppressor capabilities of the TSG, *NF2*. The potential for *NF2* to act upstream of p53 adds to the importance of retention of this gene in the maintenance of normal cell-cycle control. Research investigating the role of *NF2* in other cancers will further our knowledge on the tumor suppressor capabilities of not only *NF2*, but also the regulatory mechanisms of p53 and possibly Rb.

Reference

Ames, M. 2008. The Critical Role of Drug Metabolizing Enzyme Genotypes in Irinotecan and Tamoxifen Cancer Therapy. In *Seminar for the Department of Biomedical and Pharmaceutical Sciences* University of Montana.

Brault, E., Gautreau, A., Lamarine, M., Callebaut, I., Thomas, G., and Goutebroze, L. 2001. Normal membrane localization and actin association of the NF2 tumor suppressor protein are dependent on folding of its N-terminal domain. *J Cell Sci* **114**(Pt 10): 1901-1912.

Jongsma, J., van Montfort, E., Vooijs, M., Zevenhoven, J., Krimpenfort, P., van der Valk, M., van de Vijver, M., and Berns, A. 2008. A conditional mouse model for malignant mesothelioma. *Cancer Cell* **13**(3): 261-271.

McClatchey, A.I. and Giovannini, M. 2005. Membrane organization and tumorigenesis--the NF2 tumor suppressor, Merlin. *Genes Dev* **19**(19): 2265-2277.

Trofatter, J.A., MacCollin, M.M., Rutter, J.L., Murrell, J.R., Duyao, M.P., Parry, D.M., Eldridge, R., Kley, N., Menon, A.G., Pulaski, K., and et al. 1993. A novel moesin-, ezrin-, radixin-like gene is a candidate for the neurofibromatosis 2 tumor suppressor. *Cell* **72**(5): 791-800.

Yohay, K.H. 2006. The genetic and molecular pathogenesis of NF1 and NF2. *Semin Pediatr Neurol* **13**(1): 21-26.

APPENDIX A

Vector Maps Used in Chapters 1 and 2

Gene Expression Array Relevant to Chapter 1

Figure 29. Vector map of plasmid used in Chapter 1.

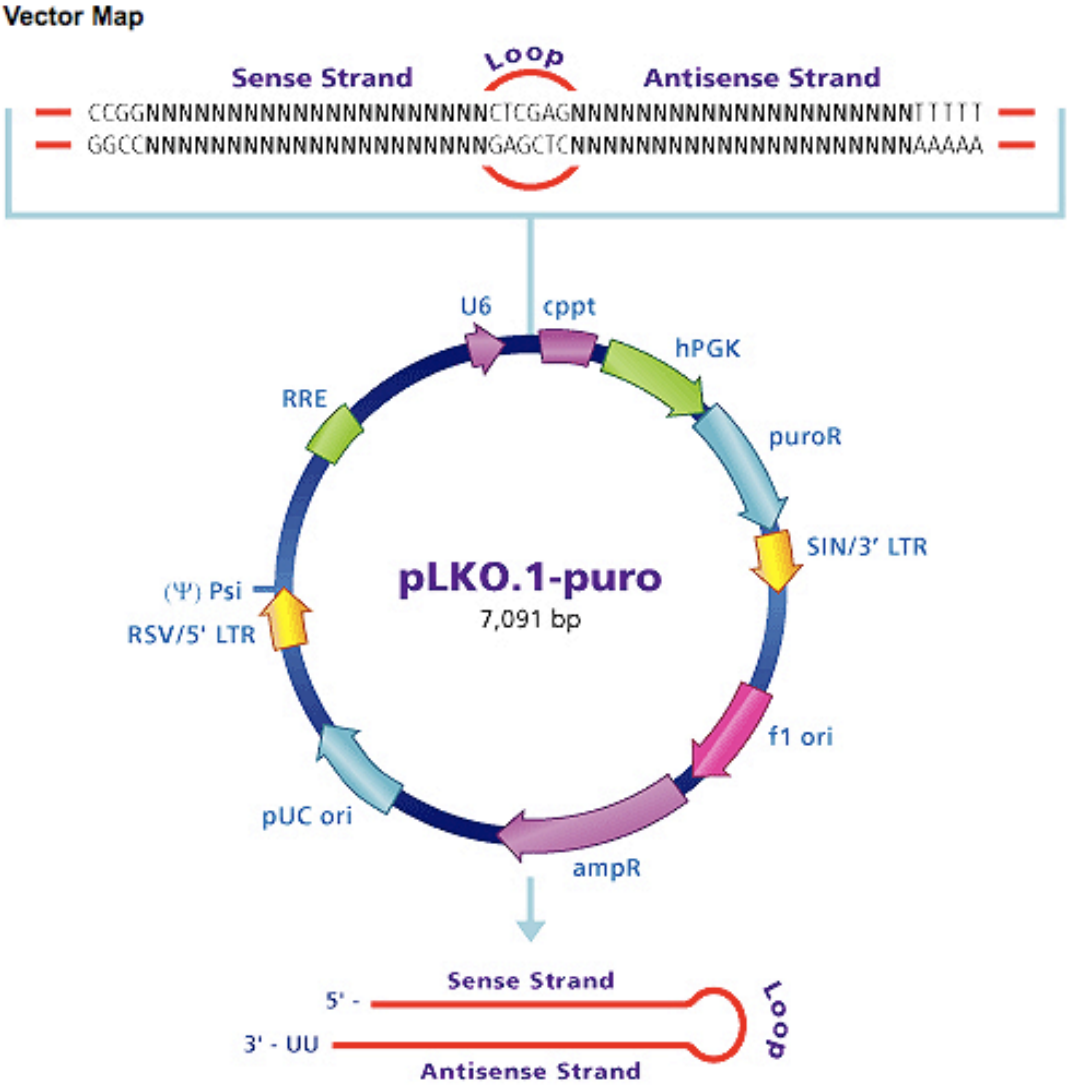

pLKO.1-puro vector description and features

Name	Description
cppt	Central polypurine tract
hPGK	Human phosphoglycerate kinase eukaryotic promoter
puroR	Puromycin resistance gene for mammalian selection
SIN/LTR	3' self inactivating long terminal repeat
f1 ori	f1 origin of replication
ampR	Ampicillin resistance gene for bacterial selection
pUC ori	pUC origin of replication
5' LTR	5' long terminal repeat
Psi	RNA packaging signal
RRE	Rev response element

Figure 30. Vector map of control plasmid used in Chapter 1.

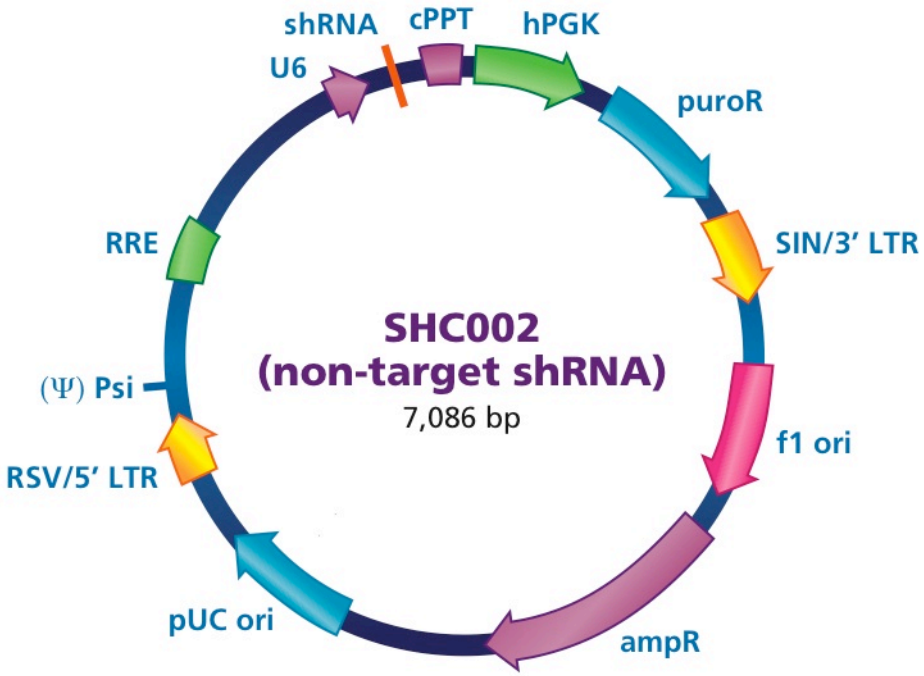

Figure 31. Vector map of plasmid used in Chapter 2.

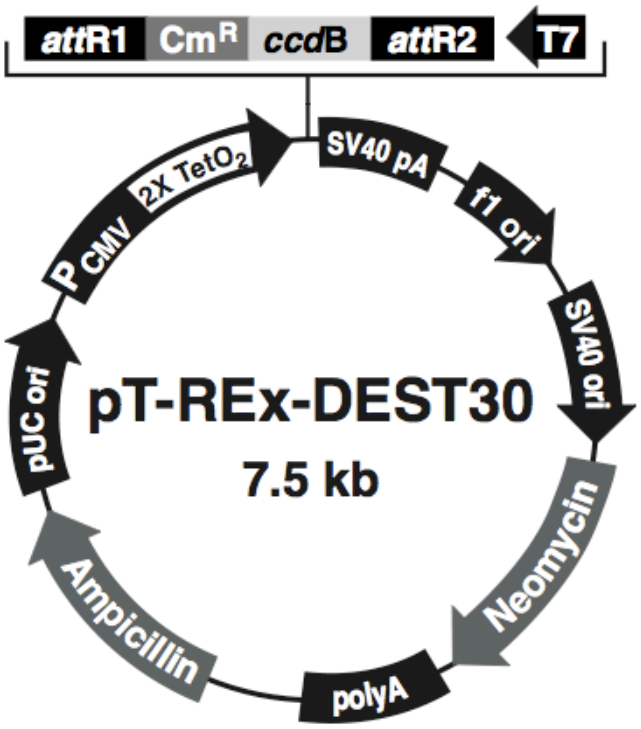

Comments for pT-REx-DEST30
7544 nucleotides

CMV promoter: bases 1-588
TATA box: bases 502-508
Tetracycline operator (2X $TetO_2$) sequence: bases 518-557
attR1 recombination site: bases 699-823
Chloramphenicol resistance gene: bases 932-1591
ccdB gene: bases 1933-2238
attR2 recombination site: bases 2279-2403
T7 promoter: bases 2464-2483 (complementary strand)
SV40 polyadenylation region: bases 2915-3045
f1 origin: bases 3175-3603
SV40 early promoter and origin: bases 3790-4098
Neomycin resistance ORF: bases 4157-4951
Polyadenylation region: bases 5015-5063
Ampicillin (*bla*) resistance ORF: bases 5474-6334
pUC origin: bases 6479-7152

Figure 32. Vector map of control plasmid used in Chapter 2.

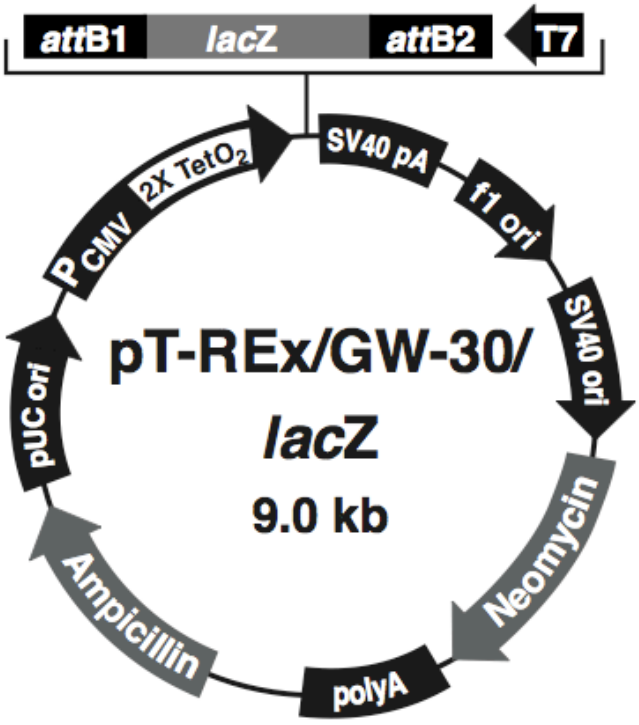

Comments for pT-REx/GW-30/*lacZ*
8999 nucleotides

CMV promoter: bases 1-588
TATA box: bases 502-508
Tetracycline operator (2X $TetO_2$) sequence: bases 518-557
attB1 recombination site: bases 699-723
lacZ ORF: bases 743-3799
attB2 recombination site: bases 3834-3858
T7 promoter: bases 3919-3938 (complementary strand)
SV40 polyadenylation region: bases 4370-4500
f1 origin: bases 4630-5058
SV40 early promoter and origin: bases 5245-5553
Neomycin resistance ORF: bases 5612-6406
Polyadenylation region: bases 6470-6518
Ampicillin (*bla*) resistance ORF: bases 6929-7789
pUC origin: bases 7934-8607

Figure 33. Vector map of Tet-Repressor plasmid used in Chapter 2.

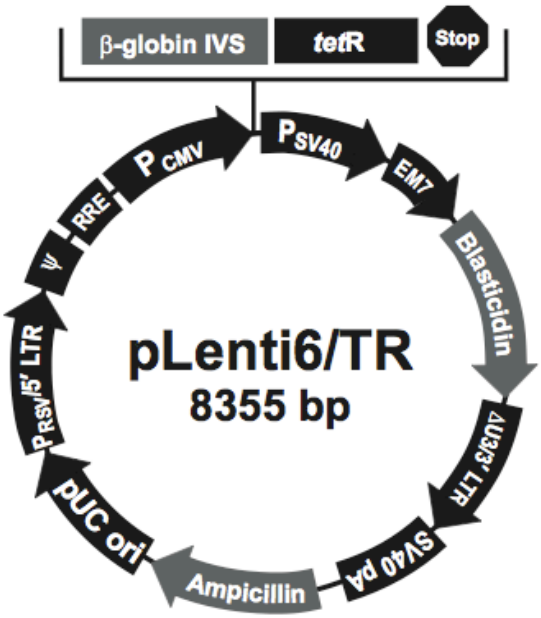

Comments for pLenti6/TR
8355 nucleotides

RSV/5′ LTR hybrid promoter: bases 1-410
RSV promoter: bases 1-229
HIV-1 5′ LTR: bases 230-410
5′ splice donor: base 520
HIV-1 psi (ψ) packaging signal: bases 521-565
HIV-1 Rev response element (RRE): bases 1075-1308
3′ splice acceptor: base 1656
3′ splice acceptor: base 1684
CMV promoter: bases 1809-2392
Rabbit β-globin intron II (IVS): bases 2552-3124
*tet*R gene: bases 3208-3855
SV40 early promoter and origin: bases 3960-4269
EM7 promoter: bases 4324-4390
Blasticidin resistance gene: bases 4391-4789
ΔU3/3′ LTR: bases 4875-5109
ΔU3: bases 4875-4928
3′ LTR: bases 4929-5109
SV40 polyadenylation signal: bases 5181-5315
bla promoter: bases 6171-6269
Ampicillin (*bla*) resistance gene: bases 6270-7130
pUC origin: bases 7275-7948

A microarray was performed on MeT5a clones generated in Chapter 1 to understand some of the gene expression changes that take place following *NF2* suppression. Two Nf2-suppressed clones generated from two different *NF2*-shRNA targets (9973-6 and 9974-5) were used for this analysis and compared to MeT5a-CNT9 cells. The resulting upregulated and down regulated gene expression changes that were shared between the two clones are listed in Table 3 and Table 4, respectively.

Table 3. Genes upregulated in MeT5a clones following *NF2*-suppression.

Gene Symbol	Gene Name	Biological Processes	Cellular Component	Fold Change	p-value
EMP3	Epithelial membrane protein 3	Cell growth	Integral to membrane	1.76	0.021
PRDX6	Peroxiredoxin 6	Cell redox homeostasis	nucleus, cytoplasm, lysosome	1.77	0.039
FPRL1	Formyl peptide receptor-like 1	Inflammatory response, cell adhesion, signaling pathways	Integral to membrane	1.55	0.022
CLCA4	Chloride channel, calcium activated, family member 4	Transport	Extracellular region, integral to membrane	1.83	0.023
KCNMB4	Potassium large conductance calcium-activated channel, subfamily M, beta member 4	Ion Transport	Membrane	1.75	0.013
SDHC	Succinate dehydrogenase complex, subunit C, integral membrane protein, 15kDa	Transport	Integral to membrane	1.57	0.022
SLC11A2	Solute carrier family 11 (proton-coupled divalent metal ion transporters), member 2	Transport	integral to membrane	1.65	0.020
GJA4	Gap junction protein, alpha 4, 37kDa (connexin 37)	Cell Communication, Cell-Cell Junction Assembly, Transport	Integral to membrane	1.63	0.009
EIF4A1	Eukaryotic translation initiation factor 4A, isoform 1	Translation	Cytosol	1.55	0.023
GDF3	Growth differentiation factor 3	Growth factor activity	Extracellular region	1.73	0.020
HTR2C	5-hydroxytryptamine (serotonin) receptor 2C	Signaling pathway	Integral to membrane, cytoplasm	1.64	0.016
PDLIM5	PDZ and LIM domain 5	Actin Binding	Cytosol, actin cytoskeleton	1.66	0.008
NFIX	Nuclear factor I/X (CCAAT-binding transcription factor)	DNA replication	Nucleus, intracellular	1.74	0.009
CALB1	Calbindin 1, 28kDa	Locomotory behavior	Cytosol, nucleus	1.52	0.018
ITGAV	Integrin, alpha V (vitronectin receptor, alpha polypeptide, antigen CD51)	Cell adhesion, integrin-mediated signaling	Cytoplasm, plasma membrane	1.84	0.037

Table 4. Genes down regulated in MeT5a clones following *NF2* suppression.

ene ymbol	Gene Name	Biological Processes	Cellular Component	Fold Change	p-value
SPN	Asporin (LRR class 1)	Protein binding	Membrane	-4.68	0.005
MEM104	Transmembrane protein 104	Not Found	Integral to membrane	-4.49	0.017
ABIN1	Calcineurin binding protein 1	Cell surface receptor linked signal transduction	Nucleus	-4.16	0.025
ARS	Alanyl-tRNA synthetase	Translation	Cytoplasm	-3.40	0.006
CN1	Lipocalin 1 (tear prealbumin)	Transport	Extracellular region	-3.23	0.022
ABRE	Gamma-aminobutyric acid (GABA) A receptor, epsilon	Ion Transport	Integral to membrane, Cell junction	-2.51	0.027
C	Pyruvate carboxylase	Metabolic Process	Mitochondrion	-2.25	0.036
CF1	Neutrophil cytosolic factor 1	Cell communication	Cytoplasm	-2.21	0.016
LOC1	Translocation protein 1	Intracellular protein transmembrane transport	Integral to membrane	-2.21	0.020
MSB10	Thymosin, beta 10	Actin cytoskeleton organization	Cytoplasm	-1.93	0.016
NO1	Enolase 1, (alpha)	Negative regulation of cell growth	Cytoplasm	-1.69	0.006

Methods

RNA Isolation

Total RNA was isolated from cell lines using the standard Trizol Reagent (Invitrogen, Carlsbad, CA) according to manufacturer's protocol. A further RNA cleanup step was performed using an RNeasy (Qiagen, Valencia, CA) to remove contaminants. RNA quantity and quality were assessed using a Nanodrop Spectrophotometer (Nanodrop Technologies, Wilmington, DE) and Agilent Bioanalyzer (Agilent Technologies, Santa Clara, CA).

Microarray Analysis

Gene expression changes following suppression of NF2 were assessed for MeT5A 9973-6 and MeT5A 9974-5 cell lines compared to MeT5A control-9 cells. Reverse transcription and cDNA labeling were performed using 8 µg of total RNA according to the Superscript Plus Direct cDNA Labeling Kit (Invitrogen). Labeling efficiency was determined using a Nanodrop Spectrophotometer (Nanodrop). Labeled cDNA was hybridized overnight at 42°C to in-house spotted arrays of oligonucleotides produced by MWG Biotech, Inc. (High Park, NC). Arrays were scanned and analyzed using an Axon GenePix 4000B microarray scanner and Axon GenePix Pro 5.1 software (Molecular Devices, Sunnyvale, CA) . Further analyses were performed using Iobion GeneTraffic Duo (Stratagene, La Jolla, CA), GoMiner (NCBI), and PathwayStudio (Ariadne Genomics, Rockville, MD).